

# UNCLASSIFIED

AD NUMBER
ADB038157
NEW LIMITATION CHANGE
TO Approved for public release, distribution unlimited
FROM Distribution authorized to U.S. Gov't. agencies only; Test and Evaluation; NOV 1978. Other requests shall be referred to US Naval Explosive Ordnance disposal Facility, Indian Head, MD 20640.
AUTHORITY
NAVEODFAC, DoDD 5200.20

THIS PAGE IS UNCLASSIFIED

✓

2 LEVEL 11/7

NAVEODFAC TECHNICAL REPORT TR-211 ✓

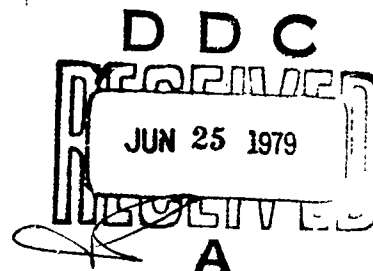
# SPECTROSCOPIC INVESTIGATIONS OF ENERGETIC MATERIALS AND ASSOCIATED IMPURITIES

AD B038157

DEPARTMENT OF PHYSICS  
BOSTON COLLEGE  
Chestnut Hill, MA 02167

JUNE 1979

INTERIM REPORT



DDC FILE COPY

Distribution limited to U.S. Government agencies only; Test and Evaluation;  
November 1978. Other requests for this document must be referred to the  
Commanding Officer, Naval Explosive Ordnance Disposal Facility, Indian Head,  
Maryland 20640.

Prepared for  
NAVAL EXPLOSIVE ORDNANCE DISPOSAL FACILITY  
INDIAN HEAD, MARYLAND 20640

29

Released by  
**LIONEL A. DICKINSON**  
Technical Director

Under Authority of  
**W. S. CADOW, JR., CDR, USN**  
Commanding Officer

REPORT DOCUMENTATION PAGE		READ INSTRUCTIONS BEFORE COMPLETING FORM	
1. REPORT NUMBER TR-211		2. RECIPIENT'S CATALOG NUMBER NAVEOZTAC	
3. TITLE (and Subtitle) SPECTROSCOPIC INVESTIGATIONS OF ENERGETIC MATERIALS AND ASSOCIATED IMPURITIES		4. TYPE OF REPORT & PERIOD COVERED Interim 1 September 1977 - 31 August 1978	
5. AUTHOR(s) B. Di Bartolo, D. P. Pacheco, M. J. Shultz		6. PERFORMING ORG. REPORT NUMBER N00174-77-C-0287	
7. PERFORMING ORGANIZATION NAME AND ADDRESS Department of Physics Boston College Chestnut Hill, MA 02167		8. CONTRACT OR GRANT NUMBER(s) N00174-77-C-0287	
9. CONTROLLING OFFICE NAME AND ADDRESS Naval Explosive Ordnance Disposal Facility Research and Development Department (Code 50) Indian Head, MD 20640		10. PROGRAM ELEMENT, PROJECT, TASK AREA & WORK UNIT NUMBERS	
11. MONITORING AGENCY NAME & ADDRESS (if different from Controlling Office) 12) 144F		12. REPORT DATE November 1978	
		13. NUMBER OF PAGES 140	
		14. SECURITY CLASS (of this report) Unclassified	
		15. DECLASSIFICATION DOWNGRADING SCHEDULE	
16. DISTRIBUTION STATEMENT (of this Report) Distribution limited to U.S. Government agencies only; Test and Evaluation; November 1978. Other requests for this document must be referred to the Commanding Officer, Naval Explosive Ordnance Disposal Facility, Indian Head, MD 20640.			
17. DISTRIBUTION STATEMENT (of the abstract entered in Block 20, if different from Report) Approved for public release; distribution unlimited.			
18. SUPPLEMENTARY NOTES			
19. KEY WORDS (Continue on reverse side if necessary and identify by block number) UV spectroscopy Explosive vapors Explosives in solution Flash photolysis of TNT			
20. ABSTRACT (Continue on reverse side if necessary and identify by block number) The detection of explosive devices through analysis of the characteristic emitted vapors has been attempted in the past using a variety of techniques. However, little work has been performed on the spectroscopic properties of these vapors. Optical detection has the potential for high sensitivity if the species being monitored has the proper optical properties. By obtaining fundamental data on these properties, the feasibility of employing such a detection technique can be determined. Along these lines, we have performed extensive studies of the absorption characteristics of a number of explosive and			



UNCLASSIFIED

SECURITY CLASSIFICATION OF THIS PAGE (When Data Entered)

explosive-related compounds, both in the vapor phase and in solutions. Specifically, the materials studied include 2,3 DNT, 2,4 DNT, 2,6 DNT, TNT, nitroglycerine, diphenylamine, ethyl centralite, monomethylamine, RDX, cyclohexanone, and PETN. The solution spectra were recorded in order to obtain useful supplementary information on the general behavior of the absorbing species. In addition to the absorption work, we have performed preliminary flash photolysis experiments on TNT\* in solution in order to identify and study the characteristic dissociation products. This technique can be extremely useful in determining whether the photodecomposition properties of certain explosive materials can be used as a basis for their detection. Initially, this work has been done in solution as a prelude to vapor-phase dissociation studies.

↑

\* were conducted

UNCLASSIFIED

SECURITY CLASSIFICATION OF THIS PAGE (When Data Entered)

## PREFACE

The authors would like to thank Dr. Edward Billo for his help with some of the absorption measurements performed during the course of this study. They would also like to acknowledge Dr. Lyle Malotky of Naval Explosive Ordnance Disposal Facility, Indian Head, Maryland and Dr. William Wall for a number of valuable discussions on the subject of this work. Some of the samples examined were provided by Dr. Lyle Malotky and Dr. John Hobbs of the Department of Transportation, Cambridge, Massachusetts. Dr. Hobbs also ran a gas chromatogram of the Eastman TNT sample investigated. Finally, the authors would like to thank Dr. Horace Furumoto for his advice regarding the vapor absorption apparatus, Jeffrey Franklin and Miguel Delgado for performing some of the experiments, Marie Thibeault and Ruth Boyer for drafting the figures for this report, and Patricia O'Neal for typing the manuscript.

1	
Distribution	
L.S.	
Distribution/	
Availability Codes	
Dist.	Avail and/or special
B	

## TABLE OF CONTENTS

	<u>Page</u>
INTRODUCTION	10
EXPERIMENTAL FACILITIES	13
Absorption Spectrometer	13
Flash Photolysis Apparatus I	15
Flash Spectroscopic Mode	15
Kinetic Spectrophotometric Mode	17
Flash Photolysis Apparatus II	19
Fluorescence Apparatus	20
Dye-Laser Apparatus	21
SPECTRA OF EXPLOSIVE MATERIALS IN SOLUTION	26
Introduction	26
Experimental Details	27
Analysis of the Spectra	28
Benzene, Toluene, 2,4 DNT and 2,4,6 TNT in Ethanol	28
2,4 DNT in Solvents from Pure Ethanol to Pure Water	30
2,4 DNT in Isobutanol and 2-Propanol	31
Isomers of DNT in Ethanol	32
Isomers of DNT in 95% Water-5% Ethanol	33
Three Purities of TNT Examined	36
TNT in Ethanol and 95% Water-5% Ethanol	36
Absorption Spectrum of RDX	37
Absorption Spectrum of Diphenylamine	38
Absorption Spectrum of Ethyl Centralite	39
Absorption Spectrum of Nitroglycerine and Pentaerythritoltetranitrate (PETN)	39

	<u>Page</u>
General Remarks	40
Conclusions	42
SPECTRA OF EXPLOSIVE MATERIALS IN THE VAPOR PHASE	70
Introduction	70
Experimental Details	73
Experimental Results	74
Isomers of DNT	75
TNT	77
Nitroglycerine	78
Amines	78
Cyclohexanone and RDX	80
PETN	81
Discussion of Results	81
Isomers of DNT	81
TNT	86
Nitroglycerine	87
Amines	88
Cyclohexanone and RDX	92
PETN	93
General Remarks	94
FLASH PHOTOLYSIS DATA	124
Introduction	124
Flash Photolysis of Ethanol	125
Spectral Characteristics of TNT	126
Flash Photolysis of TNT in Solution	128
CONCLUSIONS AND RECOMMENDATIONS	134
REFERENCES	138

## LIST OF ILLUSTRATIONS

	<u>Page</u>
Figure 1: Layout of the Absorption Apparatus Operating in the "Spectrometer" Mode	23
Figure 2: Layout of the Flash Photolysis Spectroscope	24
Figure 3: Layout of the Kinetic Spectrophotometer	25
Figure 4: Molecular Formulae of Materials Investigated	54
Figure 5: Absorption Spectra of Benzene, Toluene, 2,4 DNT and 2,4,6 TNT in Ethanol	56
Figure 6: Absorption Spectra of 2,4 DNT in Mixtures of Ethanol and Water	57
Figure 7: Absorption Spectrum of 2,4 DNT in Water	58
Figure 8: Absorption Spectra of 2,4 DNT in Isobutanol and 2-Propanol.	59
Figure 9: Absorption Spectra of Isomers of DNT in Ethanol.	60
Figure 10: Absorption Spectra of Isomers of DNT in 95% Water-5% Ethanol	61
Figure 11: Absorption Spectra of Three Purities of Trinitrotoluene (TNT) in Ethanol	62
Figure 12: Absorption Spectra of TNT in Ethanol and 95% Water-5% Ethanol	63
Figure 13: Absorption Spectra of RDX in Ethanol and 95% Water-5% Ethanol	64
Figure 14: Absorption Spectra of Diphenylamine in Ethanol and 95% Water-5% Ethanol	65
Figure 15: Absorption Spectrum of Diphenylamine in Water	66
Figure 16: Absorption Spectra of Ethyl Centralite in Ethanol and 95% Water-5% Ethanol	67
Figure 17: Absorption Spectra of Nitroglycerine in Ethanol and 95% Water-5% Ethanol	68

	<u>Page</u>
Figure 18: Absorption Spectra of Pentaerythritoltetranitrate in Ethanol and in 95% Water-5% Ethanol	69
Figure 19: Absorption Spectrum of Toluene Vapor (Vapor Generated at 23°C)	98
Figure 20: Absorption Spectrum of Benzene Vapor (Vapor Generated at 32°C)	99
Figure 21: Absorption Spectrum of 2,4 DNT Vapor (Vapor Generated at 40°C)	100
Figure 22: Absorption Spectrum of 2,4 DNT Vapor (Vapor Generated at 51°C)	101
Figure 23: Absorption Spectrum of 2,4 DNT Vapor (Vapor Generated at 60°C)	102
Figure 24: Absorption Spectrum of 2,6 DNT Vapor (Vapor Generated at 40½°C)	103
Figure 25: Absorption Spectrum of 2,6 DNT Vapor (Vapor Generated at 51°C)	104
Figure 26: Absorption Spectrum of 2,6 DNT Vapor (Vapor Generated at 59°C)	105
Figure 27: Absorption Spectrum of 2,3 DNT Vapor (Vapor Generated at 42°C)	106
Figure 28: Absorption Spectrum of 2,3 DNT Vapor (Vapor Generated at 52°C)	107
Figure 29: Absorption Spectrum of Vapors Evolved from Military Grade TNT (Vapors Generated at 29°C)	108
Figure 30: Absorption Spectrum of Vapors Evolved from Military Grade TNT (Vapors Generated at 50°C)	109
Figure 31: Absorption Spectrum of Vapors Evolved from Military Grade TNT (Vapors Generated at 69°C)	110

	<u>Page</u>
Figure 32: Absorption Spectrum of Vapors Evolved from TNT (Recrystallized from Military Grade and Pumped on for 32 Hours. Vapors Generated at 60°C)	111
Figure 33: Absorption Spectrum of Vapors Evolved from Eastman 2,4,6 TNT (Vapors Generated at 42°C)	112
Figure 34: Absorption Spectrum of Vapors Evolved from Eastman 2,4,6 TNT (Vapors Generated at 60°C)	113
Figure 35: Absorption Spectrum of Vapors Evolved from Eastman 2,4,6 TNT (Pumped on Overnight. Vapors Generated at 60°C)	114
Figure 36: Absorption Spectrum of Nitroglycerine Vapor (Vapor Generated at 60°C)	115
Figure 37: Absorption Spectrum of Nitroglycerine Vapor (Vapor Generated at 79°C)	116
Figure 38: Absorption Spectrum of Diphenylamine Vapor (Vapor Generated at 24°C)	117
Figure 39: Absorption Spectrum of Diphenylamine Vapor (Vapor Generated at 45°C)	118
Figure 40: Absorption Spectrum of Monomethylamine (Room Temperature)	119
Figure 41: Absorption Spectrum of Ethyl Centralite Vapor (Vapor Generated at 76°C)	120
Figure 42: Absorption Spectrum of Cyclohexanone Vapor (Vapor Generated at 64°C)	121
Figure 43: Absorption Spectrum of Vapors Evolved from RDX (Vapors Generated at 80°C)	122
Figure 44: Absorption Spectrum of Vapors Evolved from PETN (Vapors Generated at 80°C)	123
Figure 45: Absorption Spectrum of Ethanol (Flashed 50 Times) versus Ethanol	130

	<u>Page</u>
Figure 46: Absorption Spectrum of Recrystallized TNT in Ethanol	131
Figure 47: Absorption Spectrum of Recrystallized TNT in Ethanol (Flashed 25 Times)	132
Figure 48: Absorption Spectrum of Recrystallized TNT in Ethanol (Flashed 100 Times)	133



# LIST OF TABLES

	<u>Page</u>
Table 1: Classification of Materials of Interest	43
Table 2: Physical Properties	44
Table 3: Absorption Peaks and Extinction Coefficients for the Spectra Shown in Figure 5	46
Table 4: Absorption Maxima and Extinction Coefficients of 2,4 DNT in Solvents from Pure Ethanol to Pure Water	47
Table 5: Absorption Maxima and Approximate Extinction Coefficients of 2,4 DNT in Different Solvents	47
Table 6: a) Absorption Maxima and Extinction Coefficients of Isomers of DNT in Ethanol b) Listing of the Major Peaks	48
Table 7: a) Absorption Maxima and Extinction Coefficients of Isomers of DNT in 95% Water-5% Ethanol b) Listing of the Major Peaks	49
Table 8: Shift in Absorption Caused by Addition of a Nitro Group or Methyl Group to Nitrobenzene	50
Table 9: Predicted and Observed Absorption Maxima for the Isomers of Dinitrotoluene	51
Table 10: Absorption Maxima and Extinction Coefficients of TNT	51
Table 11: Absorption Maxima and Extinction Coefficients of RDX	51
Table 12: Absorption Maxima and Extinction Coefficients of Diphenylamine	52
Table 13: Absorption Maxima and Extinction Coefficients of Ethyl Centralite	52
Table 14: Summary of the Solvent Effects on the Compound Studied	53
Table 15: Summary of Data Obtained in Vapor-Phase Absorp- tion Studies	96
Table 16: Minimum Detectable Concentrations of Explosive- Related Materials (Using the Technique Employed)	97

## INTRODUCTION

Over the past 10 years there has been a significant amount of money and effort devoted to the development of instrumentation capable of detecting the presence of explosives prior to detonation. Various analytical techniques familiar in the laboratory for detection and identification of trace quantities of materials have been examined as to their suitability for detection of the vapors emanating from explosives situated in a real-world environment. Among the methods investigated have been mass spectrometry, gas chromatography, plasma chromatography, and various types of optical spectroscopy. Recent or ongoing studies in optical spectroscopy for detection of explosive vapors have included laser optoacoustic absorption, two-photon, and Raman scattering approaches, while for detection of pollutants and other chemicals they have included infrared absorption, Raman scattering, and laser-induced fluorescence techniques.

In reviewing past spectroscopic approaches to the detection of explosive vapors, one is struck by the fact that there is a lack of fundamental information on the spectral characteristics of the gaseous molecular systems to be detected. First of all, if such information existed, it could give investigators in the area of detection a basis for predicting the probability of success of a given approach. For example, certain problems in the two-photon approach would have been apparent. More importantly, fundamental optical data would reveal any unusual spectral features of the molecular systems under study, and might

well point out techniques for inducing detectable spectral characteristics (for instance, by photodissociation of the original molecular system), either of which could be exploited in new spectroscopic detection approaches.

The detection of a wide range of vapors of explosives is a very difficult task to accomplish. The concentration of vapor available (expressed as a mole ratio of explosive vapor to air) at room temperature and under saturated vapor conditions runs from roughly a part per billion for cyclonite (RDX) to parts per million for ethylene glycol dinitrate (EGDN). In order to enhance the sensitivity of a detector it is sometimes possible to use some sort of preconcentration techniques whereby the sample reaching the detector has an increased concentration of explosive vapor. Such techniques were not considered in carrying out the current work, but could be relevant in the design of future spectroscopic instrumentation.

Some advantages of spectroscopic techniques are that a great deal of information is available almost instantaneously, and the response from different regions of the spectrum may be easily correlated to enhance specificity of detection. These features, plus the availability of tunable laser light sources and ultrasensitive detectors of light, make optical detection techniques appear very promising. What has been needed is a study to determine the fundamental optical properties in the gas phase of explosives and of the higher vapor-pressure impurities which are present in the explosives. A study of the optical properties of the impurities is required because there may be an

insufficient number of molecules of certain explosives available as a vapor for detection by any technique. Also, the presence of two or more components for a given explosive allows for a higher degree of specificity.

The purpose of the current study is to provide the needed optical data for a number of explosive and explosive-related compounds. Specifically, the systems studied include 2,3 DNT, 2,4 DNT, 2,6 DNT, TNT, nitroglycerine, diphenylamine, ethyl centralite, monomethylamine, RDX, cyclohexanone, and PETN. These materials were studied both in the vapor phase and in solution. The solution data provided important supplementary information which facilitated interpretation of the vapor-phase results.

In addition to these absorption studies, we have done some preliminary experiments on the photodecomposition of TNT in solution. This line of research can be useful in determining whether photodissociation properties of explosive materials can be utilized as a basis of detection.

## EXPERIMENTAL FACILITIES

### Absorption Spectrometer

An absorption spectrometer has been built at Boston College for the purpose of studying low-absorbing gaseous species in a wide spectral region (figure 1). Two light sources are available:

- a) A 30-watt deuterium lamp (Beckman, Mod. 9300962-80). This lamp is powered by a Beckman Mod. B "Hydrogen Lamp Power Supply."
- b) An Osram XB0-150W/1 xenon lamp housed in an Oriel Model 6137 source housing. This lamp uses an Oriel Corp. Model 8510-2 power supply. This supply has an operating current of 2.5 - 10A and an operating voltage of 12-70V.

The light beam is collimated by means of a lens and passes through a long-path cylindrical optical cell. The output beam from this cell is focused onto the entrance slit of a Spex 3/4-meter Czerny-Turner Spectrometer/Spectrograph (Model 1800).

The optical signal may be recorded on Kodak spectroscopic plates when the Spex instrument is used in the "spectrograph" mode. In order to identify the position of the spectrum, the light from a low-pressure Hg "Pen Ray" lamp (Ultra-Violet Products Corp., Calif.) is focused onto the slit of the spectrograph and recorded on the same plate before or after the experiments are performed. The characteristic Hg emission lines are previously identified by inserting interference filters with wavelengths 2852, 3500 and 5200 Å to eliminate higher-order lines.

Alternatively the beam emerging from the absorption cell can be chopped by means of a Bulova Model L-40-C tuning fork, and then focused onto the entrance slit of the Spex instrument,

operating in the "Spectrometer" (monochromator) mode. The optical signal is in this case detected by means of an EMI 9662B photomultiplier. The electric signal from this photomultiplier is sent to a Model 122 P.A.R. lock-in amplifier which in turn feeds a strip-chart recorder.

The optical cell is a cylindrical quartz tube 1m in length and 1 inch in diameter and is capped at both ends by quartz windows. The cell is also provided with two Kontes Kel-F high vacuum valves suited for vacuum applications down to  $5 \times 10^{-7}$  mm Hg and suitable for operation up to  $\sim 200^{\circ}\text{C}$ . Consequently, the design is such that the cell may be heated or evacuated. The exciting radiation is directed along the axis of cylindrical symmetry of the cell. The exiting vapor is vented into a hood.

In addition to the apparatus just described, a Cary 14 Spectrophotometer is available for absorption measurements. This instrument is designed for the automatic recording of absorption spectra in the wavelength region 1860-26000 Å with good resolving power. It is provided with interchangeable light sources:

1. a hydrogen lamp for the ultraviolet region,
2. a tungsten lamp for the visible region, and
3. a tungsten lamp for the infrared region.

It is also provided with the detectors:

1. 1P-28 RCA photomultiplier tube for the ultraviolet and visible region, and
2. a lead-sulphide cell for the infrared region.

## Flash Photolysis Apparatus I

The flash photolysis apparatus built at this laboratory has been designed for use in two complementary modes.

(a) "Flash spectroscopic mode:" the absorption spectrum of a chemical system is recorded on a film at different times after the irradiation of the sample, and (b) "kinetic spectrophotometric mode:" a particular chemical species is examined by monitoring the absorption of the species at a selected wavelength; it is used for accurate kinetic study.

### Flash Spectroscopic Mode

For convenience, the apparatus (figure 2) will be discussed according to the following units: (i) the exciting system, (ii) the analysing system, and (iii) the detecting and recording system.

#### (i) The Exciting System

The reaction cell is made of suprasil, a material which has transmission extending below 2000 Å. It consists of a cylinder of 25 cm length and 1-inch diameter with fused-on optically flat end-windows. The cell is mounted on an adjustable support at the center of a silver- and rhodium-plated metal cavity. Two high-energy micropulse flashtubes (FP - 10 or N-739, Xenon Corp.), which provide short-duration, high-intensity "photolysing" pulses of radiation in the ultraviolet region, lie on either side of the cell, approximately 2.8 cm from its axis and supported by the end plates of the cavity.

The energy for the electric discharge is given by a Model A high-energy micropulser (Xenon Corp.) which has a DC operating voltage from 0 to 10 kV and is capable of providing output energies of 100 to 2000 joules per flash with pulse widths 10 to 100  $\mu$  sec. The electric discharge is triggered by a Model C trigger module (Xenon Corp.) which provides pulses with a peak voltage of 40 kV and a rise time of 0.3  $\mu$  sec.

(ii) The Analysing System

It consists of a probing (spectral) flash light source, a light baffle 30 cm long which defines a monitoring beam of  $0.7\text{cm}^2$  cross section and two double convex quartz lenses of focal length 16.5 cm.

The light source is a "spectral" flash tube (Suntron 6C, Xenon Corp.) housed in an FH-1282 flash tube housing (Xenon Corp.). The energy is provided by a Model B spectroscopic micropulser (Xenon Corp.), with output energy 10 to 100 joules per flash, and pulse duration 5-10  $\mu$  sec. The flash tube is set to discharge with a trigger pulse which occurs at a predetermined delay setting ranging from 10  $\mu$  sec to 1 sec and is provided by a Model D delay trigger module (Xenon Corp.). This pulse has a peak output voltage of 40 kV and a rise time of 0.3  $\mu$  sec.

The probing spectral flash passes through the first lens, traverses the reaction cell and the baffle, and is then focused by the second lens onto the slit of the spectrograph.

(iii) The Detecting and Recording System

A Jarrell-Ash 3-meter Wadsworth type spectrograph (JA 78) is used; it employs a  $63 \times 41\text{ mm}^2$  grating blazed at  $4000\text{ \AA}$  with



590 lines/mm. This spectrograph is provided with a 51 cm camera and film holder which holds a 35 mm x 100 ft. roll of Kodak spectrum analysis film.

The Kodak spectrum analysis film type No. 1 is used; this film is suitable for the spectral region 2500 to 4000 Å and is able to distinguish weak absorption spectra from the heavy continuum of background radiation. The spectrograph responds quite linearly to the spectral wavelengths; i.e., 1 cm of the film corresponds to ~110 Å.

#### Kinetic Spectrophotometric Mode

When used in the kinetic spectrophotometric mode (figure 3) this apparatus also consists of three units: (i) the exciting system, (ii) the analysing system, and (iii) the detecting and recording system.

##### (i) The Exciting System

The exciting system is exactly the same as that described in the flash spectroscopic mode.

##### (ii) The Analysing System

This system consists of a constant intensity, continuous light source, an iris diaphragm, a monochromator, a light baffle and two converging lenses; the latter two components are the same as those used in the spectroscopic mode.

The continuous monitoring light is provided by a K-1 lamp (Xenon Corp. or Illumination Industries, Inc.) housed in a FH-1288 source housing (Xenon Corp.). The K-1 lamp is a high-pressure xenon point source operated at 5 amperes and 14 Volts

for the most stable output signal. This lamp is powered by two 12-Volt batteries and a control electrical circuit.

The 1/4-meter ( $f = 3.6$ ) Jarrell-Ash Ebert-type monochromator is equipped with two gratings blazed at  $3000 \text{ \AA}$  (2365 lines/mm) and  $6000 \text{ \AA}$  (1180 lines/mm).

The light passes through a lens and the iris, traverses the reaction cell and is focused onto the entrance slit of the monochromator.

For studying the species which absorb in the region 6000 to  $7000 \text{ \AA}$ , a Corning cut-off filter (C.S. 3-73) is inserted to eliminate the light with wavelengths below  $4200 \text{ \AA}$ . This ensures that the signal being detected is not the effect of a second- or third-order spectrum of other species.

#### (iii) The Detecting and Recording System

The detecting system uses a photomultiplier, with its high-voltage supply, and an oscilloscope. An EMI 9783 B photomultiplier tube (sensitive region 2000 to  $6000 \text{ \AA}$ ) is mounted in a light-tight holder on the exit slit of the monochromator; alternatively an RCA 1P-28 tube may be used. An RCA 4840 photomultiplier tube (sensitive region 2500 to  $7500 \text{ \AA}$ ) can be substituted for investigation over the 6000 to  $7000 \text{ \AA}$  region. The high voltage for the photomultiplier is provided by a Fluke Model 415 - B power supply. The output signal from the photomultiplier is fed to a Tektronix Model 564 B storage oscilloscope. The storage display is recorded by a Polaroid oscilloscope camera.

## Flash Photolysis Apparatus II

The peculiarity of this apparatus is the use of a coaxial flash lamp. This lamp, powered by a low 1.5- $\mu$ f capacitor and charged to a high voltage (up to 25 kV), can provide 500-Joule pulses down to  $\sim 1 \mu$  sec. in width. It consists of two coaxial quartz cylinders; the inner cylinder serves as a reaction cell and the annular part contains xenon gas and serves as a flash-tube. This system provides a close optical coupling between the photolysing source and the sample. The reaction cell has a length of 33 cm and a diameter of 1.6 cm, and has two removable, optically flat quartz windows at each end. Thus, it can be connected to another identical flashlamp in series if a double cell length is desired.

The outside wall of the flashlamp is covered with a highly reflective metal coating so as to maximize the light incident on the sample. The cell is air-tight and is connected to a vacuum system through two glass joints near each end. The electric pulse for the lamp is provided by a low impedance electric driver unit.

The probing light source consists of a high-pressure xenon arc lamp (K-1 lamp, Xenon Corp.) operated normally at 5 amperes and 14 Volts, and powered by two 12-Volt batteries. The absorption is monitored at different wavelengths with the Spex 3/4-meter Czerny-Turner Spectrometer/Spectrograph cited earlier.

The detection system uses a 1P-28 photomultiplier tube with its high-voltage power supply (Fluke 415-B), and a Tektronix 535-A

oscilloscope. The display on the oscilloscope is then recorded by using a Polaroid camera.

The 3/4-meter Spex instrument can be used as a monochromator in the mode described above or as a spectrograph when a photograph detection is desired.

### Fluorescence Apparatus

Several fluorescence studies of laser systems are currently under way at Boston College. The facilities in the fluorescence laboratory allow one to obtain fluorescence spectra, excitation spectra, and pulsed fluorescence data for the systems under study.

The fluorescence spectra of the samples are obtained by exciting the samples with the light from a Sylvania DVY 650 W tungsten halogen lamp, passed through a  $\text{CuSO}_4$  filter. The fluorescence is observed at  $90^\circ$  to the direction of excitation, chopped, and focused onto the entrance slit of a Model 2051 McPherson 1-m scanning monochromator. Optical signals are detected by an RCA 7102 (S-1) photomultiplier tube cooled by crushed dry ice, and amplified by a Model 122 P.A.R. lock-in amplifier. An RCA 7265 (S-20) photomultiplier is also available. In the infrared region, a lead-sulphide detector and a built-in preamplifier replaces the photomultiplier tube.

Pulsed fluorescence measurements are made by using EG & G FX-12 or FX-33 flash tubes, and observing the fluorescence at right angles through an interference filter and a lead-sulphide detector or an RCA 7102 or an RCA 7265 photomultiplier tube.

The detector is housed in a light-tight enclosure. The fluorescence decay is observed and photographed on a Tektronix 533 oscilloscope.

The excitation spectra are obtained by selectively pumping the samples by means of a Model 82-410 Jarrell-Ash monochromator and detecting the fluorescence output through an interference filter. A Sylvania DVY 650 W tungsten halogen lamp is used as the exciting source. Three gratings are available for use with this monochromator: the first has 2365 lines/mm and is blazed at 3000 Å; the second has 1180 lines/mm, blazed at 6000 Å; the third has 590 lines/mm, and is blazed at 1.2μ. The resolutions are given by:

	500μ slits	2000μ slits
3000 Å blaze	~16 Å	~50 Å
6000 Å blaze	16 Å	50 Å
1.2μ blaze	35 Å	145 Å

#### Dye-Laser Apparatus

A Molelectron Dye Laser Model DL-12 pumped by a Molelectron UV-12 (250 kW) N<sub>2</sub> laser is available for spectroscopic measurements. This laser can deliver pulses of duration down to 7 nsec. at repetition rates 1-50 pps. The laser output is monochromatic to within 0.1 Å (at 4600 Å). The spectral region covered with 16 dyes is 3600-7400 Å.

The detection of the optical signal following the laser excitation of the samples is accomplished by a P.A.R. Model 164 gated integrator whose output feeds a P.A.R. Model 162 boxcar averager.

The combination dye-laser/boxcar integrator allows a wide variety of measurements such as absorption, fluorescence, excitation, lifetime and time-resolved spectroscopy.

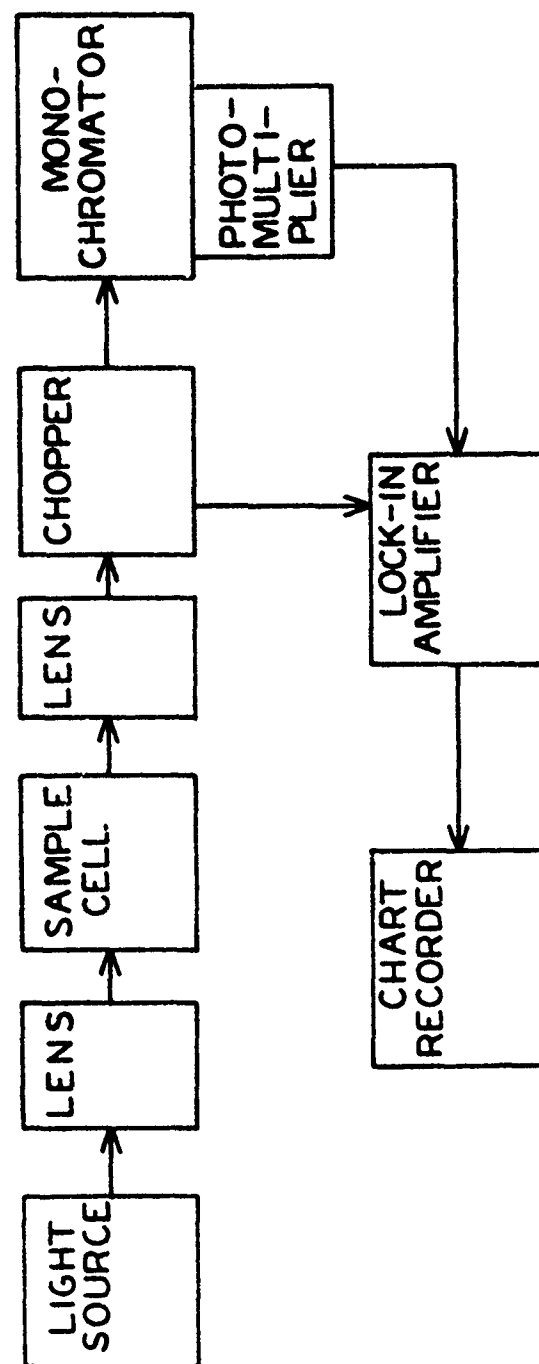


Figure 1: Layout of the Absorption Apparatus Operating in the "Spectrometer" Mode

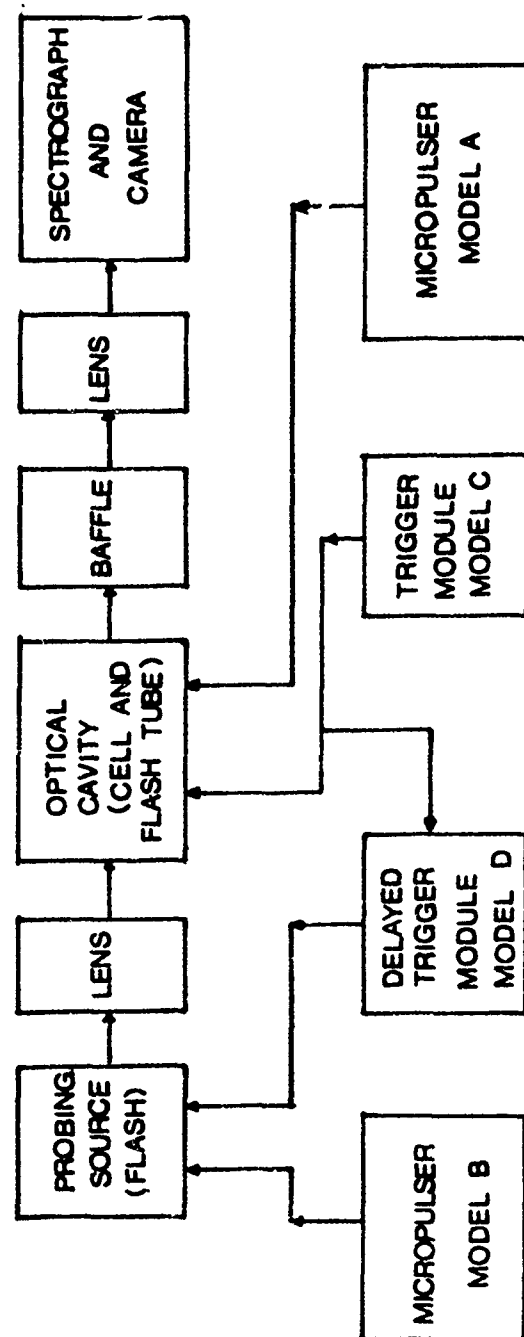


Figure 2: Layout of the Flash Photolysis Spectroscopy



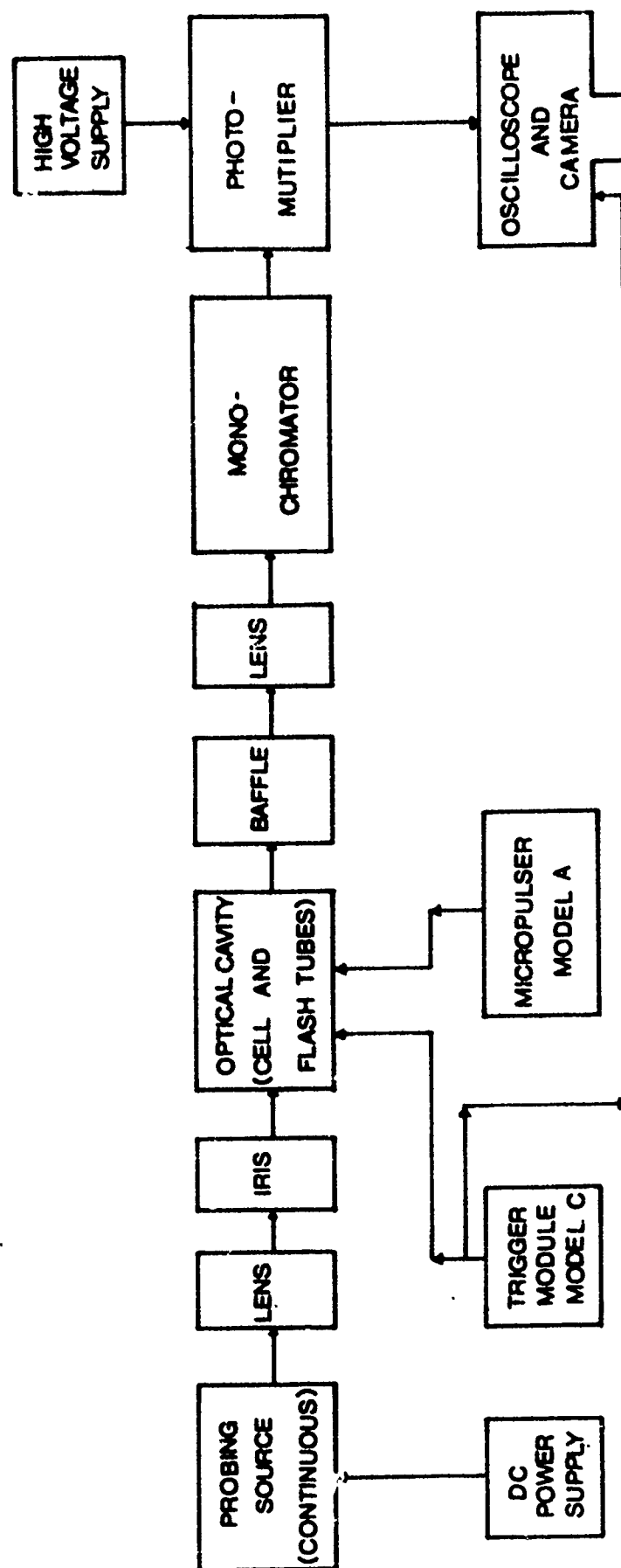


Figure 3: Layout of the Kinetic Spectrophotometer

## SPECTRA OF EXPLOSIVE MATERIALS IN SOLUTION

### Introduction

This section presents absorption data for several explosives or explosive-related materials in solution. The materials investigated are: benzene, toluene, isomers of dinitrotoluene (DNT); 2,4,6 trinitrotoluene (TNT); 1,3,5 triazinehexahydro 1,3,5 trinitrocyclohexane (RDX); diphenylamine (DPA), ethyl centralite (EtC); nitroglycerine (NG); and pentaerythritol-tetranitrate (PETN). The molecular formulae of these materials are shown in figure 4.

Of these materials, benzene and toluene were investigated because they are the structural core of the DNT's and TNT. Thus, comparison of the spectra of benzene and toluene with the nitrotoluenes reveals interesting information about the effect of the  $-\text{NO}_2$  groups on the absorption. Aside from benzene and toluene, the remaining materials are all either explosive or present in explosive materials. Their common denominator is that they contain nitrogen. Since the nitrogen is believed to form the basis for the energetic behavior of these materials, it is interesting to classify them according to the type of nitrogen they contain. The compounds fall into three classes: (a) compounds which are basically amines, (b) compounds containing one or more nitro ( $-\text{NO}_2$ ) groups and (c) compounds containing one or more nitroxy ( $-\text{ONO}_2$ ) groups. These are listed in table 1. This classification will be useful when we begin to analyze the electronic band structure of these compounds. Also, for reference, table 2 lists the physical properties of the materials of interest.

### Experimental Details

All spectra were run on a Cary 14 spectrophotometer in one-centimeter quartz cells. Unless otherwise noted, all solids were recrystallized twice in either toluene or ethanol and pumped on to remove the solvent. 2,4 DNT was recrystallized in toluene, all other DNT's in ethanol; TNT was recrystallized in ethanol; RDX was obtained pure from Dr. Lyle Malotky, Naval Explosive Ordnance Disposal Facility, Indian Head, Maryland, and used without further purification; DPA was obtained "Baker Analyzed" from J. T. Baker and used without further purification; EtC was twice recrystallized in ethanol; NG was obtained on  $\alpha$ -lactose and used without separation; and PETN was obtained in detonation cord as pure PETN and used without further purification. Both benzene and toluene were ordered spectropure from Baker and used without further purification. The solvents used are either ethanol (which was ordered spectropure for ultraviolet spectroscopy from Baker and was used without further purification), distilled water, ACS certified spectroanalyzed isobutanol, or ACS certified spectroanalyzed 2-propanol as noted. The 5% ethanol-95% water solutions were prepared by dissolving the sample in ethanol to make a solution 20 times more concentrated than desired, filling 5% of the volume of a volumetric flask with this solution and, finally filling the flask with distilled water.

We note that although water is transparent throughout the ultraviolet region, ethanol is not. When the solvent begins to absorb strongly, it can mask out some absorption of the solute. Thus, the spectra obtained in 95% water-5% ethanol are accurate down to 1900  $\text{\AA}$  while those in ethanol are only accurate down to about 2050  $\text{\AA}$ .

## Analysis of the Spectra

### Benzene, Toluene, 2,4 DNT and 2,4,6 TNT in Ethanol

The first group of spectra is shown in figure 5 and consists of benzene, toluene, 2,4 dinitrotoluene (DNT) and 2,4,6 trinitrotoluene (TNT), each in ethanol. The peaks and extinction coefficients for these spectra are listed in table 3. (The table includes relevant data from the literature.<sup>(1,2)</sup>) These spectra indicate the effect of various substituents on the absorption of the benzene ring. Looking first at benzene (figure 5.a) we see a structured absorption between 2350 and 2600 Å and a second, very intense absorption below 2150 Å. A comparison of the spectrum of toluene with that of benzene indicates the effect the -CH<sub>3</sub> group has on the absorption. Figure 5.b shows that toluene also has a structured absorption from 2500 to 2700 Å, the extinction coefficient of which is comparable to that of benzene. The difference in the shape of the structure seems to be mainly due to an alteration in the intensity of the benzene bands. Toluene also has an intense band below 2200 Å. (The CRC Handbook<sup>(1)</sup> lists its peak at 2070 Å with log  $\epsilon$  = 3.97.) (Note: Because ethanol begins to absorb very strongly at 2000 Å, it is not possible to make an accurate determination of this peak on our apparatus.)

---

(1) CRC Handbook of Chemistry and Physics, CRC Press, 57th Ed. (1976-1977).

(2) W. A. Schroeder, P. E. Wilcox, K. N. Trueblood, and A. O. Dekker, Anal. Chem. **23**, 1740 (1951).

Comparison of DNT with toluene indicates the effect of the  $\text{-NO}_2$  groups on the absorption. Figure 5.c shows that the effect is very marked, washing out all structure, broadening the absorption, and increasing its intensity by about two orders of magnitude. It is strongly suspected that the structured ring absorption of benzene and toluene is still present, however, it is masked by the much more intense absorption in this region. DNT also has an absorption near  $2000 \text{ \AA}$ , but this absorption is difficult to observe in ethanol. Previous authors (see reference (3) and references therein) have interpreted the  $2410 \text{ \AA}$  band of DNT as corresponding to the  $2000 \text{ \AA}$  band of benzene; this interpretation is reasonable based on the similar behavior of nitrobenzene and the fact that the nitro group is known to exert a strong influence on ring properties.<sup>(4)</sup> This  $2410 \text{ \AA}$  band, therefore, is the so-called "First Primary Band," which characteristically possesses an extinction coefficient  $\sim 10^4 \text{ l/mole-cm}$ . This identification explains the large difference between the extinction coefficients for benzene and 2,4 DNT in the  $2500 \text{ \AA}$  region. The absorption band residing below  $2100 \text{ \AA}$  in the 2,4 DNT spectrum may be due to either the Second Primary Band or the  $\text{NO}_2$  groups themselves. (The Second Primary band is related to the  $1800 \text{ \AA}$  band of benzene. It is not uncommon in

---

(3) T. Abe, Bull. Chem. Soc. Japan 31, 904 (1958).

(4) H. H. Jaffé and M. Orchin, Theory and Applications of Ultraviolet Spectroscopy (John Wiley and Sons, Inc., New York, 1962) ppg. 255-257.

substituted benzenes for this band to extend into the 2000 Å region<sup>(5)</sup>). The Secondary Band in 2,4 DNT (which would correspond to the benzene fingers) is essentially completely masked by the intense First Primary Band. This is the reason no sharp line absorption is seen in the 2,4 DNT spectrum. Finally, the comparison of DNT with TNT indicates the effect of adding yet another -NO<sub>2</sub> group. As with DNT, the absorption spectrum presents a broad band. Compared with the band of DNT, the broad band in TNT is shifted to higher energies and is more intense by about one-third. Again, the peak near 2000 Å seems to be present, but is out of our reach.

In summary, all four samples exhibit an absorption below 2100 Å, although the origins are different. Some interesting contrasts are evident in the 2200 to 2700 Å region. In this region, benzene has a relatively weak ( $\log \epsilon = 2.2 - 2.4$ ), structured absorption, toluene has a similarly weak ( $\log \epsilon = 2.2 - 2.5$ ) and slightly less structured absorption, DNT has a fairly strong ( $\log \epsilon = 4.2$ ) and broad absorption, while TNT has a similarly broad and somewhat stronger ( $\log \epsilon = 4.3$ ) absorption. As has been mentioned, the presence of the nitro groups plays an important role in masking the structured absorption.

#### 2,4 DNT in Solvents from Pure Ethanol to Pure Water

The second group of spectra consists of 2,4 dinitrotoluene (DNT) in various mixtures of ethanol and water (shown in figures

(5)

Op. Cit., pg. 243.

6.a - d and figure 7). The peak positions and absorption coefficients are summarized in table 4. Notice that the peak of the absorption shifts by  $\sim 100 \text{ \AA}$  in going from pure water to pure ethanol. In addition, the shift appears to be a linear function of the percent water in the solution. This is thought to be due to the polar nature of water: water is more polar than ethanol and thus forms stronger hydrogen bonds with the solute molecules (in this case, the DNT molecules). The effect on the DNT is to pull the electrons out from the ring toward the  $-\text{NO}_2$  groups. It is known<sup>(6)</sup> that such an inductive effect lowers the electron density of the benzene ring and hence lowers the absorption energy. We will have more to say about this effect in the section on general conclusions.

#### 2,4 DNT in Isobutanol and 2-Propanol

As further evidence that the solvation shift observed above for 2,4 DNT is due to the more polar nature of water (compared with ethanol), we dissolved 2,4 DNT in two other solvents which are also less polar than water, namely isobutanol and 2-propanol. Since these two solvents have polarity closer to that of ethanol than to that of water, we expect to observe absorption maxima nearer to that in ethanol. As shown in figure 8 and summarized in table 5, our expectation is correct. In isobutanol the maximum is at  $2390 \text{ \AA}$  while in 2-propanol it is at  $2395 \text{ \AA}$ ; both of these values are closer to  $2410 \text{ \AA}$  than to  $2520 \text{ \AA}$ . It should be noted that 2,4 DNT does not readily dissolve in either isobutanol or 2-propanol and hence an accurate determination of the

---

(6) C. P. Conduit, J. Chem. Soc., 3273 (1959).

concentration is not possible. Thus, no significance should be attached to the difference in the calculated extinction coefficients in these solvents.

#### Isomers of DNT in Ethanol

The fourth group of spectra shows the absorption of five of the six isomers of DNT. (The 3,5 isomer is missing because we were unable to find a source for it.) This group of spectra indicates how the position of the  $\text{-NO}_2$  groups on the ring affects the absorption position and intensity.

We would like to begin the discussion of these spectra by making two general observations about them. First, notice that not only the peak position, but also the general shape of the spectrum varies greatly from one isomer to another. Secondly, notice that while some isomers exhibit fairly well-defined peaks (e.g., 2,4 and 2,5) others merely have shoulders (e.g., 2,3 and 3,4). Thus, in a few cases, it is difficult to unambiguously assign the position of the absorption maximum. In these ambiguous cases we have identified the peak which most closely corresponds to the literature values.<sup>(1,6)</sup> In Conduit's work, for example, he considers only the most intense maxima in the 2100-2800 Å region, and assumes these to correspond with the First Primary Band of benzene. In the case of 2,3 DNT, however, he treats this intense band as residing below 2100 Å, despite the presence of a maximum at ~2600 Å (see figure 9.a). This is justifiable for two reasons.



(1) The band at  $\sim 2600 \text{ \AA}$  has an extinction coefficient of  $\sim 5800 \text{ l/mole-cm}$ . This is rather weak for a First Primary Band, whose typical extinction coefficient is  $\sim 10,000\text{-}20,000 \text{ l/mole-cm}$ . (Note the extinction coefficients calculated for the other isomers.) (2) His model for explaining the band shifts works well for the other five isomers of DNT. When this model is applied to 2,3 DNT, it predicts a band position below  $2100 \text{ \AA}$ .<sup>(6)</sup> Based on these considerations, we will follow the assignments of Conduit in discussing the isomer shifts.

The spectra we have obtained in ethanol are shown in figures 9.a - e and the data summarized in table 6. Notice that the variation in intensity from one isomer to another is not very great. ( $\epsilon$  varies from 17,300 to 8,900). The position of the maximum absorption, however, varies by  $550 \text{ \AA}$ . The energy of the maximum increases along the series 2,5 to 3,5 to 2,4 to 2,6 to 3,4 to 2,3.<sup>(6)</sup> A similar variation is seen for the isomers of DNT in water and we postpone discussion of this isomer shift until the next section.

#### Isomers of DNT in 95% Water-5% Ethanol

As in the preceding section, this group of spectra (shown in figure 10) shows the absorption of five of the six isomers of DNT. In contrast to the last set, this set has the isomers dissolved in a mixture of 95% water-5% ethanol. This mixture was chosen instead of pure water because the isomers of DNT do not readily dissolve in water, yet this solvent is close to pure water. Our work with 2,4 DNT indicates that the spectrum in this mixture is indeed very close to that in pure water.

As with the spectra of the isomers in ethanol, this set of spectra indicates how the position of the  $\text{-NO}_2$  groups affects the energy of the absorption. As has been mentioned, this effect has been analyzed by Conduit<sup>(6)</sup> who looked at the absorption spectrum of the isomers of DNT in 5% ethanol-95% water and reported a single intense maximum in the 2100-2800 Å region. (This absorption was accompanied by one or more "inflections" on the long-wavelength side.) The exact position of this maximum depends on the precise compound considered. If nitrobenzene is taken as the parent, the absorption of the other compounds can be analyzed as shifts from the nitrobenzene absorption. In this way, three conclusions can be drawn:

- (a) A pair of  $\text{NO}_2$  groups reduces conjugation to the benzene ring by competition. The magnitude of the reduction depends on the ring position of each group.
- (b) A pair of  $\text{NO}_2$  groups (and to a lesser extent, an  $\text{NO}_2$  group and a methyl group) hinder each other sterically so that neither can be coplanar with the ring.
- (c) Methyl groups enhance conjugation of nitro groups except for ortho-nitro groups. In the latter the enhancement is canceled due to steric hindrance.

Thus, we have a method to predict where the various isomers of DNT will absorb.

Quantitatively, we can deduce the magnitude of the shift for various substituents by looking at the dinitrobenzene and the nitrotoluenes. The magnitudes of the shifts and the corre-

sponding reasons are listed in table 8. Then, crudely assuming that the effects are additive, one can predict the position of the absorption for the dinitrotoluenes. These are listed in table 9 which indicates that Conduit's model<sup>(6)</sup> does a fairly good job of predicting the absorption maxima. An understanding of this shift is important because the same electronic factors are responsible for the observed solvent shifts not only in the dinitrotoluenes, but also in the other materials investigated. Basically, an enhanced conjugation between the substituent and the benzene ring means that the electronic density is spread out over a larger area, i.e., the benzene ring plus the substituent. A larger area for the electronic cloud implies more closely spaced energy levels and hence a lower energy required for excitation to the first excited state. It is well known<sup>(7)</sup> that an  $\text{-NO}_2$  group withdraws electronic charge density from the benzene ring and competes with another  $\text{-NO}_2$  group. We shall refer to this argument again in the general remarks section of this chapter.

A final observation should be made about the isomers of DNT. Notice that all isomers show evidence of an absorption between 1900 and 2000 Å. Although the exact position and extinction coefficient are sometimes difficult to accurately deduce (particularly in ethanol which begins to absorb rather strongly in this region) there is little doubt that an absorption does exist in this region. As we have pointed out earlier,

---

(7) See any introductory organic chemistry text, e.g., Morrison and Boyd, Organic Chemistry (Allyn and Bacon, 1967).

this may be due to the Second Primary Band, or to the  $\text{NO}_2$  groups themselves. The second absorption at lower energy is the First Primary Band; this band apparently overwhelms the structured secondary band in the same general region. Such a phenomenon is also observed in nitrobenzene. (4) A quantitative explanation of these effects awaits a full molecular orbital calculation of the spectrum.

#### Three Purities of TNT Examined

In our efforts to obtain information on the spectra of explosives and explosive-related materials, we have obtained three different purities of TNT: (1) Military grade or crude TNT, (2) recrystallized military grade TNT, and (3) Eastman pure 2,4,6 TNT. A gas chromatograph of the Eastman TNT indicates no contamination with any of the isomers of DNT nor with other isomers of TNT. Our solution spectra (figure 11) indicate that the military grade TNT definitely has some impurities in it. (Gas-phase spectra -- to be discussed later -- indicate that at least part of the contamination is due to toluene.) On the other hand, our solution data show no difference between the recrystallized TNT and the Eastman pure 2,4,6, TNT. (The Eastman TNT was used without further purification.)

#### TNT in Ethanol and 95% Water-5% Ethanol

This group of spectra, (shown in figure 12) and indeed the rest of the spectral groups in this report, indicate the effect of the solvent (either ethanol or water) on the intensity and position of the peak of compounds relevant to our work.

This particular group examines trinitrotoluene (TNT). As shown in figure 12 and summarized in table 10, the extinction coefficient for TNT is slightly greater in ethanol than in 95% water-5% ethanol. At the same time, the absorption maximum is shifted to lower energy by 80 Å in 95% water-5% ethanol. This trend will be commented on in the general remarks at the end of this section.

#### Absorption Spectrum of RDX

The next pair of spectra, presented in figure 13 shows the absorption of RDX in both solvents (ethanol and 95% water-5% ethanol). As summarized in table 11, the extinction coefficient of RDX in 95% water-5% ethanol is slightly greater than in pure ethanol. This is opposite to the trend of the other materials and is certainly much less significant than the change of the overall spectrum of RDX in going from one solvent to another. In ethanol, RDX resembles TNT except for a strong, but not very well defined band at higher energy. In 95% water, this band is seen more clearly; the lower-energy absorption also becomes slightly narrower and shifts to lower energy by ~70 Å. Orloff, Mullen, and Rauch<sup>(8)</sup> have done a complete molecular orbital calculation for RDX and assigned the lower-energy absorption to a  $n \rightarrow \pi^*$  transition, while the higher-energy one is mainly  $\pi \rightarrow \pi^*$ .

---

(8) M. K. Orloff, P. A. Mullen, and F. C. Rauch, J. Phys. Chem. 74, 2189 (1970).

It is useful to compare RDX to TNT. At first glance, it appears as though RDX and TNT should be very similar; the carbons of RDX are four-fold coordinated, however, the nitrogen in the ring introduces a lone pair of electrons. Thus, RDX satisfies the  $4n + 2$  Hückel rule for aromaticity. However, both the above molecular orbital calculation and X-ray diffraction data<sup>(9)</sup> indicate that RDX is non-planar and, therefore, lacks the aromatic  $\pi$  electron cloud. Thus, RDX cannot exhibit a benzene-like  $\pi \rightarrow \pi^*$  transition. Nevertheless, RDX can and does exhibit an absorption involving the  $-\text{NO}_2$  groups. Hence, the RDX absorption resembles that of TNT because they both contain  $-\text{NO}_2$  groups.

#### Absorption Spectrum of Diphenylamine

The next set of spectra (figure 14) shows the absorption of diphenylamine (DPA). DPA represents a very interesting case for several reasons: the extinction coefficient is significantly lower, the spectrum is much broader, and the absorption maximum is at a higher energy in 95% water-5% ethanol (see table 12). The higher energy is particularly interesting because it is in contrast to our previous samples which absorb at lower energy in 95% water. More will be said about this in the general remarks section. For now, we merely note that DPA is an amine, while the previously studied compounds have all been nitro-containing compounds.

---

(9) P. L. Marinkas, "Luminescence Properties of RDX and HMX," Picatinny Arsenal Technical Report No. 4840, August, 1975.

As a final note on DPA, we would like to point out that the absorption in 95% water is not weaker than in ethanol, because although the extinction coefficient is smaller, the band is significantly wider. Thus, the integrated intensity remains the same.

#### Absorption Spectrum of Ethyl Centralite

Like diphenylamine, ethyl centralite (EtC) is an amine. Thus, it is not surprising to see the absorption maximum shift to higher energy in 95% water when compared to ethanol (see figure 16). Notice that EtC also has a significantly lower extinction coefficient in 95% water and, like DPA, the absorption peak is broader in 95% water. (See table 13 for a summary of the data on EtC.) We will say more about these trends in the final section.

#### Absorption Spectra of Nitroglycerine and Pentaerythritoltetranitrate (PETN)

We are discussing these two compounds, nitroglycerine (NG) and pentaerythritoltetranitrate (PETN), together because the similarity of their spectra. Figure 17 shows the absorption spectrum of NG, while figure 18 shows that of PETN. Both are characterized by a near zero absorption until  $\sim 2300 \text{ \AA}$ , where the absorption begins to sweep up strongly. This similarity is perhaps due to the fact that both are nitroxy compounds as contrasted with the nitro and amine compounds discussed previously. It should also be noted that in the NG spectra of figure 17, there appears to be a weak band in the 2300-3000  $\text{\AA}$  region.

Its presence is especially evident in the ethanol solution (figure 17a). This feature was also observed in the vapor spectra and will be discussed later. There is evidence of the same behavior for PETN in figure 18.

#### General Remarks

In this section we want to make a few general remarks about the absorption spectra of the compounds investigated. For these general remarks we will refer again to the classification of the compounds given in table 1. We will begin with a few remarks about the absorption spectra and then will look fairly closely at the solvent shift.

Looking at the classification and at the spectra, we notice that the amines and the nitro compounds show a maximum between 2000-2900 Å, while the nitroxy compounds show no maximum and indeed little absorption in most of the ultraviolet region. This is an important observation because it indicates that the nitroxy compounds, which interfere with some detection techniques, should be much less of a problem for a detection technique based on ultraviolet absorption.

We now look more closely at the solvent shift. This shift is summarized in table 14 and refers to the difference in the absorption maximum in ethanol and 95% water-5% ethanol. First, notice that everything except RDX absorbs more strongly in ethanol than in water. (Note that the RDX spectrum is also somewhat narrower in water which would make the extinction



coefficient somewhat larger than in ethanol). Second, notice that the nitro compounds all shift to lower energy in 95% water-5% ethanol while the amine compounds shift to higher energy. We will now discuss these in order ---first the nitro compounds, then the amines.

First a few general remarks about the solvent. Water is a more polar solvent than ethanol, showing a higher degree of hydrogen bonding. This hydrogen bonding perturbs the electronic environment of the  $\text{-NO}_2$  groups increasing conjugation to the ring, providing a larger area for the electronic charge density, and a lower-energy absorption. A corollary of this reduced electronic charge density is a reduced absorption intensity which is what we see in all nitro compounds with the minor exception of RDX which has fairly nondistinct peaks.

Looking now at the amines, we see a rather different solvation effect. First, the absorption is at a higher energy in water and second the absorption is much broader in water, thus leading to a lower extinction coefficient in this solvent. Hence, the lower extinction coefficient in water is due to a broadening of the absorption rather than to diffuseness of the electronic cloud.

Since the solvation shift in the nitro compounds appears to be due to hydrogen bonding between the solvent water and the oxygen atoms of the  $\text{-NO}_2$ , one is tempted to attribute the opposite shift in the amines to another force, discounting the ability of the amines to hydrogen-bond. However, Ito<sup>(10)</sup>

---

(10) M. Ito, J. Mol. Spectroscopy 4, 106 (1960).

has taken advantage of temperature effects to show that DPA does show hydrogen bonding in an ethanol solution. Furthermore, he has shown that increasing the hydrogen bonding leads to the usual shift to longer wavelengths. Thus, the difference in the solvation effect of ethanol and water on DPA is due to an additional force beyond the hydrogen bonding. (For further insight into the degree of hydrogen bonding between water and DPA, it would be interesting to see what effect temperature has on the spectrum.) It is clear that such an additional effect is present because of the marked broadening in water compared to ethanol.

Notice that the solvation effects, both broadening and shifting, are much less pronounced in EtC than in DPA. This may indicate that the electronic transition involved is associated with the nitrogen. This is because the nitrogen in EtC is sterically much more protected than in DPA, and therefore less susceptible to solvent perturbation. The precise mechanism for this shift awaits further study.

### Conclusions

We make the following general conclusions based on our observations. (1) Nitroxy compounds are not expected to exhibit a maximum in the near ultraviolet and should not interfere with the near U.V. absorption of other explosives. (2) Nitro compounds will absorb in the near U.V. and will exhibit a shift towards longer wavelengths in water compared to ethanol. Finally, (3) amine compounds will also exhibit a maximum in the near U.V., but will show a shift towards shorter wavelengths in water compared to ethanol.

TABLE 1

Classification of Materials of Interest According to Type

Class (a) - Basically amines

- diphenylamine
- ethyl centralite

Class (b) - Nitro compounds

- Isomers of DNT (dinitrotoluene)
- TNT (trinitrotoluene)
- RDX (1, 3, 5 trinitro 1, 3, 5 triazacyclohexane)

Class (c) - Nitroxy compounds

- NG (nitroglycerine)
- PETN (pentaerythritoltetranitrate)

substance	molecular weight	physical form	melting point (°C)	boiling point (°C)	density	w	solubility	Al	eth	ace	bz	other
NG												
nitroglycerine	227.09	col.-yel. liq $\eta=1.482$	2, 13	125 256 exp	1.5931	6	s	s	∞	v	v	MeOH CS <sub>2</sub>
DPA												
diphenylamine	169.23	col. monoc. leaf.	54-5	302	1.160	1	v	s	s	v	v	Py, CCl <sub>4</sub> AcOEt
EtC												
ethyl centralite	268.36		73	----	----	1	v	...	...	...	...	...
methylamine	31.06	col. gas $\eta=1.432$	-93.5	-6.3	.699	v	s	s	∞	s	s	s
RDX												
1, 3, 5 triazinehexahydro-	222.12											
1, 3, 5, trinitrocyclohexane		(I) ortho. (II) unat.	205-6	----	1.82	1	1	1	6	s	1	MeOH, AcOEt, 6, CCl <sub>4</sub> , CS <sub>2</sub> , 1 A.A.
TNT												
2, 4, 6 trinitrotoluene	227.13	col. mono.; rh. f. al.	82	240 exp.	1.654	1	6	s	s	v	v	tol Py.
2, 4 dinitrotoluene	182.14	yel. nd. f. al. or CS <sub>2</sub> , $\eta=1.442$ 1.662; 1.756	71	300	1.3208	1	s	s	s	v	s	tol, Py CS <sub>2</sub> , AcOEt
2, 5 dinitrotoluene	182.14	need. f. al.	52.5	----	1.282	----	s	----	s	----	s	CS <sub>2</sub> v
2, 6 dinitrotoluene	182.14	rh. need. $\eta=1.479$ ; 1.669, 1.734	66	----	1.2833	----	s	----	s	----	----	----
3, 4 dinitrotoluene	182.14	yel. need. f. CS <sub>2</sub>	58.3	----	1.2594	1	s	----	s	----	----	CS <sub>2</sub> s
3, 5 dinitrotoluene	182.14	yel. mono. need. f. w.	93	sub.	1.2772	6	s	s	s	----	s	CS <sub>2</sub>
PETN												
pentaerythritol tetra- nitrate	316.15		140-1	----	1.773	6	6	6	6	v	s	tol., Py MeOH

Abbreviations used in Table  
of Physical Properties

A.A.	acetic acid
ace	acetone
AcOEt	$\text{CH}_3\text{COC}_2\text{H}_5$
Al	alcohol
Alk	alkali
bz	benzene
col	colorless
c	cold
d	decomposes
eth	ether
exp	explodes
f	from
i	insoluble
leaf	leaflets
liq	liquid
MeOH	methanol
mono	monoclinic
need, nd	needles
ortho	orthorhombic
pl	plates
Py	Pyrimidine
rh	rhombic
s	soluble
sub	sublimes
tol	toluene
tricl	triclinic
unst	unstable
v	very soluble
w	water
yel	yellow
$\delta$	slightly soluble
n	refractive index
$\infty$	soluble in all proportions

TABLE 3

Absorption Peaks and Extinction Coefficients for the Spectra  
Shown in figure 5.

(a) Peaks of Benzene

<u><math>\lambda</math> max. (<math>\text{\AA}</math>)</u>	<u>O.D.</u>	<u><math>\log \epsilon</math></u>	literature <sup>(1)</sup>	
			<u><math>\lambda</math> max. (<math>\text{\AA}</math>)</u>	<u><math>\log \epsilon</math></u>
2600	0.40	2.25	2610	2.2
2540	0.63	2.45	2560	2.4
2480	0.51	2.36	2490	2.3
2420	0.32	2.15	2430	2.2
2370, 2380	0.20	1.95		

(b) Peaks of Toluene

<u><math>\lambda</math> max. (<math>\text{\AA}</math>)</u>	<u>O.D.</u>	<u><math>\log \epsilon</math></u>	literature <sup>(1)</sup>	
			<u><math>\lambda</math> max. (<math>\text{\AA}</math>)</u>	<u><math>\log \epsilon</math></u>
2680	0.47	2.40		
2640	0.35	2.27		
2610	0.52	2.44	2600	2.48
2590	0.43	2.35		
2550	0.38	2.31		

(c) Peaks of 2, 4 DNT

<u><math>\lambda</math> max. (<math>\text{\AA}</math>)</u>	<u>O.D.</u>	<u><math>\epsilon</math></u>	<u><math>\log \epsilon</math></u>	literature <sup>(2)</sup>	
				<u><math>\lambda</math> max. (<math>\text{\AA}</math>)</u>	<u><math>\epsilon</math></u>
2410	0.84	15,300	4.18	2390 - 2420	14,280

(d) Peaks of 2, 4, 6 TNT

<u><math>\lambda</math> max. (<math>\text{\AA}</math>)</u>	<u>O.D.</u>	<u><math>\epsilon</math></u>	<u><math>\log \epsilon</math></u>	literature <sup>(2)</sup>	
				<u><math>\lambda</math> max. (<math>\text{\AA}</math>)</u>	<u><math>\epsilon</math></u>
2230	0.45	20,500	4.31	2270	19,700

TABLE 4

Absorption Maxima and Extinction Coefficients of 2, 4 DNT in Solvents from Pure Ethanol to Pure Water

<u>% Ethanol</u>	<u><math>\lambda</math> max. (<math>\text{\AA}</math>)</u>	<u>O.D.</u>	<u><math>\epsilon</math></u>	<u><math>\log \epsilon</math></u>
100	2410	0.84	15,300	4.18
75	2430	0.84	15,300	4.18
50	2450	0.87	15,800	4.20
10	2510	0.81	14,800	4.17
0	2520	1.30	Concentration not determined	

TABLE 5

Absorption Maxima and Approximate Extinction Coefficients of 2, 4 DNT in Different Solvents

<u>Solvent</u>	<u><math>\lambda</math> max. (<math>\text{\AA}</math>)</u>	<u>O.D.</u>	<u><math>\epsilon</math></u>	<u><math>\log \epsilon</math></u>
isobutanol	2390	0.90	16,400	4.21
2-propanol	2395	0.78	14,200	4.15

TABLE 6

(a) Absorption Maxima and Extinction Coefficients of Isomers of DNT in Ethanol.

Isomer	$\lambda$ (Å)	O.D.	$\epsilon$	$\log \epsilon$	literature (2)	
					$\lambda$ (Å)	$\log \epsilon$
2,3	†2540	0.32	5,800	3.76	---	---
	<2050	≥0.95	≥17,300	≥4.24	---	---
2,4	2410	0.84	15,300	4.18	2390-2420	4.15
	<2050	>0.60	----	---	---	---
2,5	2580	0.57	10,500	4.02	---	---
	<2050	>0.95	----	---	---	---
2,6	*2800	0.06	1,100	3.04	---	---
	†2300	0.49	8,900	3.95	---	---
3,4	*2600	0.27	4,900	3.69	---	---
	†2100	0.63	11,500	4.06	---	---
3,5	---	---	----	---	---	---

(b) Listing of the Major Peaks.

Isomer	$\lambda$ (Å)	O.D.	$\epsilon$	$\log \epsilon$
2,3	<2050	≥0.95	≥17,300	≥4.24
2,4	2410	0.84	15,300	4.18
2,5	2580	0.57	10,500	4.02
2,6	†2300	0.49	8,900	3.95
3,4	†2100	0.63	11,500	4.06
3,5	---	---	----	---

†Approximate, peak not well defined.

\*Shoulder.



TABLE 7

(a) Absorption Maxima and Extinction Coefficients of Isomers of DNT in 95% Water-5% Ethanol.

					literature (6)	
Isomer	$\lambda$ (Å)	O.D.	$\epsilon$	$\log \epsilon$	$\lambda$ (Å)	$\log \epsilon$
**2,3	†2625	0.30	5,500	3.74	---	---
	2000	0.85	15,500	4.19	<2100	---
* 2,4	*2510	*0.81	*14,800	*4.17	2520	4.15
	†1980	0.60	10,900	4.04	---	---
2,5	2640	0.55	10,000	4.00	2665	4.06
	1980	0.95	17,300	4.24	---	---
2,6	†2390	0.48	8,700	3.94	2410	3.95
	<1950	---	----	---	---	---
3,4	†2680	0.27	4,900	3.69	---	---
	*2160	0.56	10,200	4.01	2190	4.00
	*2020	0.68	12,400	4.09	---	---
	<1900	>1.00	----	---	---	---
3,5	---	---	----	---	2480	4.08

(b) Listing of the Major Peaks.

					literature (6)	
Isomer	$\lambda$ (Å)	O.D.	$\epsilon$	$\log \epsilon$	$\lambda$ (Å)	$\log \epsilon$
**2,3	2000	0.85	15,500	4.19	<2100	---
* 2,4	*2510	*0.81	*14,800	*4.17	2520	4.15
2,5	2640	0.55	10,000	4.00	2665	4.06
2,6	†2390	0.48	8,700	3.94	2410	3.95
3,4	*2160	0.56	10,200	4.01	2190	4.00
3,5	---	---	----	---	2480	4.08

\*\*Due to the small quantity of this material available, the sample was vacuum-dried to remove the volatile solvents (mostly toluene) and the solution was prepared with this sample.

\* Spectrum determined in 10% ethanol-90% water.

† Approximate, peak not well defined.

\* Shoulders.

TABLE 8

Shift in Absorption Caused by Addition of a Nitro Group or a Methyl Group to Nitrobenzene.

Material	$\lambda$ (Å)	Shift from nitrobenzene (Å)	Reason
nitrobenzene	2689	---	----
o-dinitrobenzene	<2101	<-588	a, b
m-dinitrobenzene	2421	-268	a
p-dinitrobenzene	2650	- 39	a
o-nitrotoluene	2650	- 39	c
m-nitrotoluene	2740	+ 51	c
p-nitrotoluene	2836	+147	c

## NOTE:

- (a) A pair of  $\text{NO}_2$  groups reduces conjugation to the benzene ring by competition. The magnitude of the reduction depends on the ring position of each group.
- (b) A pair of  $\text{NO}_2$  groups (and to a lesser extent, an  $\text{NO}_2$  group and a methyl group) hinder each other sterically so that neither can be coplanar with the ring.
- (c) Methyl groups enhance conjugation of nitro groups except for ortho nitro groups. In the latter the enhancement is canceled due to steric hindrance.

TABLE 9

Predicted and Observed Absorption Maxima for the Isomers of Dinitrotoluene.

Isomer	2, 3	2, 4	2, 5	2, 6	3, 4	3, 5
$\lambda$ (calc.)	<2113 Å	2529 Å	2662 Å	2343 Å	<2299 Å	2523 Å
$\lambda$ (obs.)	2000 Å	2510 Å	2640 Å	2390 Å	2160 Å	2491 Å

\*Taken from ref. 6, since the 3, 5 isomer was not available to us.

TABLE 10

Absorption Maxima and Extinction Coefficients of TNT.

Solvent	$\lambda$ (Å)	O.D.	$\epsilon$	$\log \epsilon$	literature	
					$\lambda$ (Å)	$\log \epsilon$
ethanol	2230	0.45	20,500	4.31	2270 (2)	4.29
95% water - 5% ethanol	2310	0.44	20,000	4.30	2320 (6)	4.27

TABLE 11

Absorption Maxima and Extinction Coefficients of RDX.

Solvent	$\lambda$ (Å)	O.D.	$\epsilon$	$\log \epsilon$	literature <sup>(2)</sup>	
					$\lambda$ (Å)	$\log \epsilon$
ethanol	+2270	0.46	10,200	4.01	2130	4.04
95% water- 5% ethanol	+2340	0.48	10,700	4.03		
	+1960	0.62	13,800	4.14		

+Approximate, peak not well defined.

TABLE 12

Absorption Maxima and Extinction Coefficients of Diphenylamine.

literature<sup>(2)</sup>

Solvent	$\lambda$ (Å)	O.D.	width (Å)	$\epsilon$	$\log \epsilon$	$\lambda$ (Å)	$\log \epsilon$
ethanol	2850	0.59	230	20,000	4.30	2850	4.31
	2020	0.83	---	28,100	4.45	---	---
95% water-	2790	0.43	280	14,600	4.16	---	---
5% ethanol}	1990	0.89	---	30,200	4.48	---	---
water	2780	1.11		* --	* --		

\*Concentration not determined. DPA does not readily dissolve in water.

TABLE 13

Absorption Maxima and Extinction Coefficients of Ethyl Centralite.

literature<sup>(2)</sup>

Solvent	$\lambda$ (Å)	O.D.	$\epsilon$	$\log \epsilon$	$\lambda$ (Å)	$\log \epsilon$
ethanol	2460	0.81	7,200	3.86	2470	3.94
95% water-	2440	0.72	6,400	3.81		
5% ethanol}						

TABLE 14

Summary of the Solvent Effects on the Compounds Studied.

Substance	$\lambda_{\text{EtOH}}(\text{\AA})$	$\lambda_{\text{H}_2\text{O}}(\text{\AA})$	Shift in $\text{H}_2\text{O}(\text{\AA})$	O.D. EtOH	O.D. $\text{H}_2\text{O}$	
DNT {	2, 3	<2050	2000	----	$\geq 0.95$	0.85
	2, 4	2410	2510	100	0.84	0.81
	2, 5	2580	2640	60	0.57	0.55
	2, 6	2300	2390	90	0.49	0.48
	3, 4	2100	2160	60	0.63	0.56
	3, 5	---	2480	----	----	----
TNT	2230	2310	80	0.45	0.44	
RDX	2270	2340	70	0.46	0.48 <sup>+</sup>	
DPA	2450	2790	-60	0.59	0.43*	
EtC	2460	2440	-20	0.81	0.72**	
NG	---	---	----	----	----	
PETN	---	---	----	----	----	

<sup>†</sup> somewhat narrower band in 95% water-5% ethanol<sup>\*</sup> much broader in 95% water-5% ethanol<sup>\*\*</sup> somewhat broader in 95% water-5% ethanol $\lambda_{\text{EtOH}}$  = absorption peak in pure ethanol $\lambda_{\text{H}_2\text{O}}$  = absorption peak in 95% water-5% ethanol

# Molecular Formulae of Materials Investigated

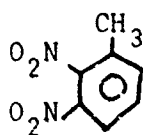
Benzene



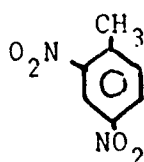
Toluene



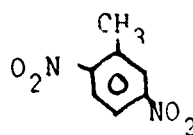
Isomers of dinitrotoluene:



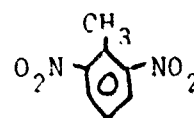
2,3



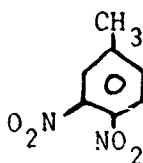
2,4



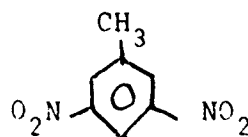
2,5



2,6



3,4



3,5

TNT

2, 4, 6 trinitrotoluene

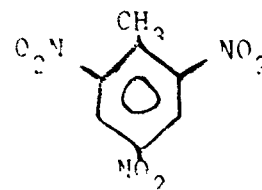
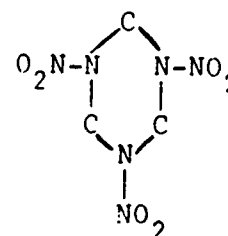


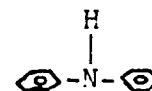
Figure 4

Figure 4, cont'd.

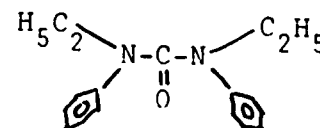
RDX { cyclotrimethylene trinitramine  
or  
1, 3, 5 triazinehexahydro-  
1, 3, 5 trinitrocyclohexane  
or  
1,3,5 trinitro 1,3,5 triazacyclohexane



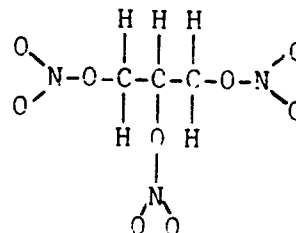
DPA diphenylamine



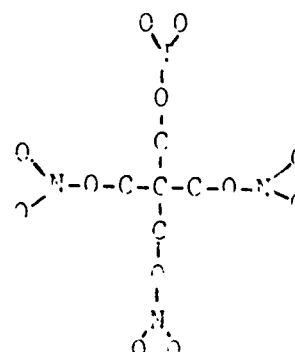
EtC ethyl centralite  
or 1, 3 diethyl  
1, 3 diphenylurea



NG nitroglycerine



PETN Pentaerythritoltetranitrate



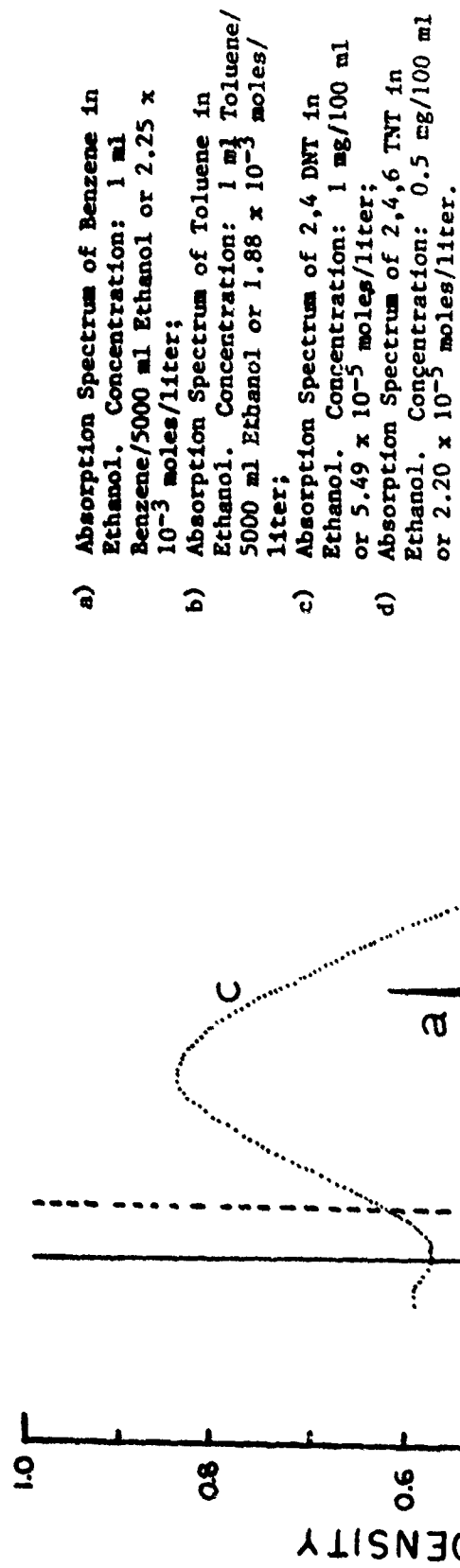


Figure 5



Absorption Spectra of 2,4 DNT in mixtures of Ethanol and Water. Concentration:  $1 \text{ mg}/100 \text{ ml}$  or  $5.49 \times 10^{-5} \text{ moles/liter}$ .

- a) 100% ethanol;
- b) 75% ethanol;
- c) 50% ethanol;
- d) 10% ethanol.

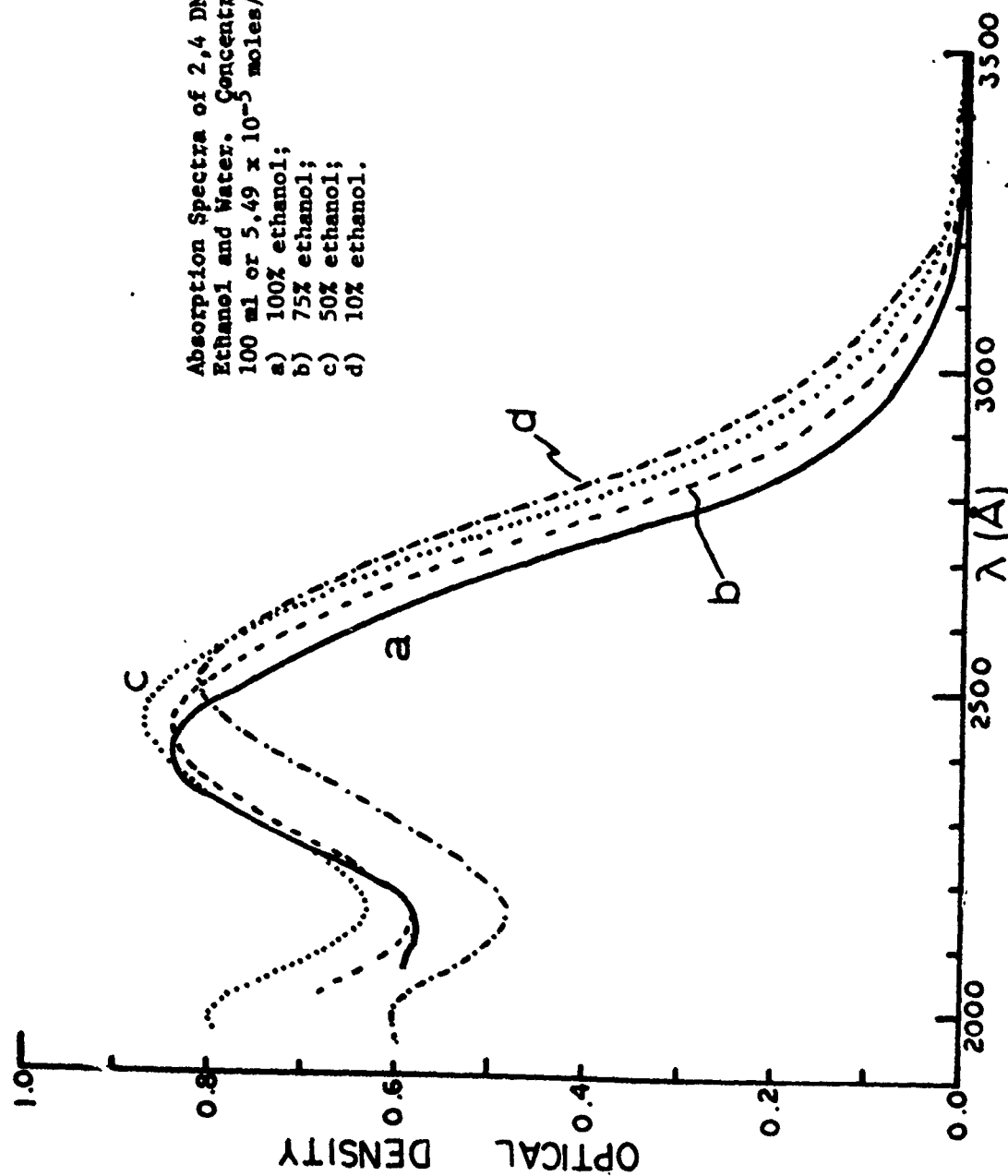


Figure 6

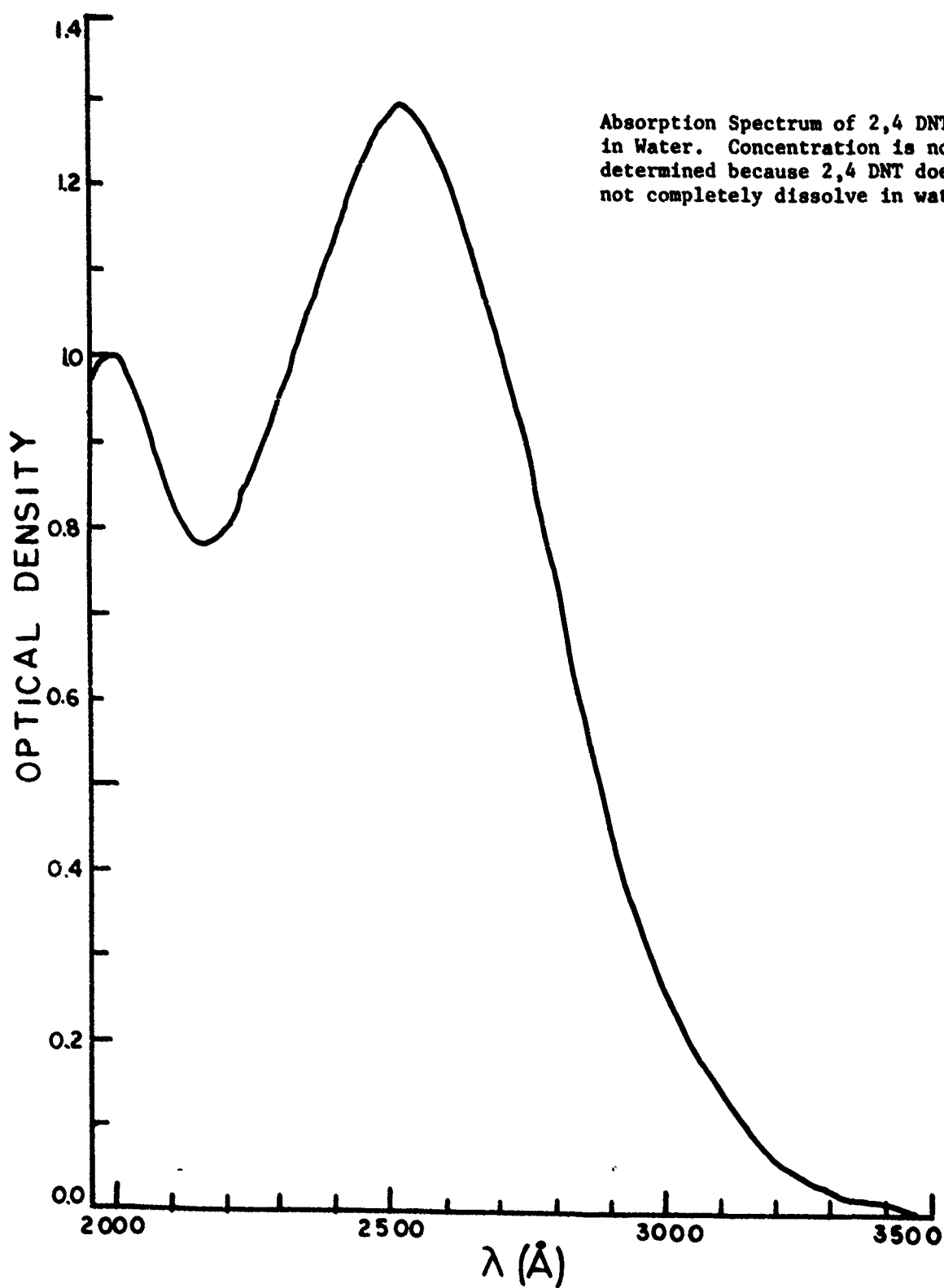


Figure 7

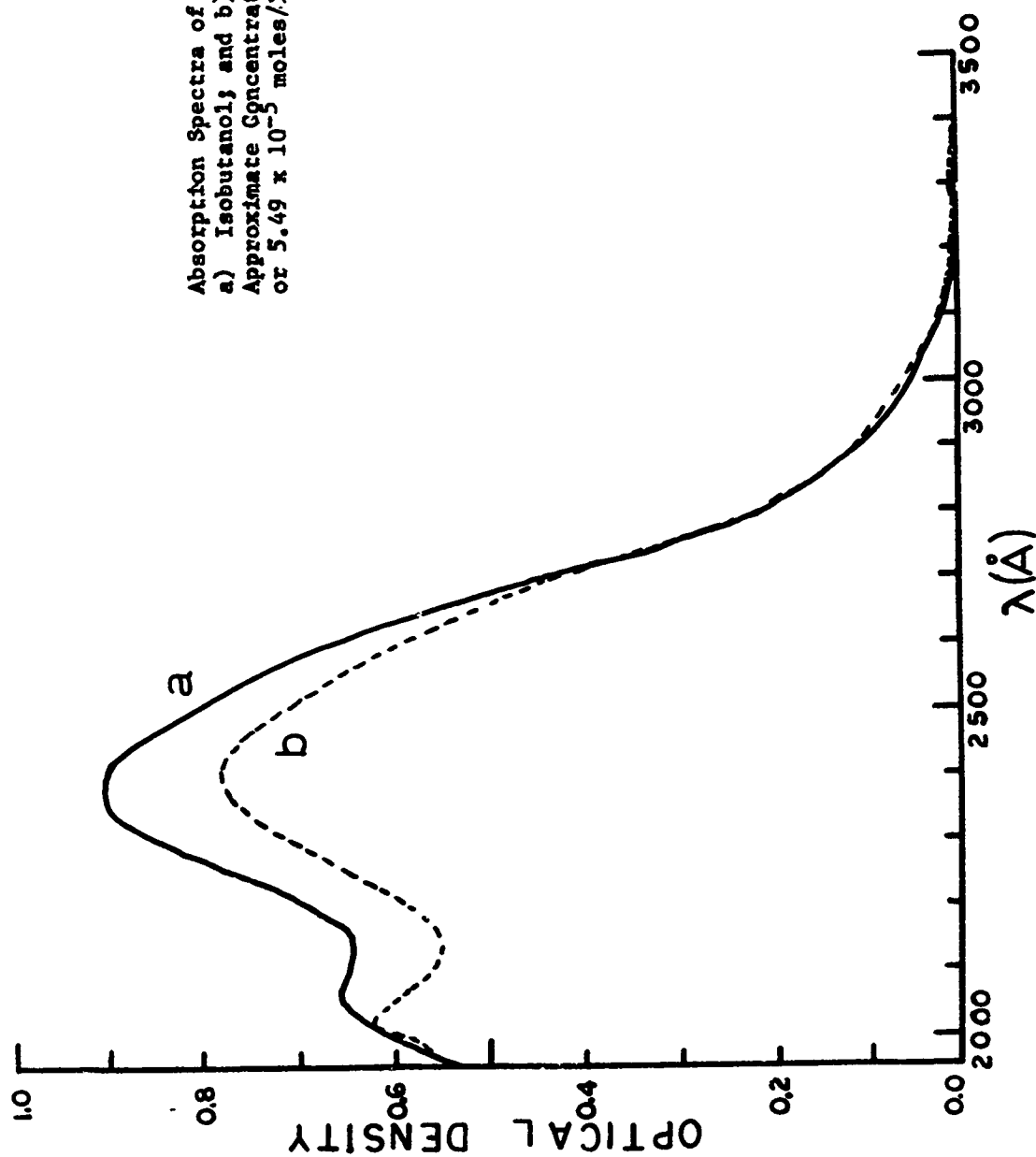


Figure 8

Absorption Spectra of Isomers of  
DNT in Ethanol. Concentration:  
1 mg/100 ml or  $5.49 \times 10^{-5}$  moles/  
liter.  
a) 2,3;  
b) 2,4;  
c) 2,5;  
d) 2,6;  
e) 3,4.

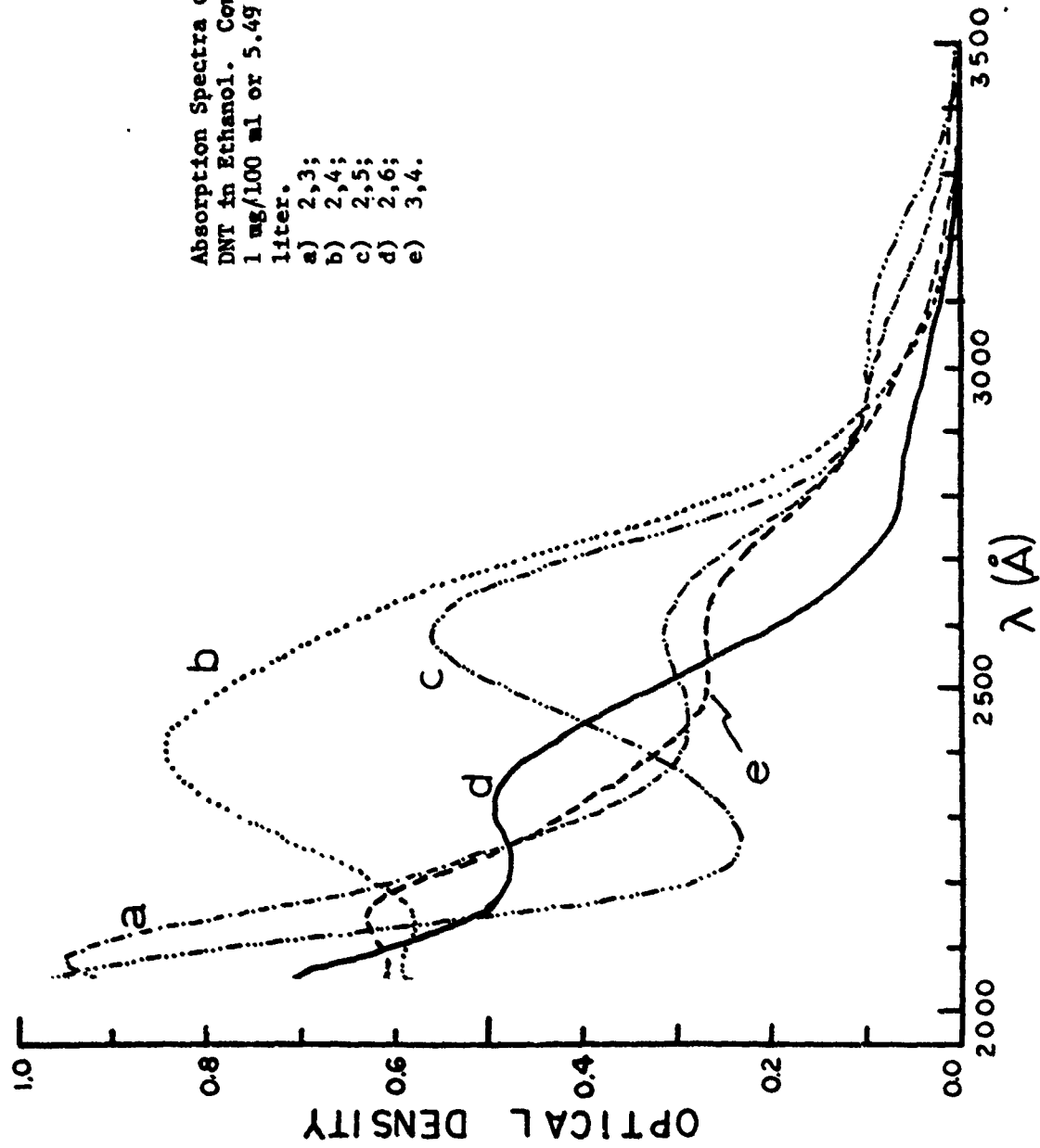


Figure 9

Absorption Spectra of Isomers of DNT  
in 5% Ethanol-95% Water. Concentration:  
1 mg/100 ml or  $5.49 \times 10^{-5}$  moles/liter.

- a) 2,3;
- b) 2,4;
- c) 2,5;
- d) 2,6;
- e) 3,4.

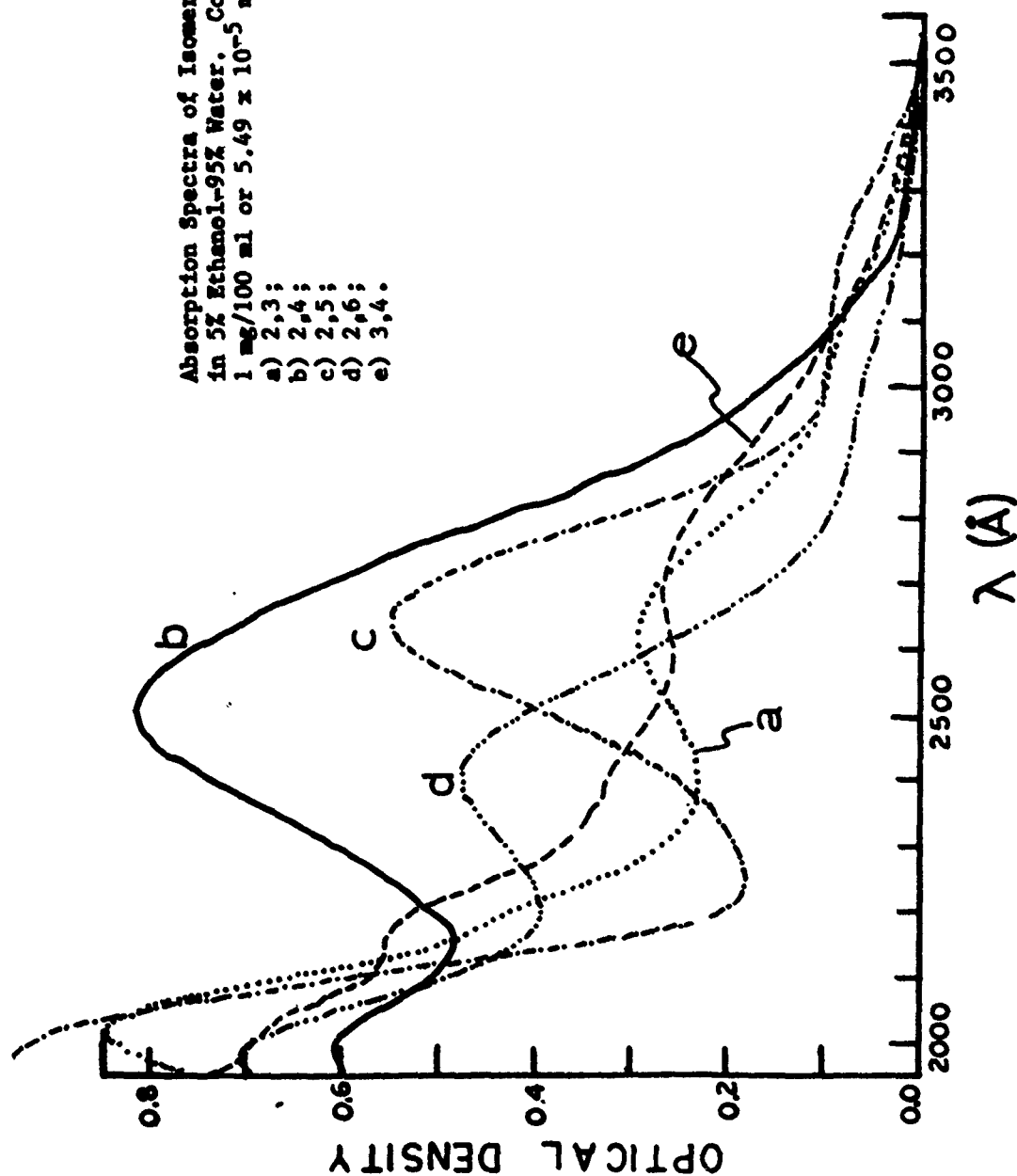


Figure 10

Absorption Spectra of Three Purities of  
Trinitrotoluene (TNT) in Ethanol.  
Concentration: 0.5 mg/100 ml or  
 $2.20 \times 10^{-5}$  moles/liter.  
a) Military grade;  
b) recrystallized;  
c) Eastman.

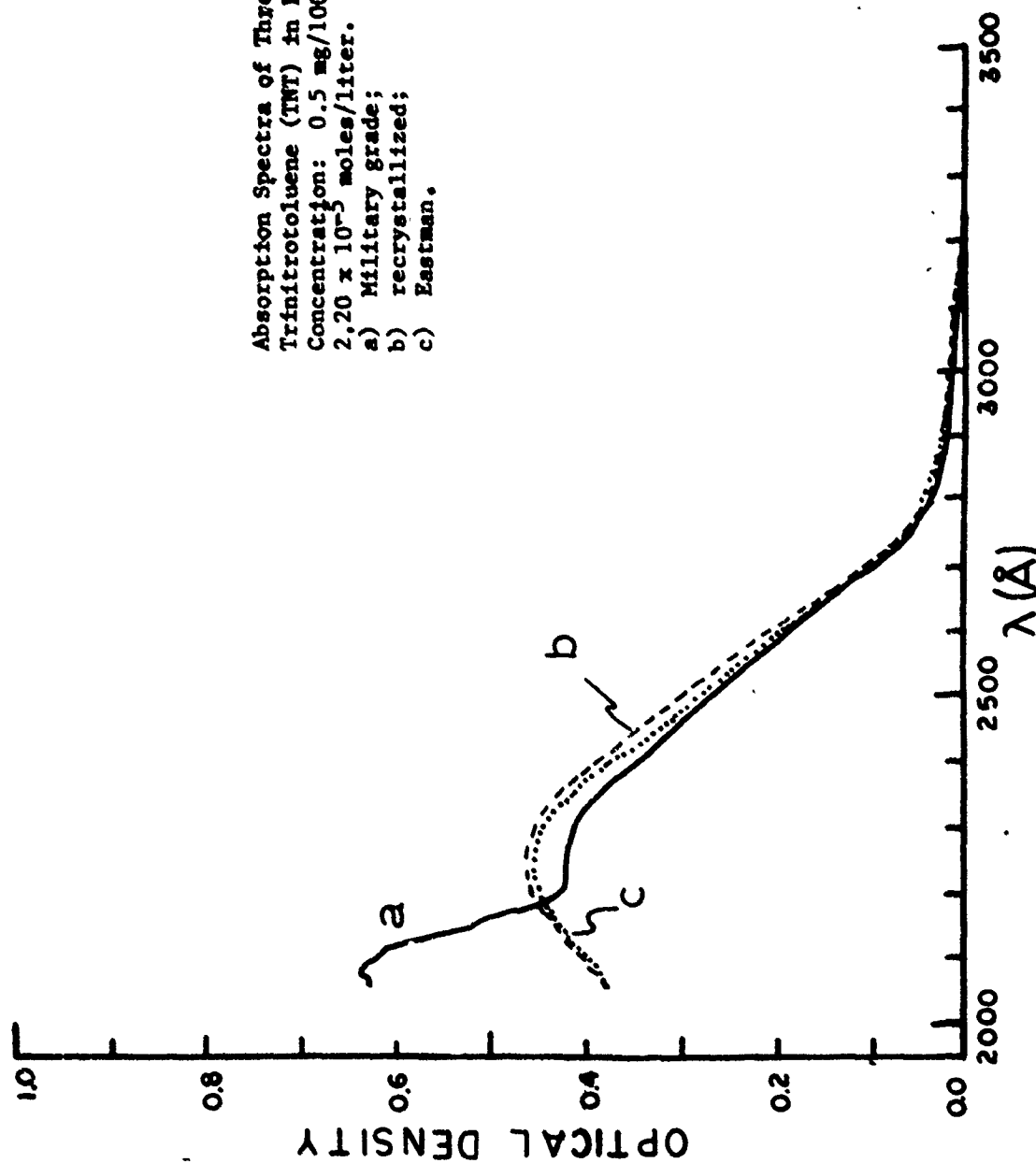


Figure 11

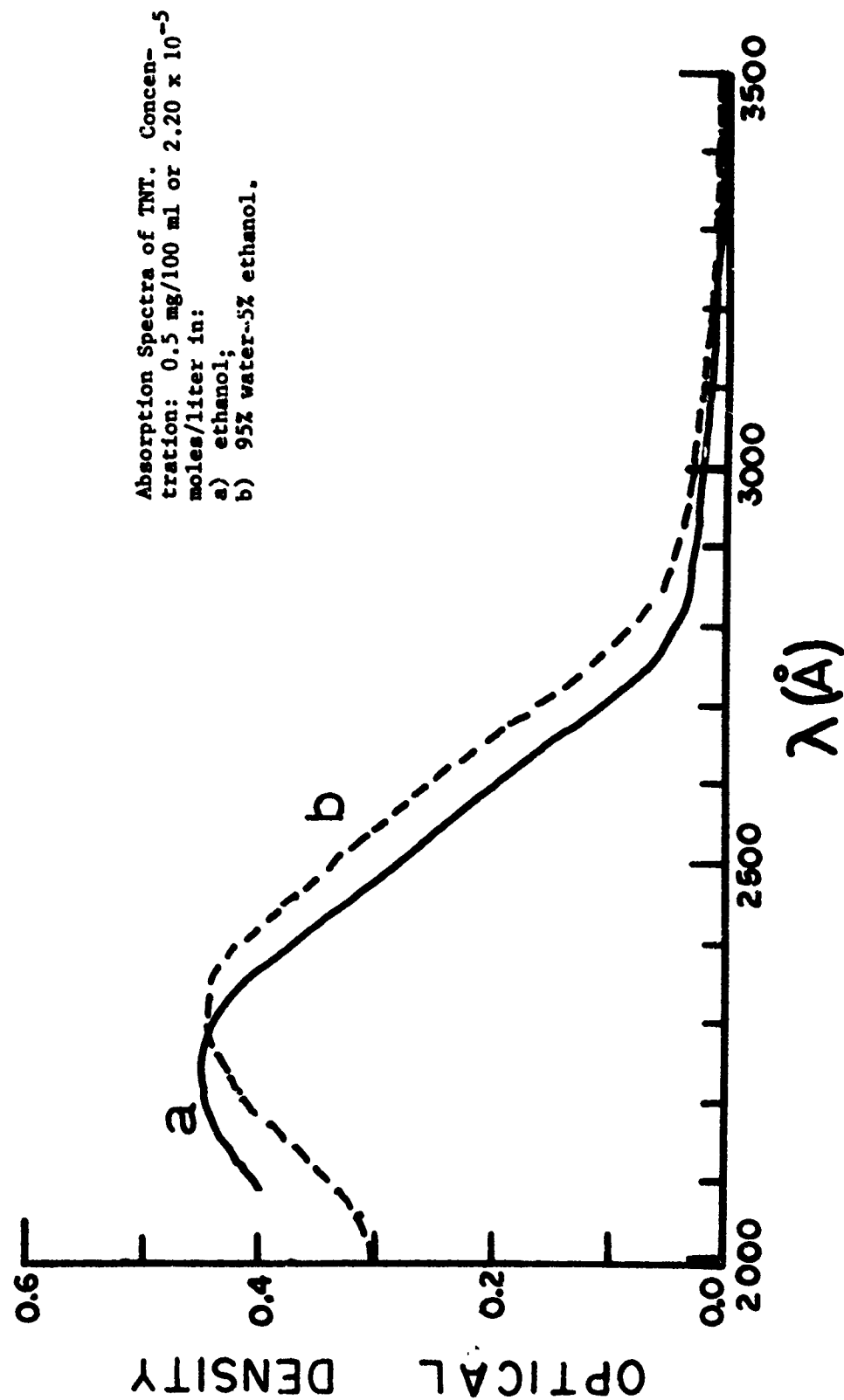


Figure 12

Absorption Spectra of ND<sub>X</sub>, Concentration:  
1 mg/100 ml or  $4.50 \times 10^{-5}$  moles/liter in:  
a) ethanol;  
b) 95% water-5% ethanol.

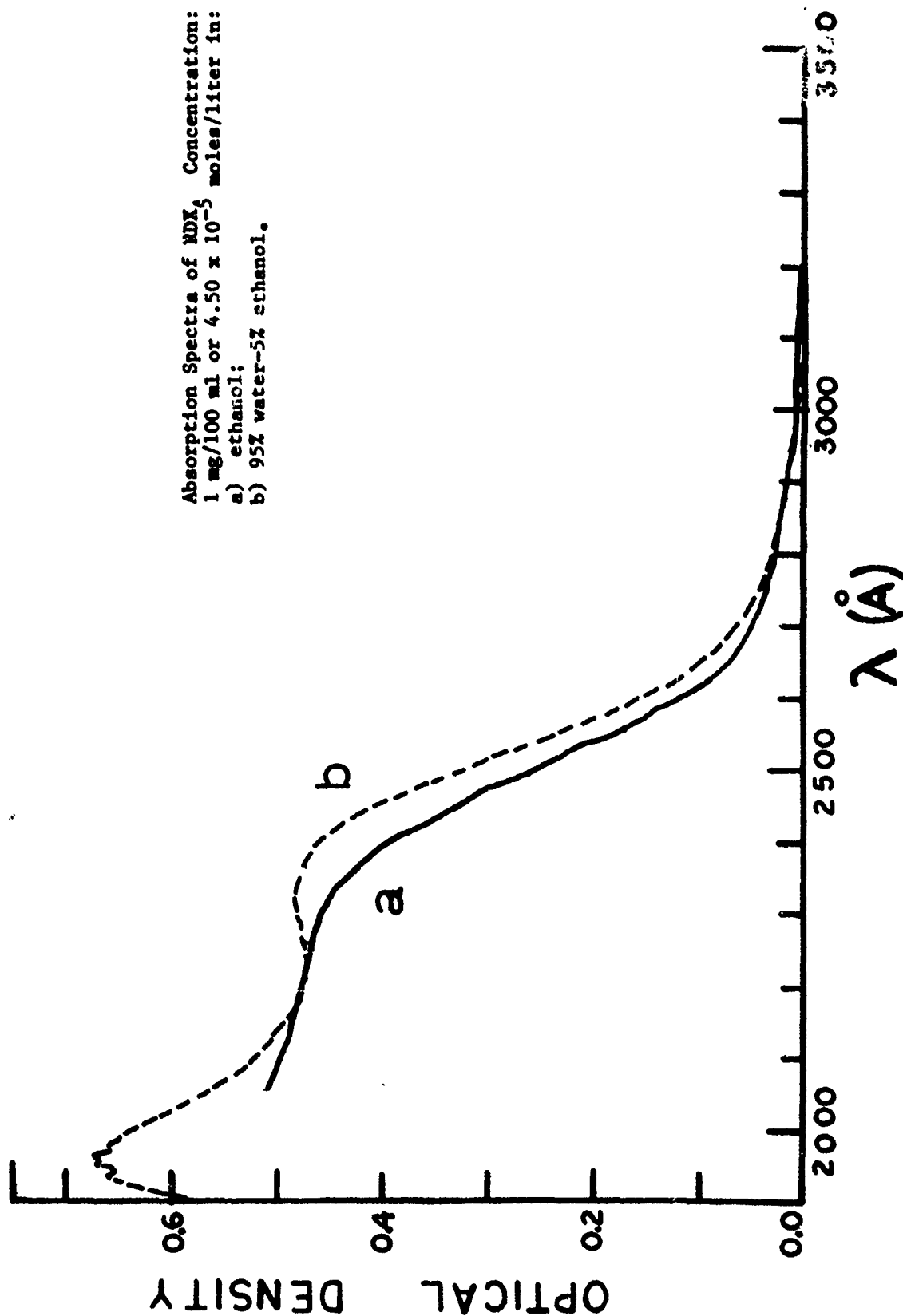


Figure 13



Absorption Spectra of Diphenylamine.  
Concentration: 0.5 mg/100 ml or 2.95 x  
10<sup>-5</sup> moles/liter in:  
a) ethanol;  
b) 95% water-5% ethanol.

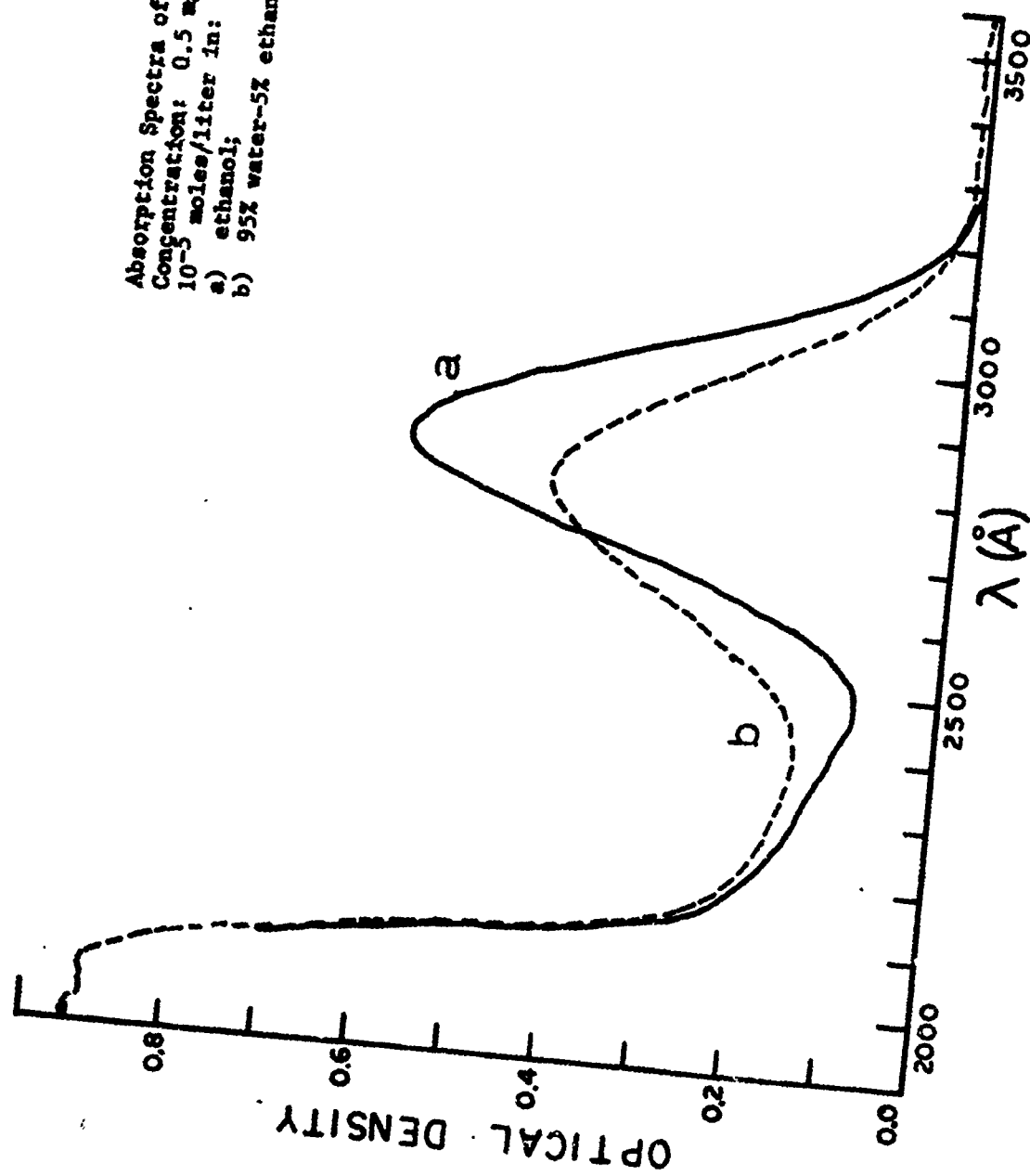


Figure 14

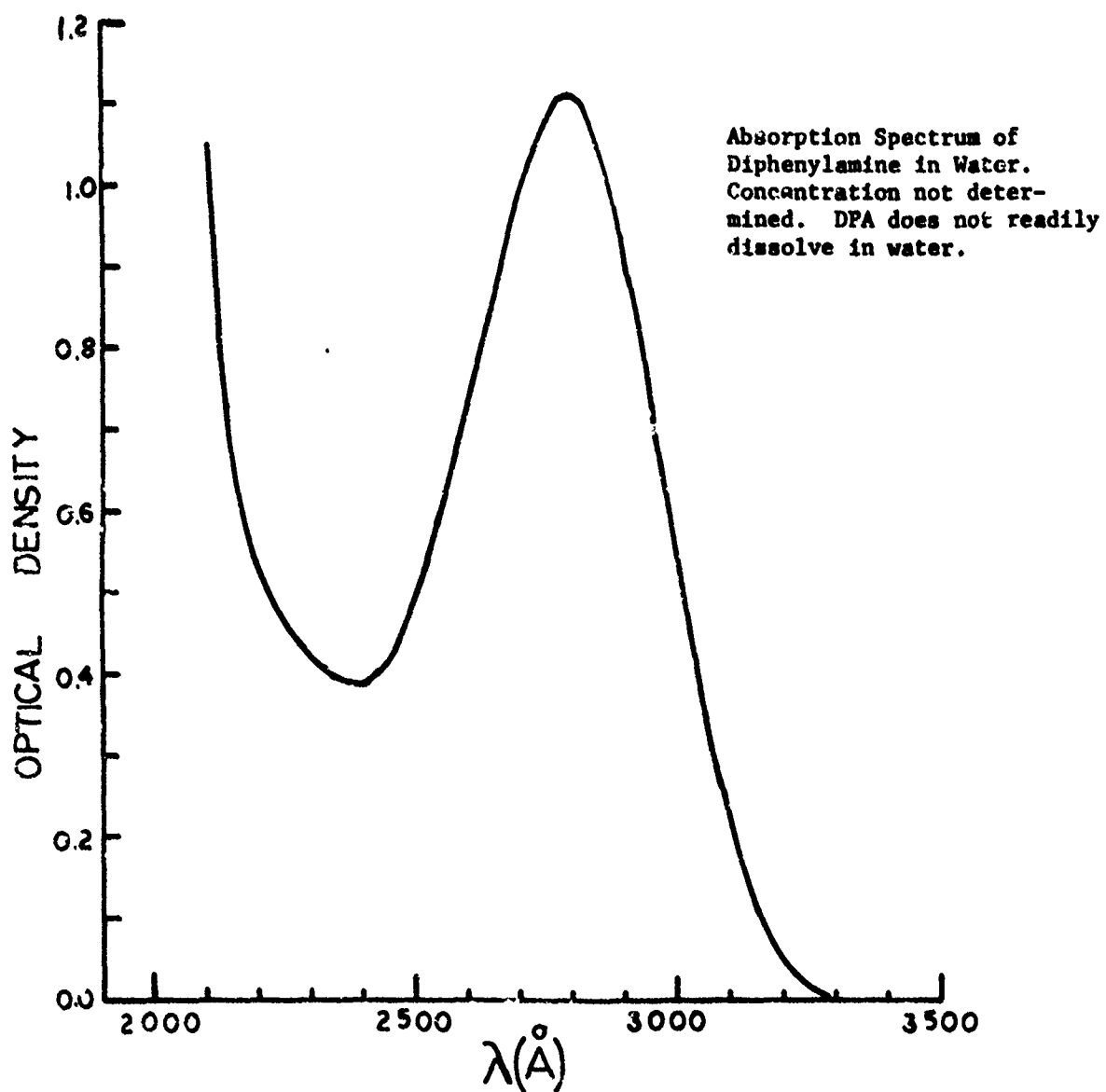


Figure 15

Absorption Spectra of Ethyl Centralite.  
Concentration: 3 mg/100 ml or  $1.12 \times 10^{-4}$  moles/liter in:  
a) ethanol;  
b) 95% water-5% ethanol.

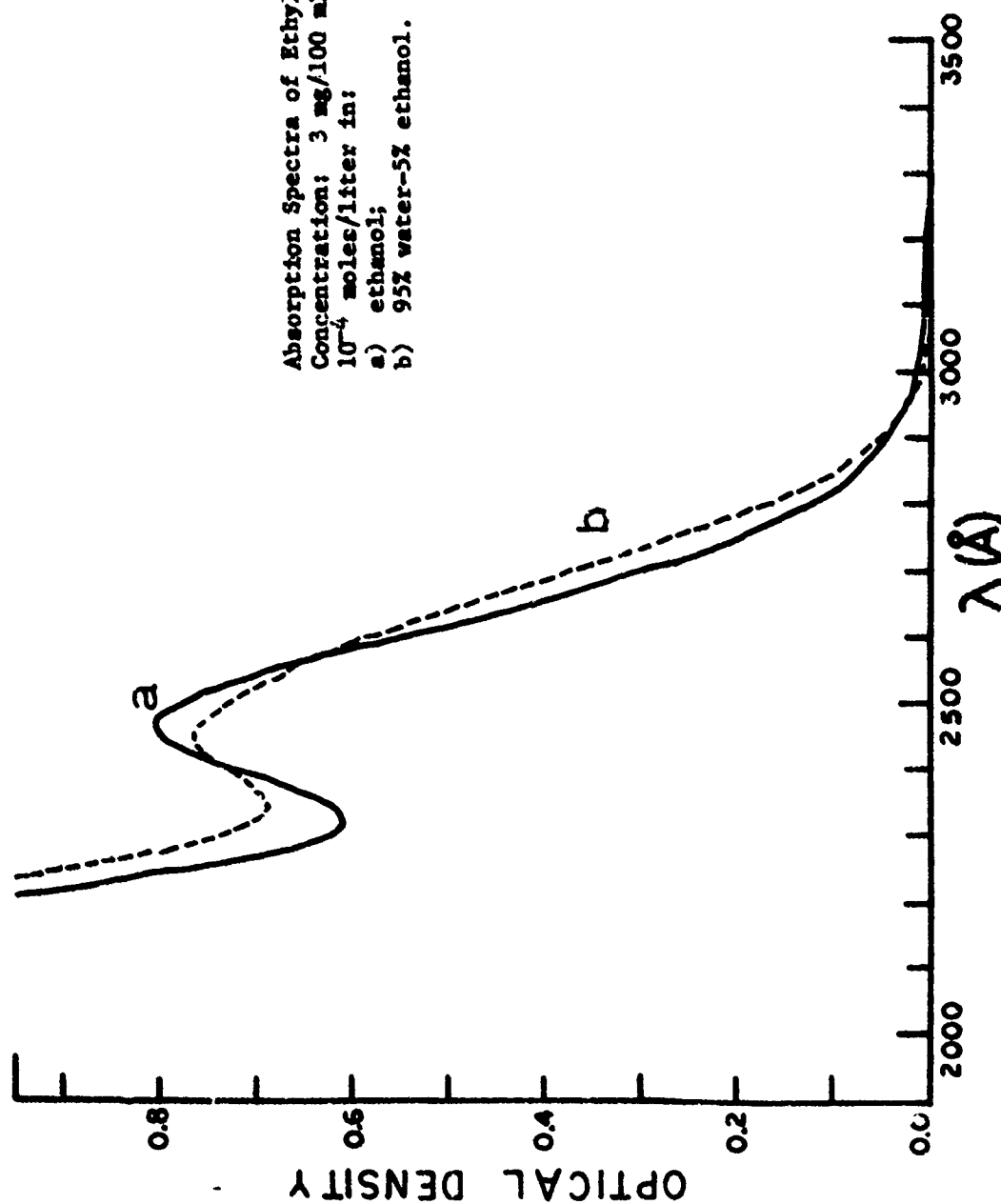


Figure 16

Absorption Spectra of Nitroglycerine.  
Concentration: 1 mg/100 ml or 4.40 x  
10<sup>-5</sup> moles/liter in  
a) ethanol;  
b) 95% water-5% ethanol.

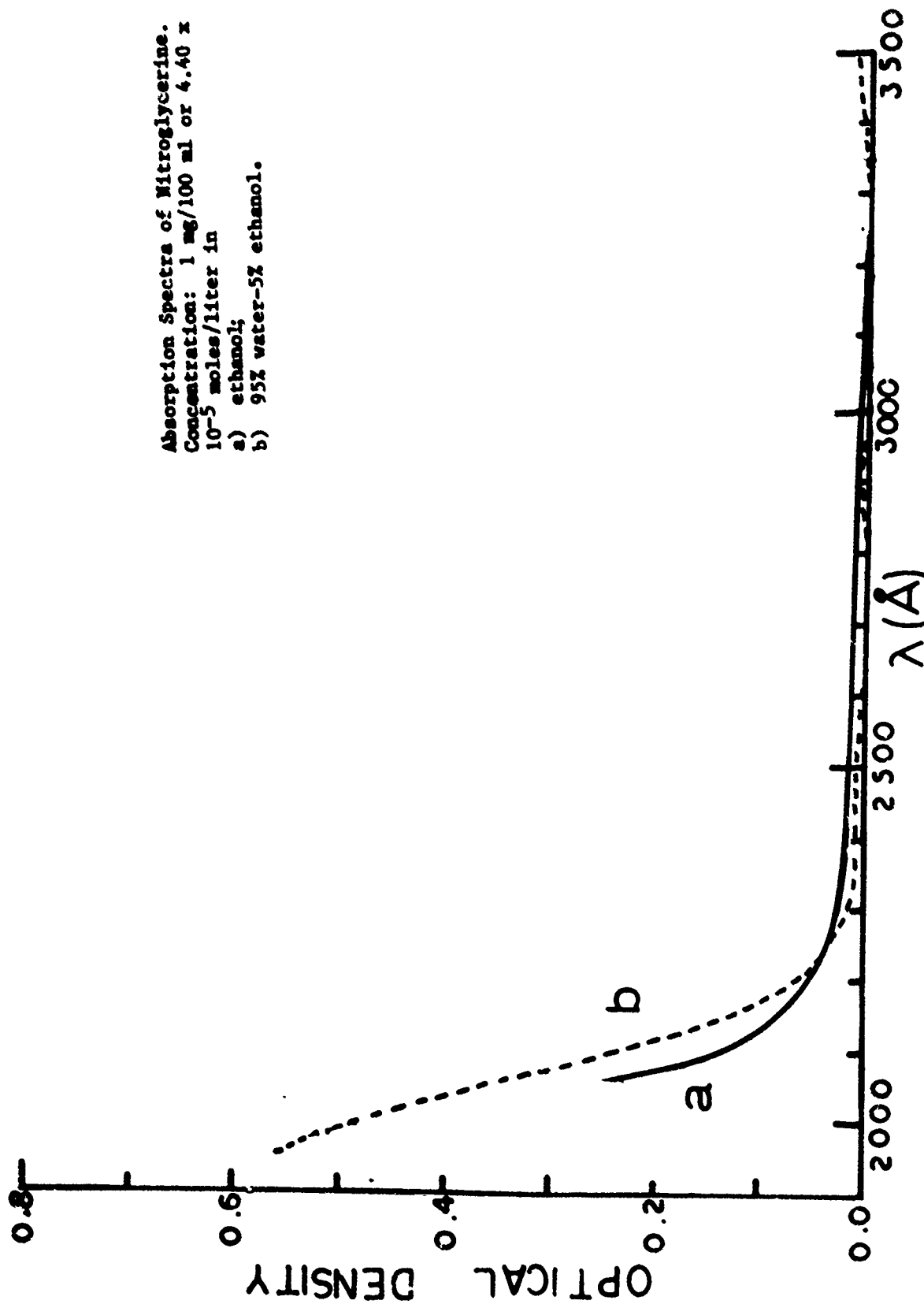


Figure 17

Absorption Spectra of Pentaerythritoltetra-  
nitrate. Concentration: 1.5 mg/100 ml or  
 $4.74 \times 10^{-5}$  moles/liter in  
a) ethanol;  
b) 95% water-5%ethanol.

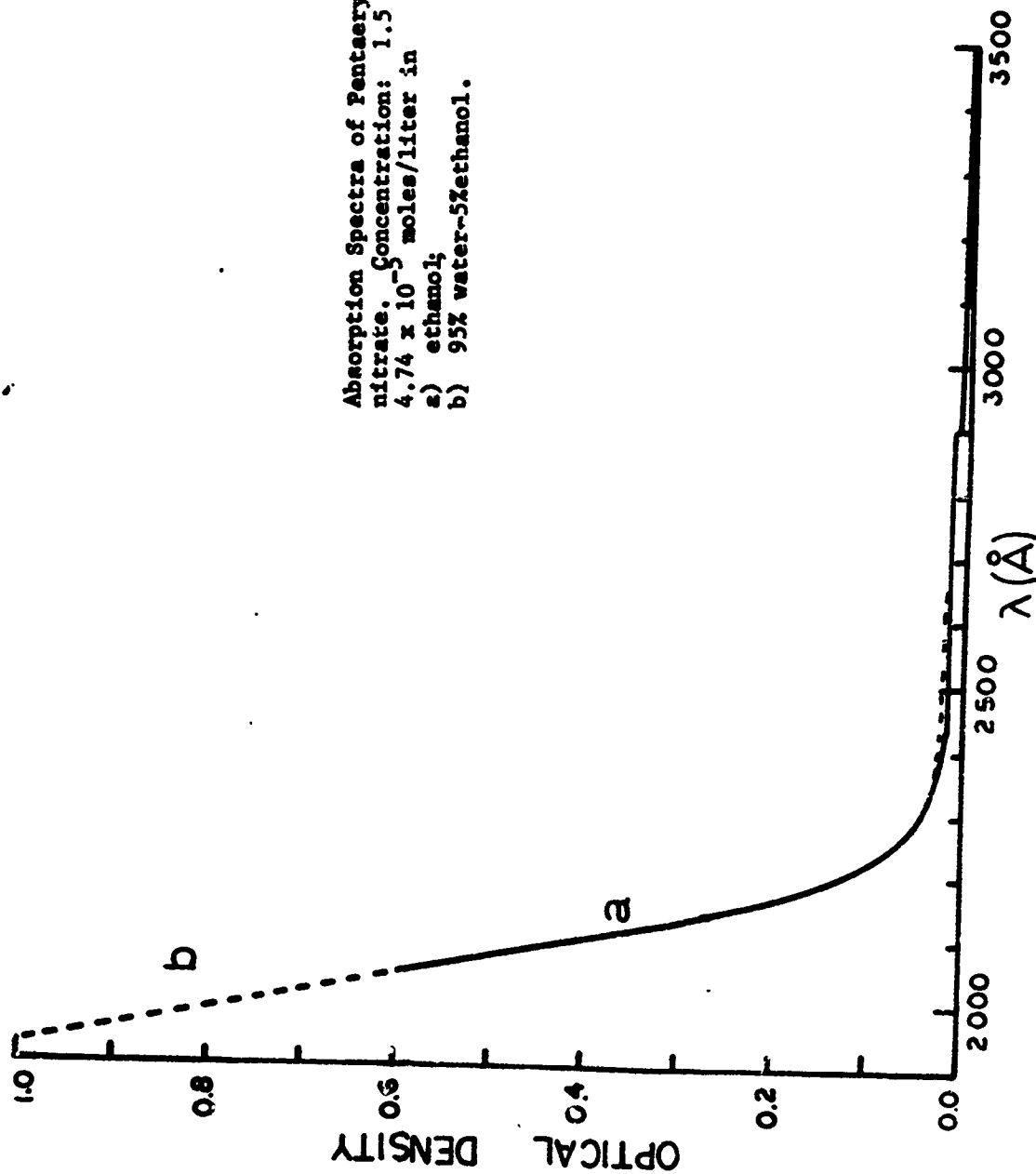


Figure 18

## SPECTRA OF EXPLOSIVE MATERIALS IN THE VAPOR PHASE

### Introduction

Over the past decade or so there has been considerable attention devoted to the development of instrumentation capable of detecting the presence of explosives prior to detonation.<sup>(11)</sup> In particular, the detection of such materials through an analysis of the characteristic emitted vapors has been attempted using a variety of approaches. These include electron capture techniques, plasma chromatography, mass spectrometry, laser photoacoustic spectroscopy and Raman scattering. Little work, however, has been done in determining the fundamental optical properties of vapors of explosives and explosive-related compounds.

Optical detection has the potential for high sensitivity if the species being monitored has the proper optical properties. By obtaining fundamental data on these properties, the feasibility of employing such a detection technique can be determined. Along these lines, we have performed extensive studies of the absorption characteristics of a number of explosive and explosive-related compounds in the vapor phase.

Previous studies of explosive vapors have concentrated on such problems as determining the vapor pressures of the relevant compounds and identifying the composition of vapors

---

<sup>(11)</sup> See, for example, the review by J. Yinon, CRC Critical Reviews in Analytical Chemistry, pg. 1 (December, 1977).

evolved from certain complex substances. For example, extensive vapor-pressure data for TNT, 2,4 DNT, 2,6 DNT, and EGDN were obtained by Pella<sup>(12)</sup> for various temperatures; room-temperature values for TNT, DNT, EGDN, nitroglycerine, PETN and RDX were measured by McReynolds et al.<sup>(13)</sup> The composition of vapors evolved from military grade TNT was recently studied by Leggett et al;<sup>(14)</sup> in their work, it was found that 2,4 DNT has a partial pressure 1 to 2 orders of magnitude higher than the vapor pressure of TNT. Jenkins et al.<sup>(15)</sup> examined the vapors over C-4 military explosives (~90% RDX) and found cyclohexanone to be a major volatile impurity. In addition, Pate<sup>(16)</sup> has investigated the vapors over certain gunpowders, dynamites, and military explosives.

---

(12) P. A. Pella, J. Chem. Thermodynamics 9, 301 (1977).

(13) J. H. McReynolds, G.A. St. John, and M. Anbar, "Determination of Concentration of Explosive Vapor from Parcels and Letters," Final Report, U.S. Postal Service Contract No. 74-00810, Stanford Research Institute (January, 1975).

(14) D.C. Leggett, T.F. Jenkins, and R.P. Murrmann, "Composition of Vapors Evolved from Military TNT as Influenced by Temperature, Solid Composition, Age, and Source," CRREL Special Report No. 77-16 (June, 1977).

(15) T.F. Jenkins, W.F. O'Reilly, R.P. Murrmann, and C.I. Collins, "Detection of Cyclohexanone in the Atmosphere Above Emplaced Antitank Mines," CRREL Special Report No. 203 (April, 1974).

(16) C.T. Pate, "Characterization of Vapors Emanating from Explosives," Final Report, LEAA Contract No. J-LEAA-025-73 (June, 1976).

Limited data on the spectroscopic properties of explosive vapors are available in the literature. Gelbwachs et al.<sup>(17)</sup> have obtained the U.V. absorption spectra of DNT, TNT, and diphenylamine vapors and have observed emission from DNT and diphenylamine. Claspy et al.<sup>(18)</sup> have detected nitroglycerine, EGDN, and DNT by photoacoustic spectroscopy techniques and have investigated the interference effects of normal atmospheric pollutants. In general, the U.V. absorption properties of explosive vapors have gone largely unexplored to date.

In any study of explosive vapors, two intrinsic problems present themselves. First, the molecules involved are polar in nature and adsorb easily on glass or metal surfaces.<sup>(19)</sup> This suggests that the absorption cell be maintained at a nominal elevated temperature. Secondly, the concentration of explosive vapor available (expressed as a mole ratio of vapor to air) at room temperature and saturated vapor conditions runs from roughly a part per billion for RDX to parts per million for EGDN. Consequently, the explosives themselves are sometimes difficult to detect. For this reason, certain higher vapor-pressure impurities characteristically found in

---

(17) J.A. Gelbwachs, C.F. Klein, and J.E. Wessel, "Feasibility of Doppler-Free Two-Photon Spectroscopy for Explosive Vapor Detection," Aerospace Report No. ATR-76 (7911)-3 (1976).

(18) P.C. Claspy, Y.-H. Pao, S. Kwong, and E. Nodov, Appl. Optics 15, 1506 (1976).

(19) J. A. Rakaczky and A.D. Coates, "The Effect of Surfaces on the Flow of Vaporized Explosives," Ballistics Research Laboratory Report No. 1597.



explosives (e.g., DNT in TNT and cyclohexanone in RDX) are also of interest as they may be easier to detect than the host material. (14), (15) If both impurity and explosive are observable, a higher degree of specificity in detection can be obtained. With this in mind, we have investigated the U.V. absorption of vapors of explosives as well as associated impurities. Specifically, the materials studied include 2, 3 DNT, 2, 4 DNT, 2, 6 DNT, TNT, nitroglycerine, diphenylamine, RDX, ethyl centralite, PETN, monomethylamine, and cyclohexanone. These materials were studied in the 30°C - 80°C temperature region; the precise range for each compound was dictated by such considerations as vapor pressure, melting point, and limitations of the apparatus.

#### Experimental Details

The basic apparatus used in this part of the experimental program has essentially been described earlier. Only a few comments are needed here. A few of the spectra were recorded on the Cary 14 Spectrophotometer. These are appropriately noted in the text. Most of the spectra, however, were obtained with the apparatus mentioned in the section on experimental facilities. The light source used was a Beckman or Pfaltz and Bauer deuterium lamp powered by a Beckman Model B supply. The light was passed through an Acton Research 230-W filter, which transmits in the 1700-3400 Å region. The detecting system employed an EMI 9662 B photomultiplier tube. The

vapors to be analyzed were contained in a specially fabricated 1-m quartz absorption cell which was designed so that it could be heated and/or evacuated. The solid sample which generated the vapors was housed in a small flask attached to one of the ports of the absorption cell. When the desired sample temperature was reached, the vapors emanating from the solid were allowed to enter the 1-m cell and equilibrate.

In order to obtain the absorption spectrum of a given compound, a spectrum with the cell evacuated was first recorded. This was followed by a spectrum obtained with the vapor present in the cell. The optical density (O.D.) at a given wavelength was then calculated from the expression:  $O.D. = \log_{10} \left\{ I_0(\lambda) / I(\lambda) \right\}$ , where  $I_0(\lambda)$  and  $I(\lambda)$  refer to the transmitted intensities for the evacuated and filled cell, respectively. Correction for fluctuation in the lamp intensity from one trace to the next was made by comparing the transmitted intensities over a region of no vapor absorption. For convenience in presenting the results, the optical density was calculated at 50-Å intervals. The resolution of the apparatus itself was typically ~3-7 Å. The resolving power may be seen directly in figures 19 and 20, which contain the recorder traces of the absorption of toluene and benzene vapors, respectively. Because the ordinate represents transmitted intensity, the dips in the spectra correspond to absorption peaks.

#### Experimental Results

The absorption spectra of the vapors evolved from the compounds of interest are divided into six groups and discussed

below. The groupings are: isomers of DNT, TNT, nitroglycerine, amines (diphenylamine, monomethylamine, and ethyl centralite), RDX and cyclohexanone, and PETN. Unless otherwise noted, all solids were recrystallized twice in either toluene or ethanol and pumped on extensively to remove the solvent. The ethanol used was ordered spectropure from Baker Chemical Company and the toluene was either Baker spectropure or Fisher A.C.S. grade.

The sample temperatures referred to in this section denote the temperature of the solid compound from which the vapors were generated. The absorption cell which contained the vapors under investigation was kept  $\sim 15-20^{\circ}\text{C}$  warmer than the solid sample. This was done to inhibit adsorption of the vapors on the cell surfaces.

#### Isomers of DNT

As was mentioned earlier, DNT is commonly found as an impurity in commercially produced TNT. Vapor analyses of military TNT have indicated the presence of all six isomers to some extent, with 2, 4 DNT as the largest contributor.<sup>(14)</sup> In view of this, it is important to investigate the absorption properties of DNT in the vapor phase. For our studies, we examined 2, 4 DNT, 2, 6 DNT, and 2, 3 DNT; the samples used were obtained from ICN K & K Laboratories. Because of the small amount of 2, 3 DNT at our disposal, this compound was not recrystallized, but rather pumped on for several hours.

The spectra obtained for 2, 4 DNT vapor at 40, 51, and  $60^{\circ}\text{C}$  are presented in figures 21 - 23 (figures 21 and 23 depict two runs each.) In general, one notices a wide absorption

band in the 2250 - 2600 Å region. Because of the broad, flat appearance of this band, the position of the maximum is difficult to gauge. (A rough estimate would be ~2300 Å. The band width is ~650 Å.) On the high-energy side of this band, there appears to be a second absorption maximum. Details of this band cannot be discerned because the data taken below 2100 Å are not sufficiently accurate. The band maximum may be in the vacuum U.V. It may be noted that no pronounced enhancement of the absorbance is observed as the temperature is raised. This increase would be expected because of the higher vapor pressure at higher temperatures. The possible reasons for this will be discussed in a later section.

The absorption spectra of 2, 6 DNT vapor at 40%, 51, and 59°C are presented in figures 24 - 26. It can be seen that the band at ~2300 Å is much less pronounced than in 2, 4 DNT. In fact, for some spectra (for example, those taken at 59°C), this band is almost absent. A second absorption appears to exist below ~2150 Å with an optical density higher than that of its lower-energy counterpart. Because of mutual interference, the width for the lower-energy band is difficult to obtain. As for 2, 4 DNT no pronounced temperature effect is observed in raising the temperature from 40°C to 60°C.

The results for 2, 3 DNT at 42°C and 52°C are presented in figures 27 and 28. The absorption of this compound in the vapor phase is relatively weak compared with that of 2, 4 DNT for the same temperatures (see figures 21 and 22). In addition, there is no clearly definable absorption peak in the 2100 - 3000 Å region.

## TNT

The absorption spectra of vapors evolved from various samples of TNT are presented in figures 29 - 35. Figures 29 - 31 contain spectra for Military Grade TNT obtained from Mr. Leo Voght of the Massachusetts State Fire Marshal's office. The results indicate a relatively strong absorption extending below 2100 Å and a weaker band peaking at ~2550 Å. Not included in these figures is some weak, sharp-line structure in the 2500 Å - 2700 Å region at 50°C and 69°C. By a comparison with spectra taken previously by us, these lines can be attributed to toluene vapor.

In order to remove the toluene and other high vapor-pressure impurities, the above sample of Military Grade TNT was then recrystallized and pumped on for a total of 32 hours. The absorption spectrum obtained at 60°C for this purified TNT is presented in figure 32. No absorption is detected in the 2200 Å - 3000 Å region, but there is still evidence of a band residing below ~2100 Å.

For purposes of comparison, we also examined a sample of Eastman 2, 4, 6 TNT. This sample was obtained from Dr. John Hobbs of the Department of Transportation and was studied initially without further purification. The spectra for 42°C and 60°C are included in figures 33 and 34. The general features are essentially the same as those observed in the Military Grade sample. There is the usual strong absorption below ~2100 Å accompanied by the broad band at ~2550 Å and the sharp-line toluene structure from 2500 Å - 2700 Å. (The

contribution of the toluene vapor can be seen in these figures as a distortion of the 2550 Å band and a tooth-like absorption at ~2650 Å.) There is a noticeable enhancement of all of these features as the temperature is increased from 42°C to 60°C. Figure 35 displays the spectrum of the Eastman TNT sample at 60°C after it was pumped on overnight. Apart from overall intensity, the spectra in figures 34 and 35 are the same.

#### Nitroglycerine

Because of the hazardous nature of pure nitroglycerine, we generated the vapor studied from a sample consisting of 10% nitroglycerine on  $\alpha$ -lactose. The absorption spectra obtained at 60°C and 79°C are presented in figures 36 and 37. (There is some scatter in the points in the 60°C spectrum, but this is due to the very low absorption at this temperature.) In general, there is a relatively strong absorption band extending below ~2500 Å and peaking below 2100 Å. In addition, there appears to be a weak band in the 2600 - 3100 Å region. The optical density of the peak is about 12 times smaller than that calculated for  $\lambda = 2100$  Å. The same features including the weak band, were observed in the solution spectra (see figure 17).

#### Amines

Three amines were examined in the course of this study: diphenylamine, ethyl centralite, and monomethylamine. The vapors of the first two emanate from smokeless powder, and

the last is found above water gel explosives. The diphenylamine was obtained "Baker-Analyzed" from J. T. Baker and used without further purification; the ethyl centralite was recrystallized twice in ethanol. The monomethylamine was obtained from Matheson Gas and used as received.

The spectra obtained for diphenylamine vapor at 24 and 45°C are reported in figures 38 and 39. There is a region of strong absorption below 2200 Å and a weaker band extending from ~2400 Å to ~3000 Å. As for nitroglycerine, one can see a definite enhancement of these features as the temperature is increased. There is some evidence of structure within the weak band; this may indicate that the absorption in this region consists of several overlapping bands. The spectra obtained in this study agree qualitatively with that obtained by Gelbwachs et al.<sup>(17)</sup> for diphenylamine vapor at 65°C.

For monomethylamine, the spectrum was recorded directly on a Cary 14 with 10cm cells. This is possible because monomethylamine is a gas at room temperature and atmospheric pressure and is, therefore, available in a relatively high concentration. The spectrum so obtained is presented in figure 40 and displays an absorption band centered at ~2170 Å with a well-defined vibrational structure extending from ~2400 Å down to at least 1900 Å. (The latter wavelength represents the limit of the apparatus used.) This spectrum agrees well with that reported by Tannenbaum et al.,<sup>(20)</sup> who were able to follow the absorption down to ~1600 Å. Their data indicate a second absorption peak at ~1740 Å whose extinction


---

(20) E. Tannenbaum, E.M. Coffin, and A.J. Harrison, J. Chemical Phys. 21, 311 (1953).

coefficient is about four times that for the lower-energy band.

In the vapor phase, ethyl centralite presents the absorption features indicated in figure 41 for a sample temperature of 76°C. (Attempts to obtain a spectrum for several lower temperatures proved unsuccessful.) A relatively strong absorption band extends below ~2300 Å and peaks below 2100 Å. On the low-energy side, there is a broad shoulder which covers the 2400-3000 Å region. This band has a peak optical density about a quarter of that obtained for  $\lambda = 2100$  Å.

#### Cyclohexanone and RDX

As has been mentioned earlier, cyclohexanone () is a prominent impurity found in the vapors above RDX and RDX-containing explosives; as such, its vapor absorption properties are also of considerable interest. Our sample was obtained purified from Fisher Scientific and placed on chromosorb. The spectrum obtained at 64°C for cyclohexanone vapor is reported in figure 42. There is evidence of an absorption maximum below 2100 Å, but the prominent feature is a relatively wide (~600 Å) absorption band centered at ~2900 Å. This band is distinctive in that no other substance examined in this study possesses an absorption peak at such a low energy.

Our sample of RDX was obtained "pure" from Dr. Lyle Malotky, Naval Explosive Ordnance Disposal Facility, Indian Head, Maryland. Because of the small amount of the compound at our disposal, it was used without further purification. The vapor absorption



spectrum of RDX at 80°C is shown in figure 43. There is the usual high-energy absorption band extending below 2100 Å and a rather wide shoulder spanning the 2200 - 2700 Å region. Compared with the other spectra already presented, this absorption is relatively weak (O.D.  $\leq$  0.1). From the data of figure 42, it is immediately evident that little or no cyclohexanone is present in the RDX sample studied.

#### PETN

Our sample of PETN was obtained in detonation cord as "pure" and used without further purification. It was received from Dr. John Hobbs of the Department of Transportation.

The absorption spectrum of PETN vapor at 80°C is reported in figure 44. There is no well-defined peak observed in the 2100 - 3000 Å region; the spectrum appears to consist of a single band extending from ~2500 Å towards the vacuum U.V. and peaking below ~2100 Å. There may be a shoulder present at ~2300 Å, but the data are not conclusive.

#### Discussion of Results

##### Isomers of DNT

The absorption spectra of 2,4 DNT reported in figures 21, 22, and 23 agree qualitatively with that obtained on a Cary 14 by Gelbwachs et al.<sup>(17)</sup> for DNT vapor. A critical comparison is not possible, since the Gelbwachs group did not know the isomeric content of the DNT sample they examined.<sup>(21)</sup> Their data indicate

---

(21) J.A. Gelbwachs, private communication.

a band centered at  $\sim 2200 \text{ \AA}$  with a shoulder at  $\sim 2500 \text{ \AA}$ . Our spectra reveal the previously mentioned band centered at  $\sim 2300 \text{ \AA}$ . As an additional check, we ran our own spectra of 2,4 DNT vapor at  $40^\circ\text{C}$  on a Cary 14 and obtained results similar to those in the above figures. The maximum at  $2300 \text{ \AA}$  represents a  $200\text{-}\text{\AA}$  shift towards shorter wavelengths compared with a 5% ethanol-water solution.<sup>(6)</sup>

If one knew the vapor pressure of 2,4 DNT as a function of temperature, the extinction coefficient of the absorption peak could be easily calculated. A recurring problem with explosive materials, however, is the wide range of vapor-pressure values quoted in the literature for a given compound at a given temperature. For example, the vapor pressure of nitroglycerine at  $20^\circ\text{C}$  has been calculated to be  $2.5 \times 10^{-4} \text{ mm Hg}$ ,<sup>(22-24)</sup> while the value for  $25^\circ\text{C}$  has been reported as  $2.4 \times 10^{-5} \text{ mm Hg}$ .<sup>(13)</sup> Vapor-pressure values for RDX at  $25^\circ\text{C}$  run from  $\sim 1.4 \times 10^{-9} \text{ mm Hg}$ <sup>(25)</sup> to  $7 \times 10^{-7} \text{ mm Hg}$ .<sup>(12)</sup> Similar scatter occurs for DNT. In fact, data are often presented for DNT without any reference to the isomeric content of the sample examined. Consequently, it does not seem advisable to calculate extinction coefficients

---

(22) T. Urbanski, Chemistry and Technology of Explosives (Peramon Press, N.Y., 1965).

(23) "Properties of Explosives of Military Interest," AMC Pamphlet 706-177, U.S. Army Materiel Command, January, 1971.

(24) A. Marshall and G. Peace, J. Soc. Chem. Ind. 109, 298 (1916).

(25) J.M. Rosen and C. Dickinson, "Vapor Pressures and Heats of Sublimation of Some High Melting Organic Explosives," NOL Report 69-67, 16 April 1969, AD 689112.

from published vapor-pressure data. What might be more enlightening is to estimate our own vapor pressures based on the extinction coefficients we have measured in solution. (It is not expected that these solution values will differ greatly from those appropriate to the vapor-phase compound.) We have consequently taken this latter approach in the presentation of the data for DNT as well as the other compounds studied. For example, we have determined the extinction coefficient of 2, 4 DNT in a 10% ethanol-water solution to be  $\sim 14,800$  l/mole-cm at  $\lambda$  max.  $\approx 2510$  Å (see table 4). This, coupled with an optical density of  $\sim 0.20$  at  $2300$  Å and  $40^\circ\text{C}$  (see figure 21) and a cell length of  $100$  cm, leads to a concentration of  $\sim 1.3 \times 10^{-7}$  mole/l. This in turn converts to a vapor pressure of  $2.6 \times 10^{-3}$  mm Hg at  $40^\circ\text{C}$ . This value compares reasonably well with that obtained by Pella<sup>(12)</sup> at the same temperature ( $1.3 \times 10^{-3}$  mm Hg). The basic data obtained by us for 2, 4 DNT (as well as the other compounds studied) are summarized in table 15.

From a cursory glance at figures 21 - 23, one observes that there is no pronounced enhancement of the absorbance as the temperature is raised from  $40^\circ\text{C}$  to  $60^\circ\text{C}$ . Such a change is expected, since the vapor pressure of 2, 4 DNT increases by an order of magnitude in this region.<sup>(12)</sup> This discrepancy is very likely due to adsorption losses on some of the glass and quartz surfaces of the set-up. To minimize these losses, the relevant surfaces had been maintained at a higher temperature than the solid sample. Because of "cold spots," it appears that much of the 2,4 DNT condenses on some of the surfaces of the

assembly at higher temperatures. This phenomenon of surface adsorption represents a recurring problem that we have encountered in dealing with these polar molecules.

In comparing the solution and vapor spectra for 2, 4 DNT, we note that there is a poorer resolution of the absorption bands in the latter case. This is most easily seen in figures 7 and 21. In figure 7, the band at 2500 Å is clearly separated from the higher-energy band peaking below 2100 Å. This is not so in the vapor-phase spectrum of figure 21, in which the two bands overlap more strongly. The same behavior can also be seen in the vapor-phase DNT spectrum of Gelbwachs et al.<sup>(17)</sup> and appears to be due to the shift of the absorption peak from ~2500 Å to ~2300 Å. (There seems to be no significant difference in the band widths.)

For 2, 6 DNT, the general situation is somewhat less clear, because the bands are more poorly resolved than in 2, 4 DNT. (Compare, for example, figures 21 and 24.)

This was also observed in the ethanol solution spectra (see, for example, figure 9.b and d). The data in figures 24 - 26 give evidence of an absorption shoulder at ~2300 Å. The stronger absorption at lower wavelengths obscures the precise position and intensity of this band. As was done for 2, 4 DNT, the vapor pressure of 2, 6 DNT at 40½°C can be estimated from the figures. Computation yields a value of  $2.2 \times 10^{-7}$  mole/l for the concentration and  $4.3 \times 10^{-3}$  mm Hg for the vapor pressure (see table 15 for the data used). Pella's value

for 2,6 DNT at 40°C is  $3.6 \times 10^{-3}$  mm Hg.<sup>(12)</sup> The optical densities of 2,4 and 2,6 DNT are comparable at a given temperature due to the fact that the vapor pressure of 2,6 DNT is 2 to 3 times higher than that of 2,4 DNT for the temperatures studied. The lack of a pronounced increase in the absorbance as the temperature is raised is once again probably attributable to adsorption effects.

An interesting trend that was first mentioned in the previous section on solution spectra can be extended to the vapor spectra for 2,4 and 2,6 DNT. It has been mentioned in the discussion of the solution spectra that the less polar the solvent, the higher the absorption energy for nitro compounds (as was seen in figures 6 and 7 for 2,4 DNT). The molecules present in the vapor phase of a compound experience no polar environment at all and should have levels shifted upwards in energy compared with the solution levels. This is in fact observed for 2,4 DNT (see figures 6, 7 and 21). In the case of 2,6 DNT, the trend is more difficult to verify, because the location of the band maximum in the vapor phase cannot be reliably determined from the figures. What can be seen, however, is the decidedly poorer band resolution in the vapor spectra. In comparing the spectra in figures 10d, 9d and 24 for 2,6 DNT, we see that the less polar the environment the less well-defined the peak is. In figures 10d and 9d this can be seen as due to the shift of the peak. This implies a further shift in the case of the vapor-phase peak in figure 24.

The results for 2, 3 DNT show no well-defined absorption maximum in the 2100 - 3000 Å region (figures 27 and 28). This is consistent with the findings of Conduit<sup>(6)</sup> who reports only an absorption tail with shoulders for  $\lambda > 2100$  Å in a 5% ethanol-water solution. Our solution data (figure 10a) reveal a weak maximum on the low-energy side of the stronger tail. This band, however, appears to be only a shoulder in the vapor phase.

Because of the weakness of the absorption for the temperatures studied, it is difficult to estimate the vapor pressure in this case. To our knowledge, there is no vapor-pressure data for 2, 3 DNT in the literature.

#### TNT

Figures 29 - 31 depict the absorption spectra of the vapors evolved from Military Grade TNT for various temperatures. By a comparison with known data<sup>(26)</sup> and spectra obtained by us, it appears that most of the absorption is due to a toluene impurity. This conclusion is supported by the fact that recrystallization and pumping virtually eliminates all the absorption (figure 32). The Eastman 2, 4, 6 TNT similarly produces mainly toluene absorption bands (figures 33 and 34). Overnight pumping results in a reduced absorption (figure 35), but the structure does not disappear. Evidently, toluene was used in the manufacturing or purification of the Eastman TNT.

---

(26) J.G. Calvert and J.N. Pitts, Jr., Photochemistry (John Wiley and Sons, Inc., N.Y., 1966) ppg. 264, 499.

Neither the Military Grade nor the Eastman 2, 4, 6 TNT showed any vapor-phase absorption due to the TNT itself. This is not surprising in view of the low vapor pressure for this compound. One can, in fact, estimate the expected optical density using known vapor pressures<sup>(12)</sup> and the extinction coefficient determined in the solution phase of this work (20,000 l/mole-cm). For 56.5°C, this leads to an optical density of ~0.04. Such a low signal is only barely recognizable with the techniques used. Furthermore, any adsorption losses would only further reduce this value and the frequent presence of toluene impurities would tend to mask this contribution.

What is somewhat surprising is the absence of any DNT absorption in the Military Grade spectra. (One would not expect to observe the presence of this compound in the pure Eastman sample.) Either the concentration of DNT is inherently low in our Military Grade sample or else adsorption losses reduced the effective concentration in the absorption cell.

#### Nitroglycerine

As is seen in figure 37, there is a rather strong absorption band for  $\lambda \leq 2500 \text{ \AA}$  and this is accompanied by a weak band centered at  $\sim 2800 \text{ \AA}$ . Both features are also observed in solution (see figure 17). Because our sample is not pure nitroglycerine, it is not clear whether the weaker band is due to the nitroglycerine or an impurity. A definitive answer would require purification of the sample.

Some of our data seem to support the contention that the nitroglycerine itself gives rise to the observed band. For example, the ratio of the optical densities at  $\lambda = 2100 \text{ \AA}$  and  $\lambda = 2800 \text{ \AA}$  is  $\sim 12$  in the vapor phase and  $\sim 14$  in an ethanol solution. If the two bands represented absorption by two different compounds, the presumably different vapor pressures would change this ratio. Such an argument is not at all conclusive, however, since it does not take into account the possible shift of the higher-energy band in going from solution to the vapor phase. Because the origin of the weak  $2800 \text{ \AA}$  band is uncertain, it is not included in table 15.

#### Amines

For diphenylamine, the band of interest lies in the  $2400\text{--}3000 \text{ \AA}$  region. The general appearance of this absorption gives an indication of overlapping bands (see figures 38 and 39). In fact, a spectrum obtained by Gelbwachs et al.<sup>(17)</sup> at  $65^\circ\text{C}$  shows this more clearly. In order to obtain a continuous curve for diphenylamine (and, therefore, better discern the structure), we attempted to record a spectrum on a Cary 14 at elevated temperatures ( $\sim 50^\circ\text{C}$ ) and with 10 cm cells. For this compound, however, we had a problem with condensation on the cell windows at these temperatures. A room-temperature spectrum revealed a general agreement with figure 38, but the absorption was too weak to show any detail.

The vapor pressure of diphenylamine at  $24^\circ\text{C}$  and  $45^\circ\text{C}$  can be calculated as described earlier. The value obtained at  $24^\circ\text{C}$  is  $8.9 \times 10^{-4} \text{ mm Hg}$ . This compares with a value of  $3.1 \times 10^{-3} \text{ mm Hg}$



which can be obtained by extrapolating the data found in the CRC Handbook of Chemistry and Physics.<sup>(1)</sup> The spectrum obtained for 45°C yields a value of  $1.2 \times 10^{-3}$  mm Hg; extrapolation of the data in the CRC Handbook results in a vapor pressure of  $1.8 \times 10^{-2}$  mm Hg at the same temperature. This trend further indicates the difficulties encountered in preventing adsorption for elevated temperatures. Table 15 summarizes these results for diphenylamine.

An interesting feature of the vapor-phase spectra can be seen through a comparison with the solution spectra (see figures 14 and 15). In the solution data, one notices that the absorption maximum for diphenylamine resides in the 2800 - 2850 Å region for the solvents used. The widths of these bands run from ~350 Å (in ethanol) to ~475 Å (in water). The vapor band is somewhat wider (~550 Å) and is centered at ~2650 Å. In going from solution to vapor, therefore, there is a broadening and a shift of 150-200 Å towards shorter wavelengths for this band. This brings the band closer to its higher-energy counterpart and increases their overlap. This is seen most readily by computing the ratio of the optical density of the band maximum to that of the intervening minimum. In the solution, this ratio is ~7, ~3, and ~3 for the ethanol, 5% ethanol-water, and water solutions, respectively. From our vapor-phase spectra, this ratio is 1.5-2; the spectrum obtained by Gelbwachs et al.<sup>(17)</sup> yields a ratio of ~1 3/4. This tendency to smear out structure was

also observed for 2, 4 and 2, 6 DNT and results in a poorer resolution of the two absorption bands. This of course, inhibits the possibility of identifying such a vapor through its absorption spectrum.

In the case of monomethylamine, the problem of adsorption does not arise, because it is a gas under normal laboratory conditions. Our spectrum at room temperature is presented in figure 40 and agrees with previously published spectra.<sup>(20,27)</sup> Because this system has been relatively well studied, there is no need to enter into great detail here. The sharp lines observed are due to vibronic transitions, with the prominent modes having frequencies of  $\sim 660 \text{ cm}^{-1}$  (amino group)<sup>(27)</sup> and  $\sim 1000 \text{ cm}^{-1}$  (CN vibration).<sup>(20)</sup> Because of the distinctive appearance of this spectrum, the presence of monomethylamine is rather easily verified as long as the signal itself is strong enough. Some data for monomethylamine are presented in table 15 for the sake of completeness. It should be noted, however, that the sample was examined at a very reduced pressure in order to obtain optical densities of the proper magnitude to be displayed on the Cary 14 chart paper. Consequently, the extinction coefficient of the absorption is not obtainable from figure 40. From the work of Tannenbaum et al.,<sup>(20)</sup> the maximum extinction coefficient for the band displayed in the figure is 600 l/mole-cm.

The spectrum of ethyl centralite presented in figure 41 reveals a broad absorption band whose maximum resides in the

---

<sup>(27)</sup> T. Förster and J.C. Jungers, Z. physik. Chem. B36, 387 (1937).

2500 Å region. This band is seen as a shoulder to the higher-energy band which peaks below 2100 Å. As such, the location and width of the lower-energy band are difficult to determine accurately. It appears, however, that this latter band has broadened considerably in going from the solution to the vapor phase. (The bandwidths are ~400 Å, ~500 Å, and ~600 Å for the ethanol solution, water solution, and vapor, respectively.) The three spectra in figures 16 and 41 point to the following trend. The shift of the absorption peak is rather small in the two solution spectra (~25 Å). The bandwidths, however, change more dramatically. This increased bandwidth for the water solution results in a poorer resolution of the two absorption bands (figure 16). In the vapor spectra, the broadening has increased and led to a complete smearing out of the lower-energy band, so that no well-defined maximum is observed. One sees, therefore, that for ethyl centralite vapor, the lack of resolution between the bands is essentially a broadening effect. In diphenylamine, the poorer resolution was a combination of shift and broadening and for the isomers of DNT simply a shift. An important point to make here is that the amine broadening, as mentioned in the section on solution spectra, is not attributable to polarity effects. This is because the broadening increases in the order ethanol-water-vapor. This progression is not in order of polarity. For the amines, therefore, an added mechanism is present which affects the width of the observed band and consequently the ability to distinguish it from the higher-energy absorption.

Based on the observed optical density, one can estimate the vapor pressure for ethyl centralite using the extinction coefficient calculated for the 5% ethanol-water solution. (We pick this value because the bandwidth in this solution is closer to the vapor bandwidth.) This computation yields a value of  $\sim 7.8 \times 10^{-3}$  mm Hg. From previous considerations, this result is, of course, a lower bound to the actual vapor pressure. To our knowledge, there are no data on the vapor pressure of ethyl centralite in the literature, so no comparisons are possible. The relevant data for ethyl centralite are summarized in Table 15.

#### Cyclohexanone and RDX

In cyclohexanone, the pronounced peak at 2900 Å is well-separated from the higher-energy peak. As a result, the resolution of the two bands is very good. This and the minimal potential interference from most of the other compounds studied make it an attractive compound for use in identification purposes. Of course, this approach ultimately depends on the U.V. spectra of other possible atmospheric constituents not studied here. From figure 42 and the extinction coefficient of 11 l/mole-cm from Calvert and Pitts,<sup>(28)</sup> the vapor pressure can be calculated to be 6.5 mm Hg. This is about a factor of five smaller than the value obtained by interpolating the vapor-pressure data given in the Handbook of Physics and Chemistry<sup>(1)</sup> (34 mm Hg). These data are included in table 15.

(28) J.G. Calvert and J.N. Pitts, Jr., Photochemistry (John Wiley and Sons, Inc., N.Y., 1966) pg. 409.

Interpreting the spectrum of vapors evolved from RDX presents an intrinsic problem. The vapor pressure of this compound is extremely low at room temperature. (The highest value quoted in the literature is  $7 \times 10^{-7}$  mm Hg.)<sup>(13)</sup> Therefore, absorption due to the impurities in the sample could easily mask any absorption due to the RDX itself. In addition, the vapor pressure of RDX at elevated temperatures is apparently not known. (We could find only room-temperature data in the literature.) Consequently, it is not possible to attribute any observed bands to RDX by appealing to vapor-pressure considerations and estimated extinction coefficients. The spectrum of figure 43, therefore, may be characteristic of vapors evolved from RDX, but may not be due to RDX itself. Although the spectra of figures 13 and 43 are not dissimilar, it would be unwarranted to make any assignment. Further study of the vapor pressure and absorption spectrum of RDX is needed. For the 2150 - 2700 Å band to be due to RDX, the vapor pressure of this compound at 80°C would have to be at least  $1.5 \times 10^{-3}$  mm Hg. Because the origin of this band is not certain, it is not included in table 15.

#### PETN

The spectrum of vapors emanating from this compound (figure 44) shows a measurable absorption up to ~2500 Å. This is in contrast to the solution spectra of figure 18, which indicates a cut-off at ~2300 Å. The reason for this is not clear. There is some evidence of a shoulder at ~2300 Å in the

vapor data. Based on the solution work, it would appear that such a shoulder would have to be attributed to a higher vapor-pressure impurity. Further work on a purified sample is advisable at this stage. The solution data of the previous chapter indicate that PETN, like the other nitroxy compound nitroglycerine, does not itself absorb appreciably above  $\sim 2300 \text{ \AA}$ .

#### General Remarks

In evaluating the detectability of the above compounds by means of U.V. absorption spectra, one must keep several points in mind. First, with the exception of monomethylamine, none of the explosive-related compounds studied reveal any sharp-line absorption due to the pure compound itself. In fact, only the spectra of monomethylamine and cyclohexanone show any distinguishing features. (In the latter case, the absorption occurs at a relatively high wavelength:  $\sim 2900 \text{ \AA}$ .) Secondly, the vapor spectra of most of the compounds studied show a poorer resolution between the higher and lower energy bands than is evident in solution. For the nitro-containing compounds (2, 4 and 2, 6 DNT), this is due to a shift of the lower-energy band. We have been able to correlate this effect with the polarity of the environment of the molecule. For the amines, a broadening also contributes to the poorer resolution in the vapor phase. In the case of diphenylamine, a broadening and a shift both play a major role; for ethyl centralite, the effect seems to be purely a broadening of the lower-energy band.

The nitroxy compounds (nitroglycerine and PETN), on the other hand, appear to have a very weak absorption for  $\lambda \approx 2300 \text{ \AA}$ . Detection of these compounds through their U.V. spectra is not at all feasible, but at the same time they do not interfere with the detection of the other compounds.

For RDX, detection is difficult because of the low vapor pressure. Perhaps detection through cyclohexanone would be the only practical approach. As was seen in our study, though, RDX can be purified so as to remove all optical traces of the cyclohexanone. (The low extinction coefficient of the relevant band of cyclohexanone,  $\sim 11 \text{ l/mole-cm}$ , adds to the problem.) Many of the same problems exist for detecting TNT through the presence of DNT. As was mentioned earlier, the compounds RDX and PETN require further study.

Finally, in table 16 we estimate the minimum concentrations detectable with the technique employed in this study. It is evident that our absorption technique could be improved upon (for example, by making it a dual-beam apparatus and employing a multiple-pass cell). In particular, if the exciting light is allowed to make  $\sim 10^2$  passes through the cell, we can increase the sensitivity by about two orders of magnitude. The table, however, presents figures only for the experimental set-up actually used in this study. In computing the values, we have considered that an optical density of at least 0.05 is needed for reliable detection if no interfering species are present. In the real world, however, the inevitable interferences could substantially affect the applicability of the figures in the table. These limits, therefore, are to be interpreted as the minimum detectable concentrations under optimal conditions. Because of the previously mentioned problems with literature vapor-pressure values, no attempt is made to relate these concentrations to a temperature.

TABLE 15

Summary of Data Obtained in Vapor-Phase Absorption Studies

Compound	T(°C)	$\lambda$ max. ( $\mu$ )	$\epsilon(\lambda \text{ max.})$ in l/mole-cm*	O.D. ( $\lambda$ max.)	V.P. (mm Hg) (calculated)	V.P. (mm Hg) (literature)	Reference
2, 4 DNT	40	~2300	14,800	0.20	$2.6 \times 10^{-3}$	$1.3 \times 10^{-3}$	12
2, 6 DNT	40½	~2300	8,700	0.19	$4.3 \times 10^{-3}$	$3.6 \times 10^{-3}$	12
Diphenylamine	24	~2600	14,600	0.07	$8.9 \times 10^{-4}$	$3.1 \times 10^{-3}$	1
	45	~2600	14,600	0.09	$1.2 \times 10^{-3}$	$1.8 \times 10^{-2}$	1
Monomethylamine	23	~2170	600	0.25	-----	-----	-----
Ethyl Centralite	76	~2500	6,400	0.23	$7.8 \times 10^{-3}$	-----	-----
Cyclohexanone	64	~2900	11	0.34	6.5	34	1

96

\*Except for monomethylamine and cyclohexanone, these values are taken from the solution data of Chapter 3. The values for monomethylamine and cyclohexanone are from references (20) and (28), respectively.



TABLE 16

Minimum Detectable Concentrations of Explosive-Related Materials  
(Using the Technique Employed in This Study)

Compound	Minimum Detectable Concentration (moles/l)
2, 4 DNT	$3.4 \times 10^{-8}$
2, 6 DNT	$5.7 \times 10^{-8}$
TNT	$2.5 \times 10^{-8}$
Ethyl Centralite	$7.8 \times 10^{-8}$
Diphenylamine	$3.4 \times 10^{-8}$
Monomethylamine	$8.3 \times 10^{-7}$
RDX	$4.8 \times 10^{-8}$
Cyclohexanone	$4.5 \times 10^{-5}$

Note: Above concentrations were calculated from the formula:  
 $C = O.D./\epsilon L$ , where  $O.D. = 0.05$ ,  $L = 100$  cm, and  $\epsilon$  is obtained  
from table 15. The extinction coefficients for TNT and RDX  
were taken from our solution data.

Absorption Spectrum of Toluene Vapor.  
(Vapor Generated at 23°C)  
Absorption peaks correspond to minima in the  
transmitted intensity. The spectrum has not  
been corrected for lamp intensity and system  
response.

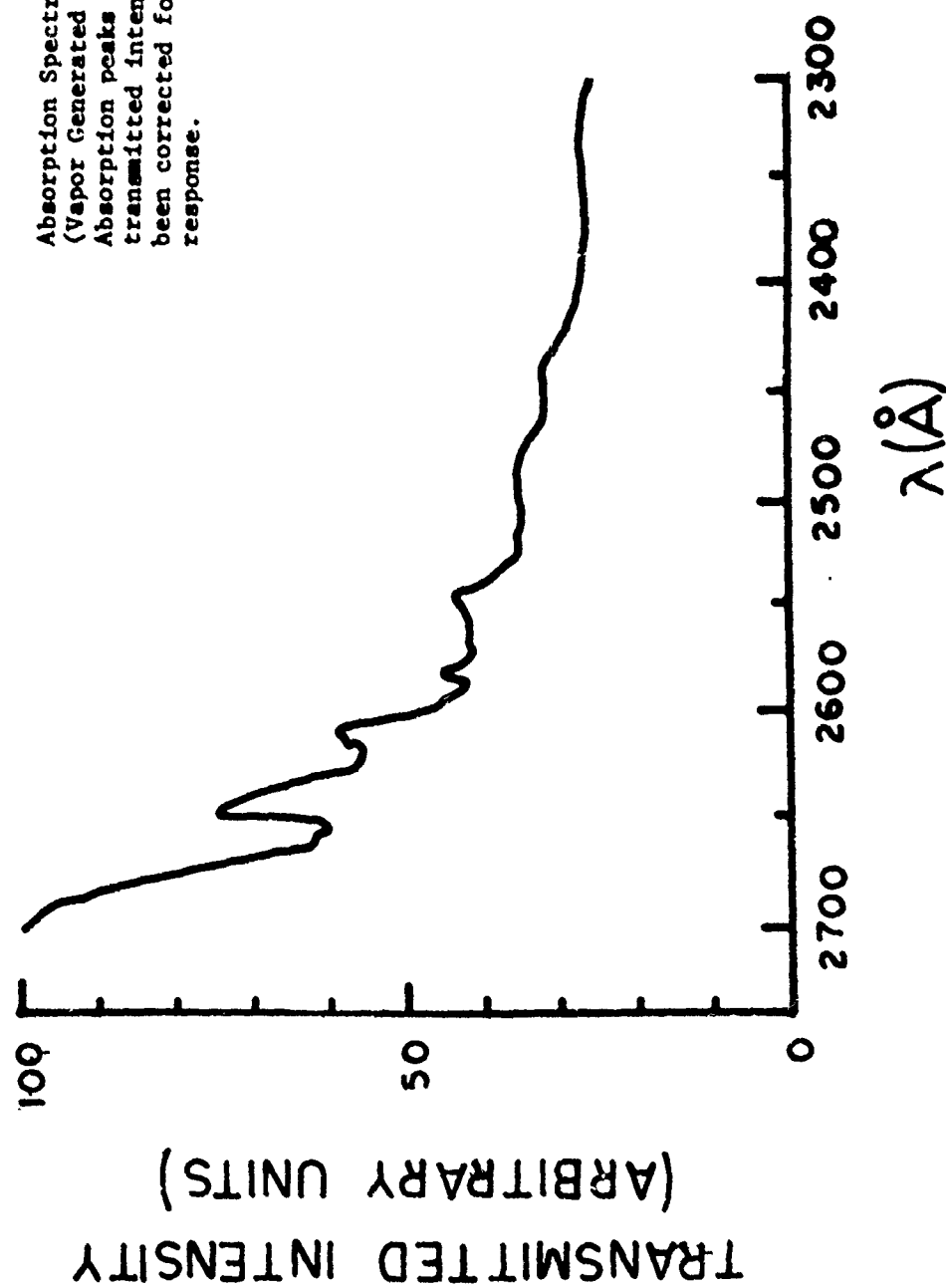


Figure 19

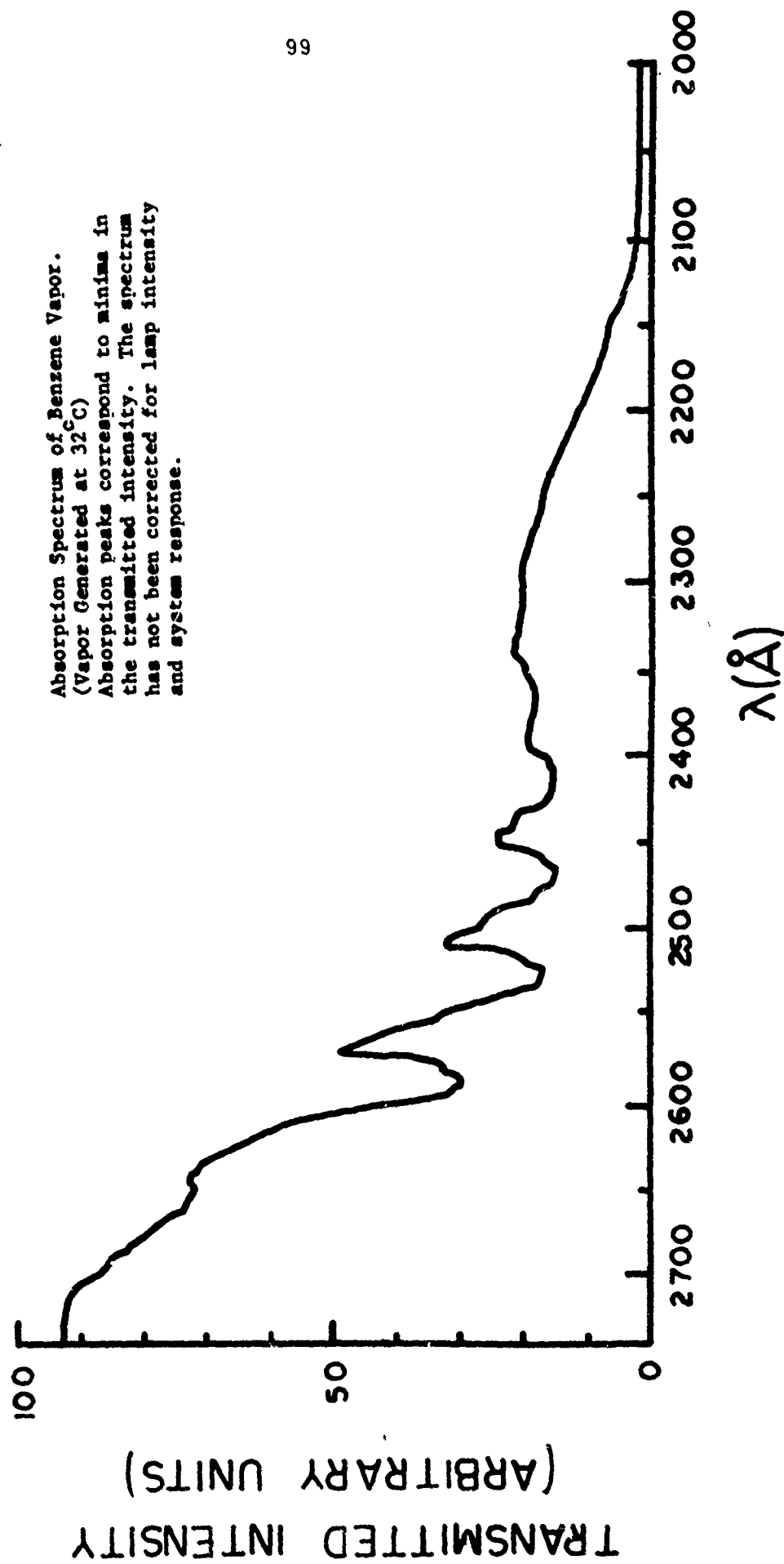


Figure 20

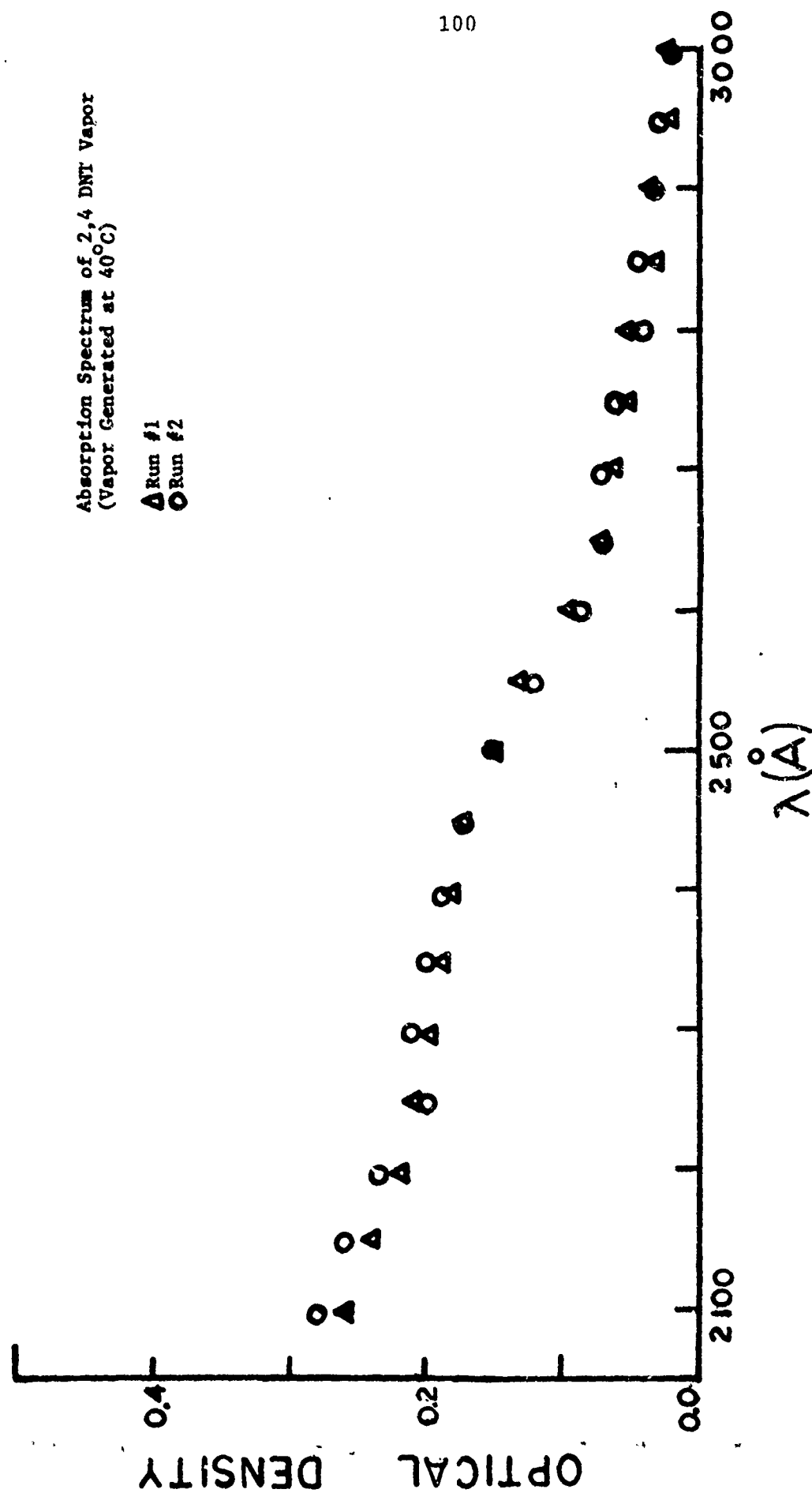


Figure 21

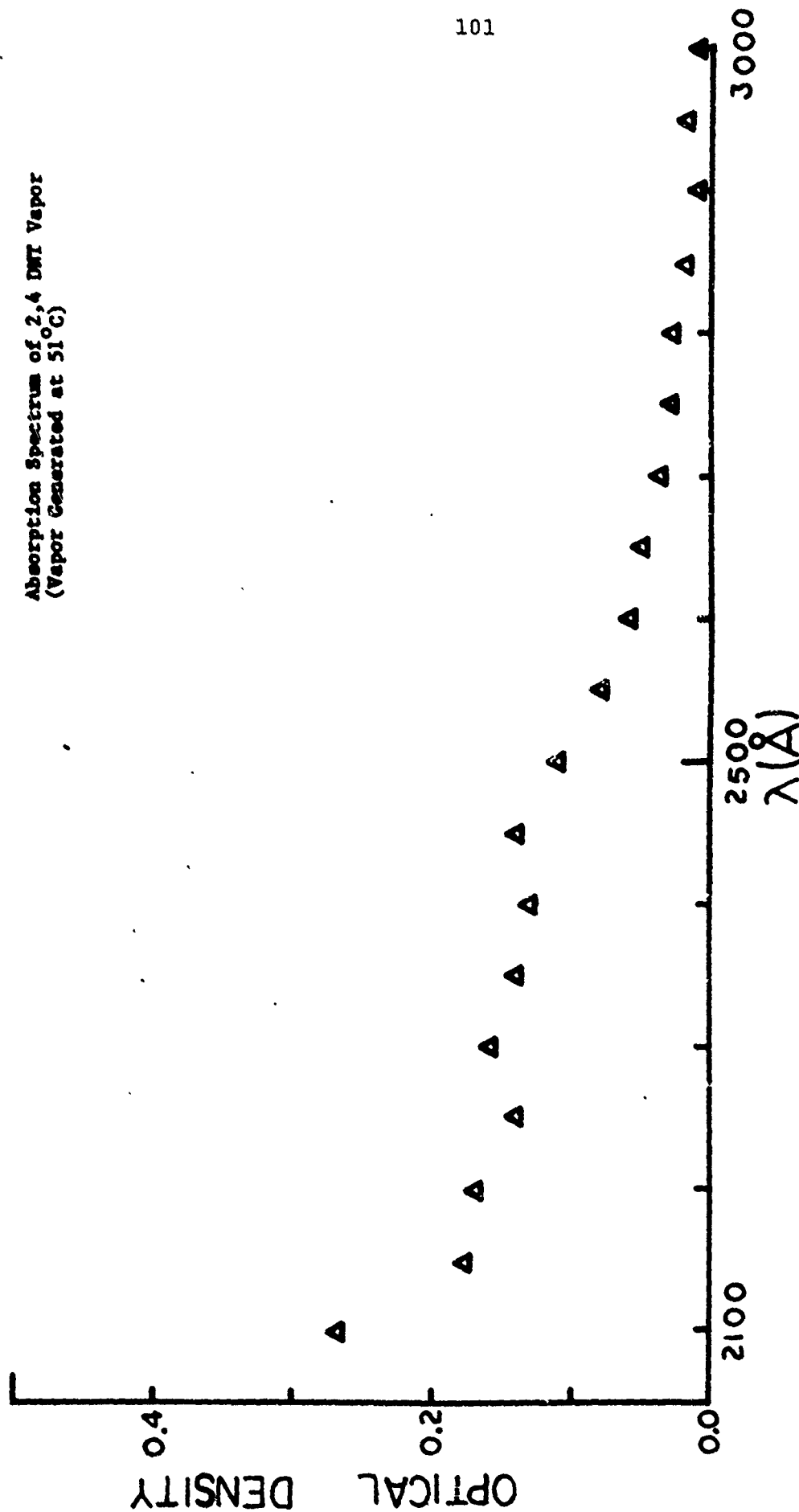


Figure 22

Absorption Spectrum of 2,4 DNT Vapor  
(Vapor Generated at 60°C)

△ Run #1  
○ Run #2

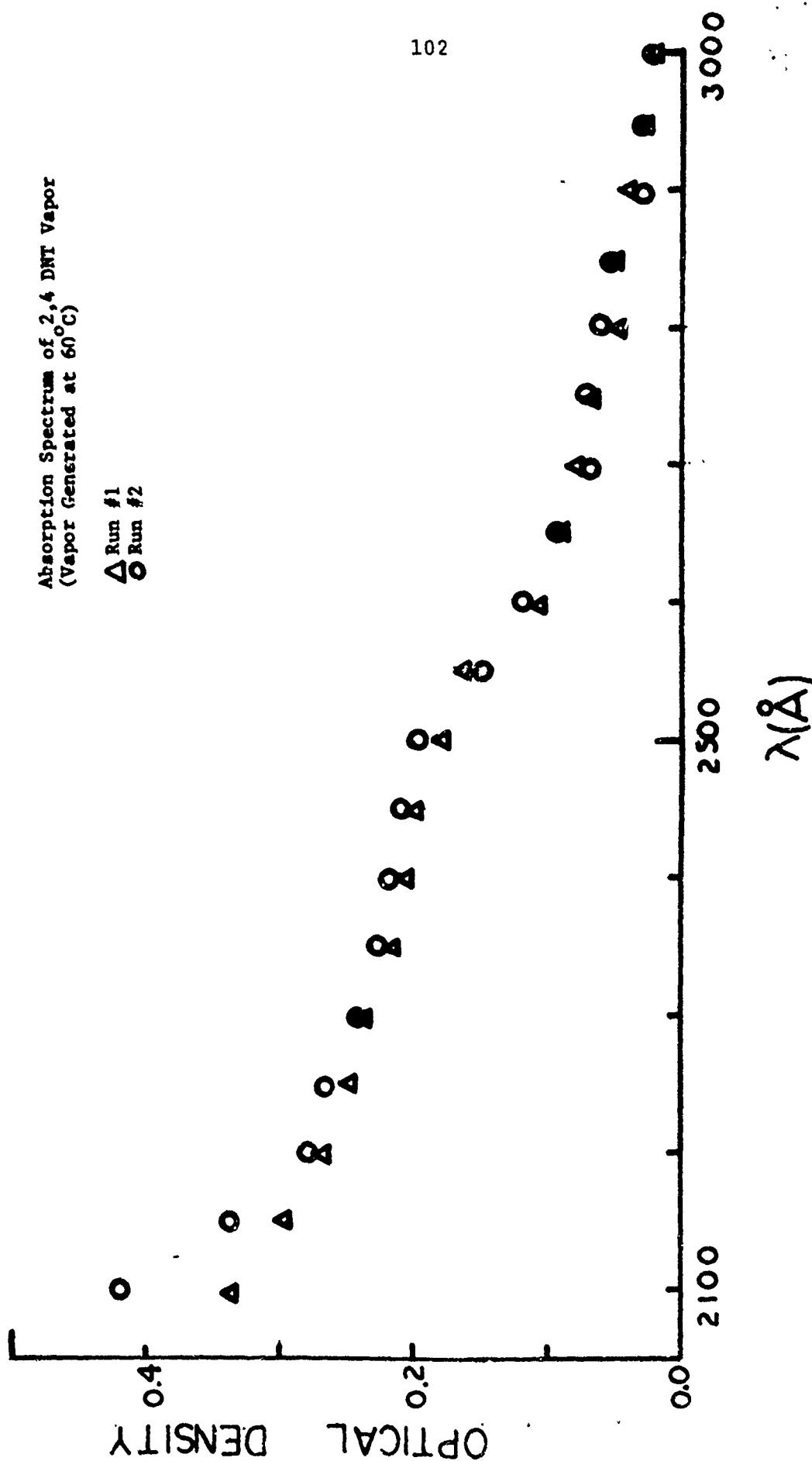


Figure 23

Absorption Spectrum of 2,6 DNT Vapor  
(Vapor Generated at 40 $\frac{1}{2}$ °C)

$\Delta$  Run #1  
 $\circ$  Run #2

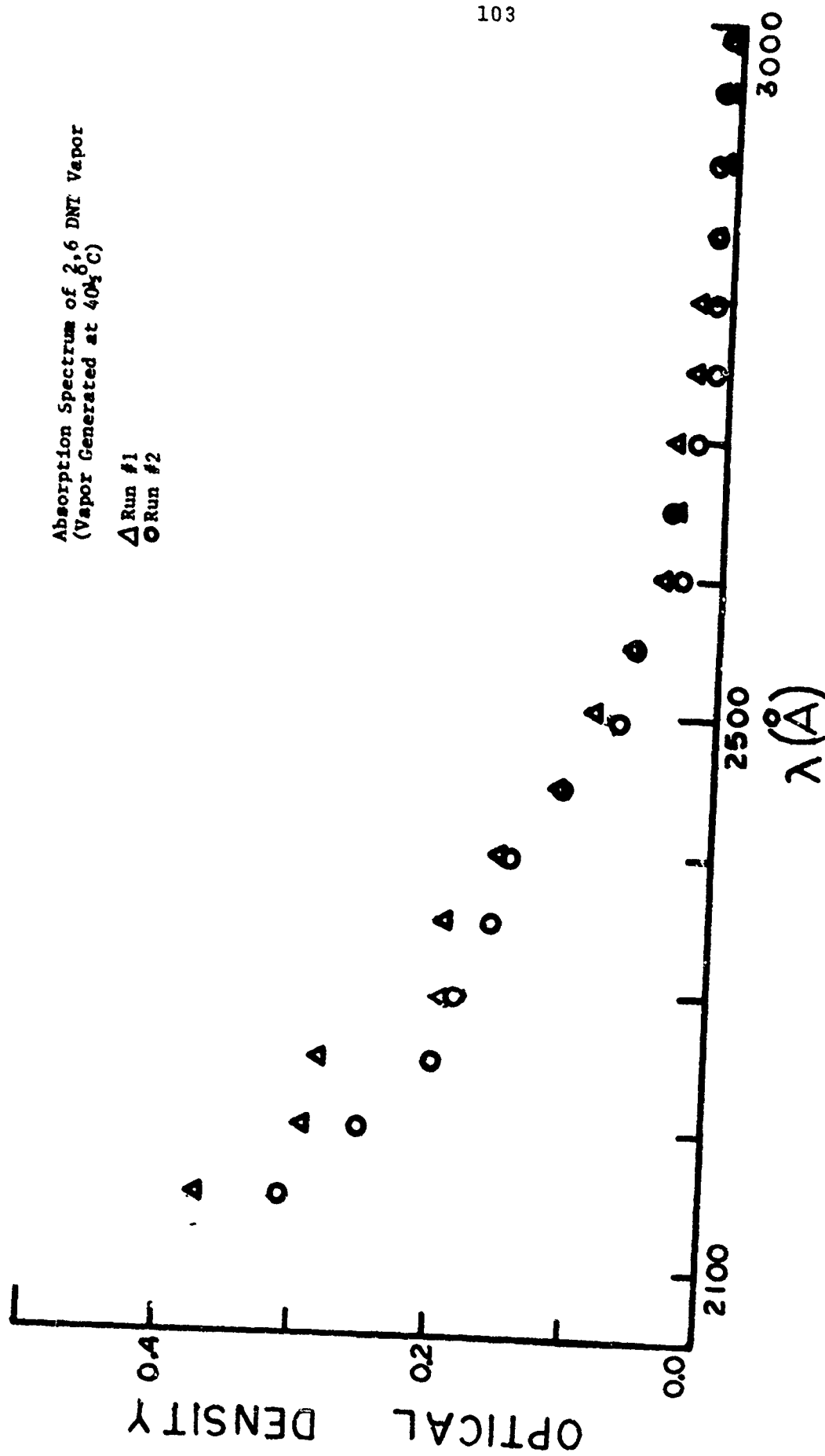


Figure 24

Absorption Spectrum of 2,6 DMT Vapor  
(Vapor Generated at 51°C)

Δ Run #1  
○ Run #2

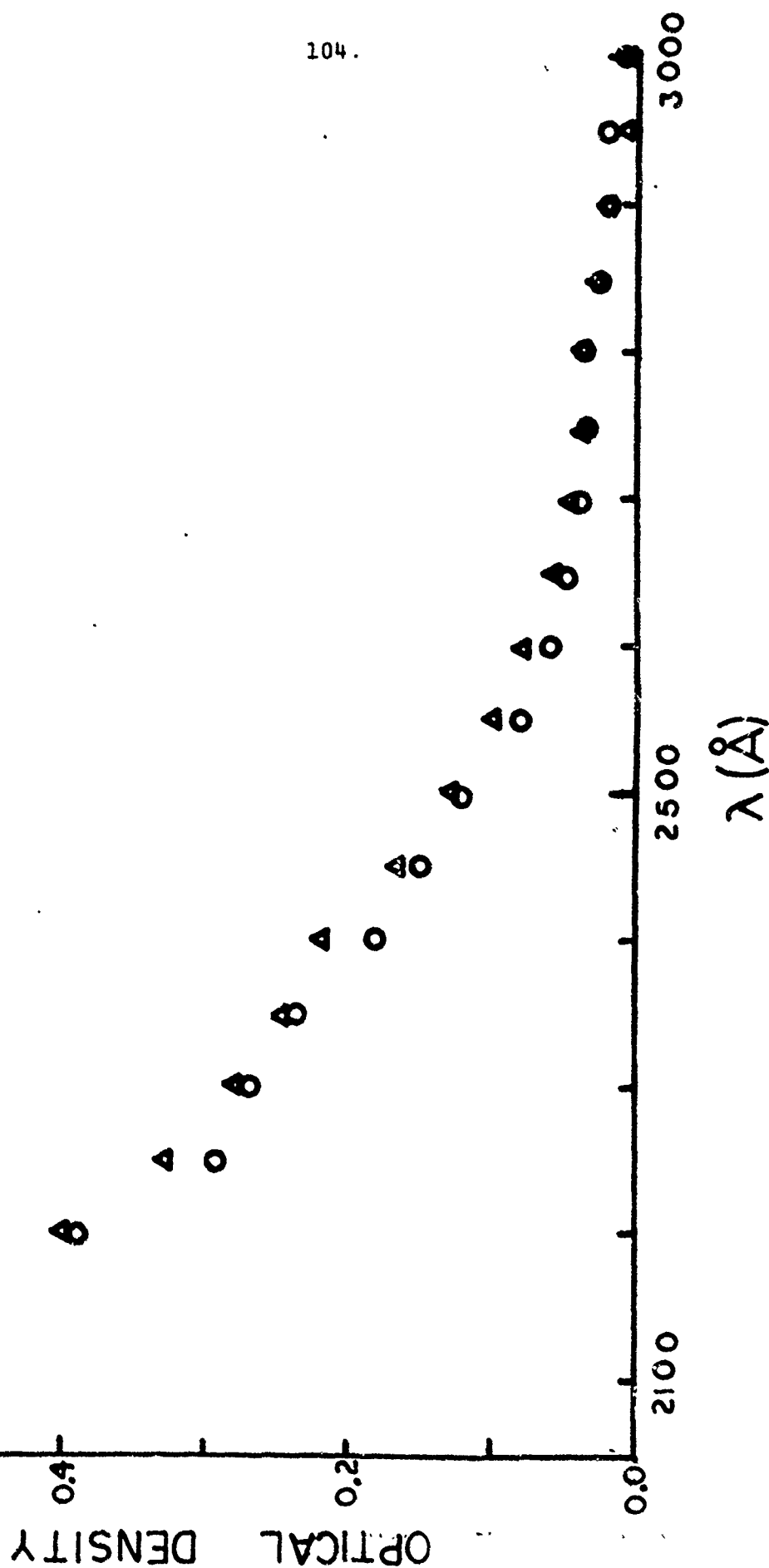


Figure 25



Absorption Spectrum of 2,6 DMT Vapor  
(Vapor Generated at 59°C)

Δ Run #1  
○ Run #2

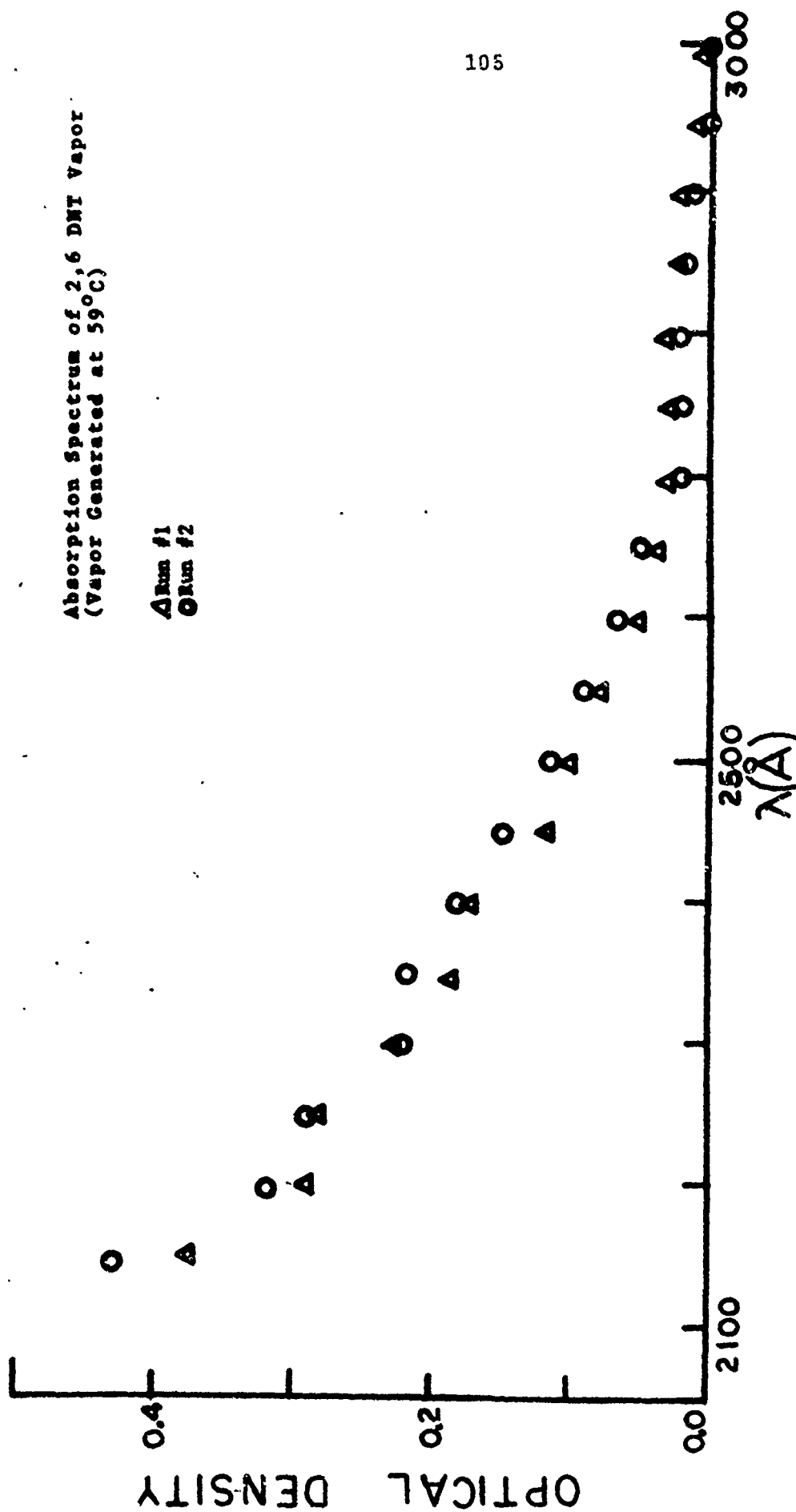


Figure 26

Absorption Spectrum of 2,3 DNT Vapor  
(Vapor Generated at 42°C)

$\Delta$  Run #1  
O Run #2

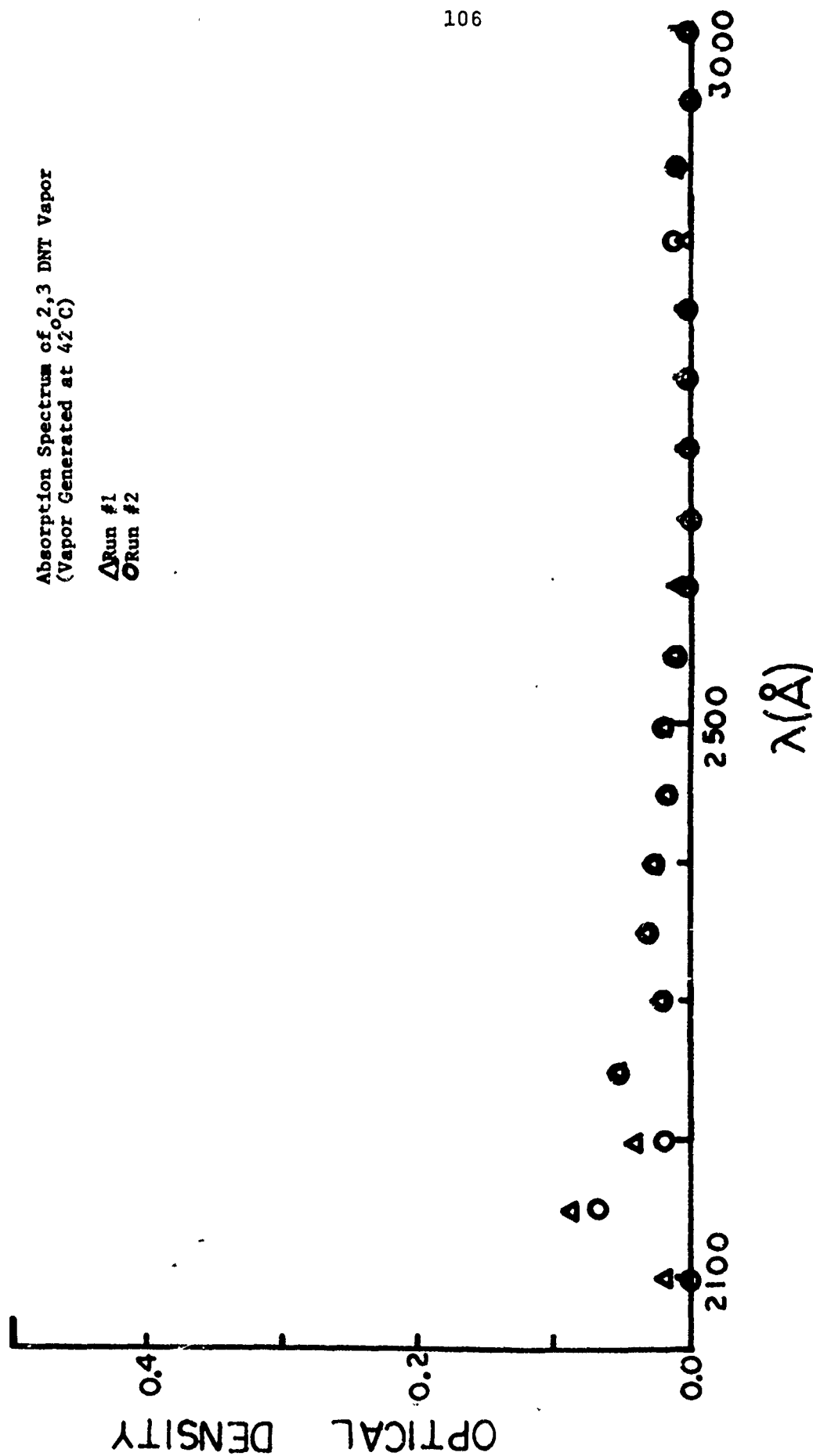


Figure 27

Absorption Spectrum of 2,3 DNT Vapor  
(Vapor Generated at 52°C)

△ Run #1  
○ Run #2

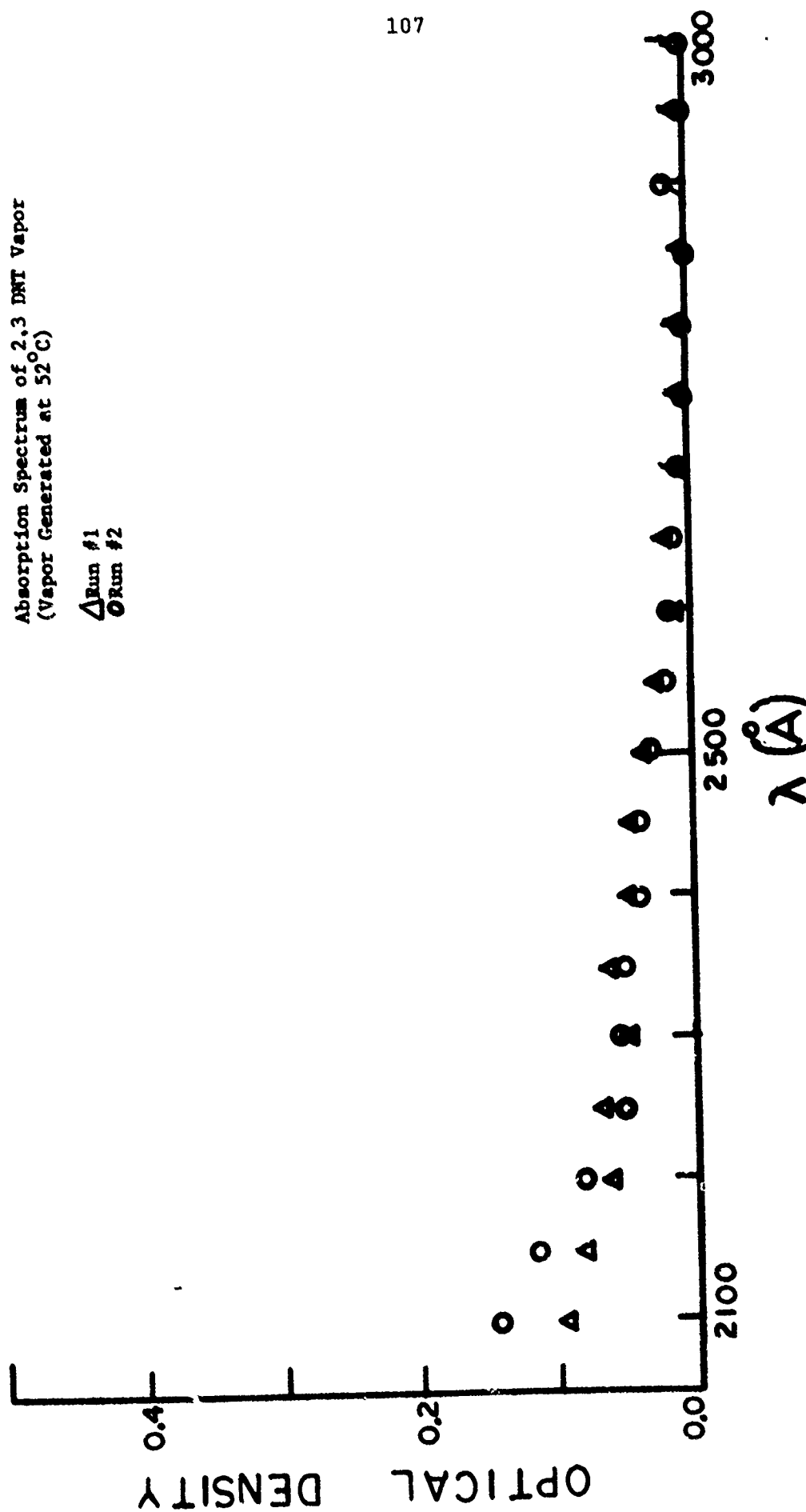


Figure 28

Absorption Spectrum of Vapors Evolved from  
Military Grade TNT  
(Vapors Generated at 29°C)

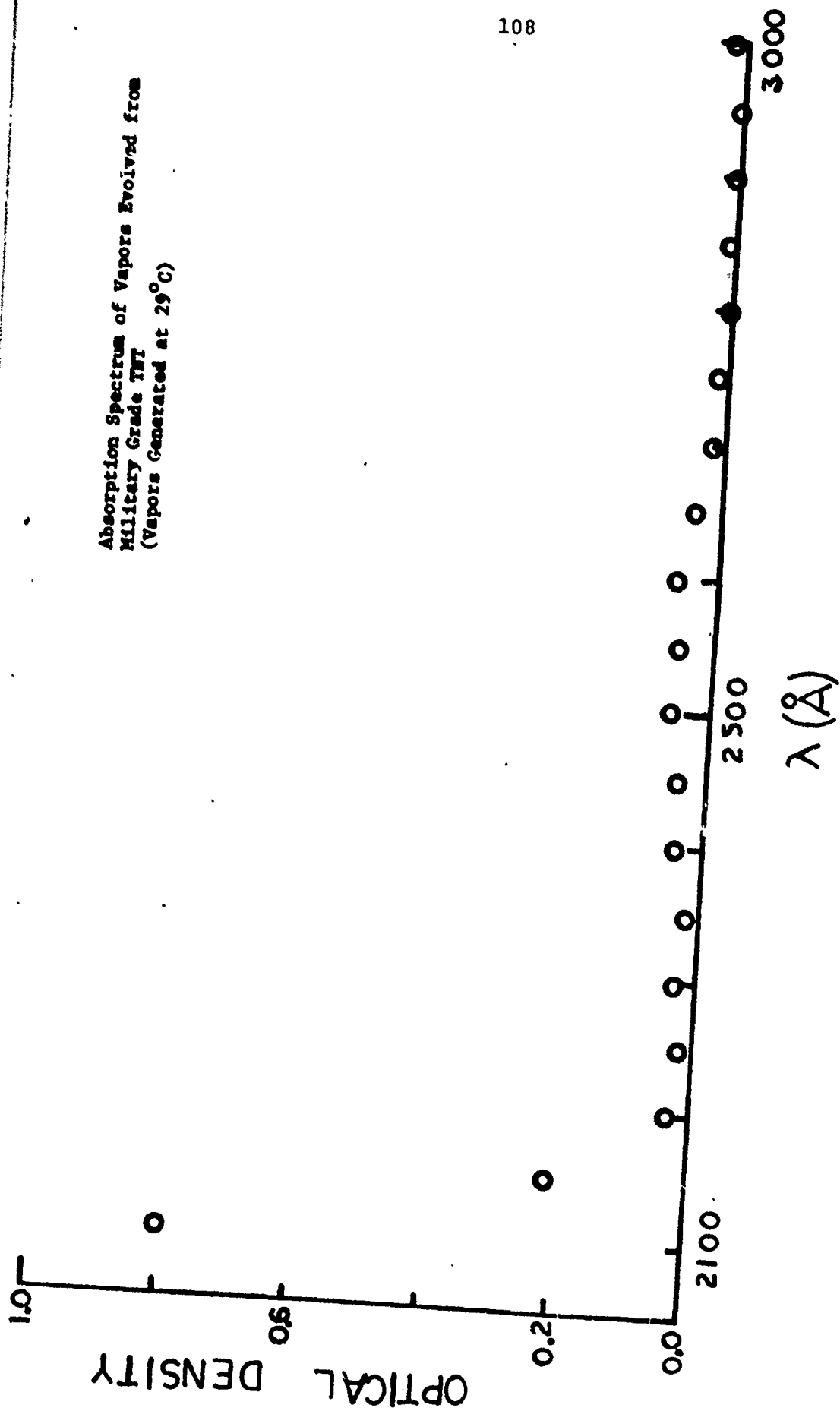


Figure 29

Absorption Spectrum of Vapors Evolved from  
Military Grade TNT  
(Vapors Generated at 50°C)

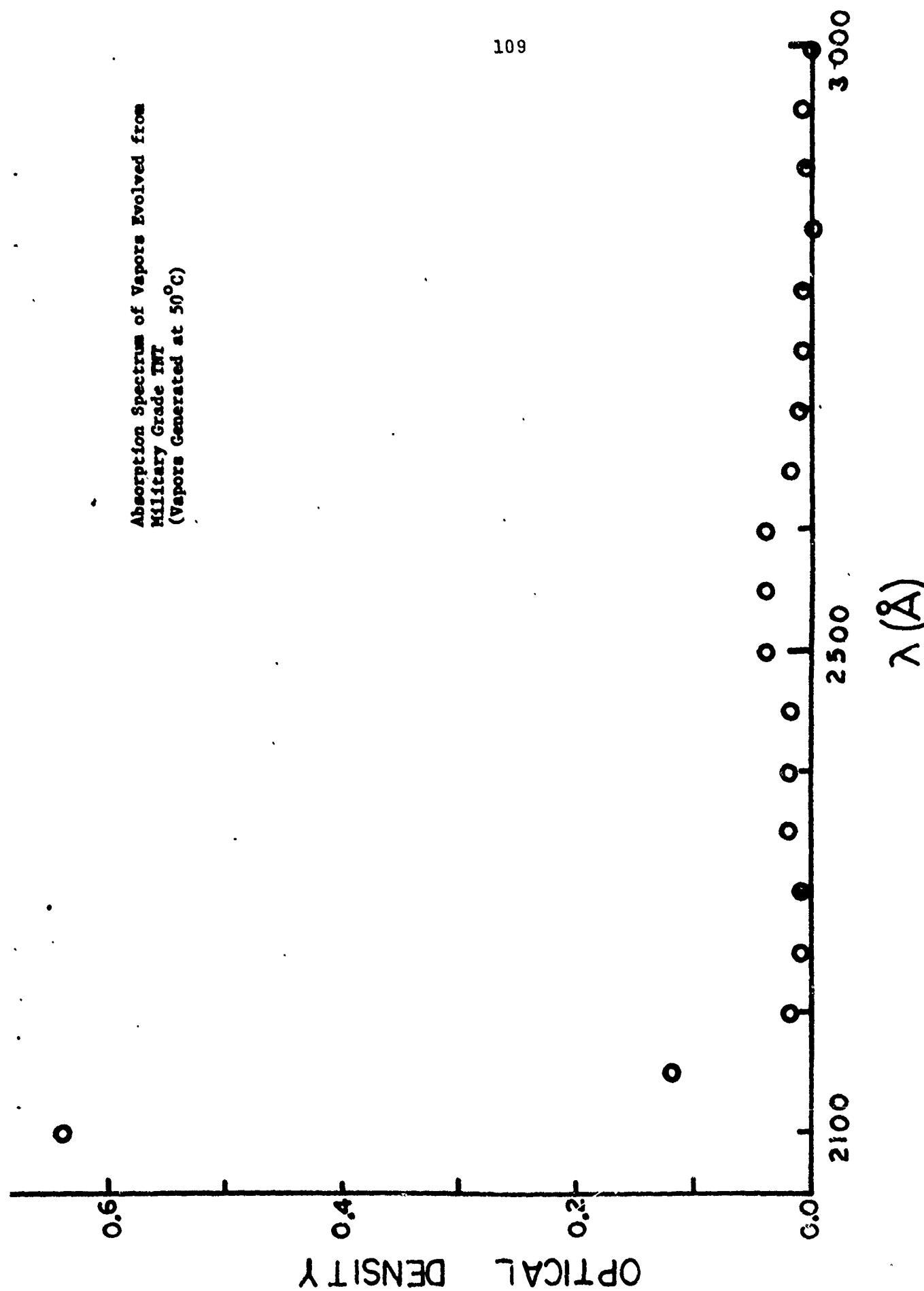


Figure 30

Absorption Spectrum of Vapors Evolved from  
Military Grade TNT  
(Vapors Generated at 69°C)

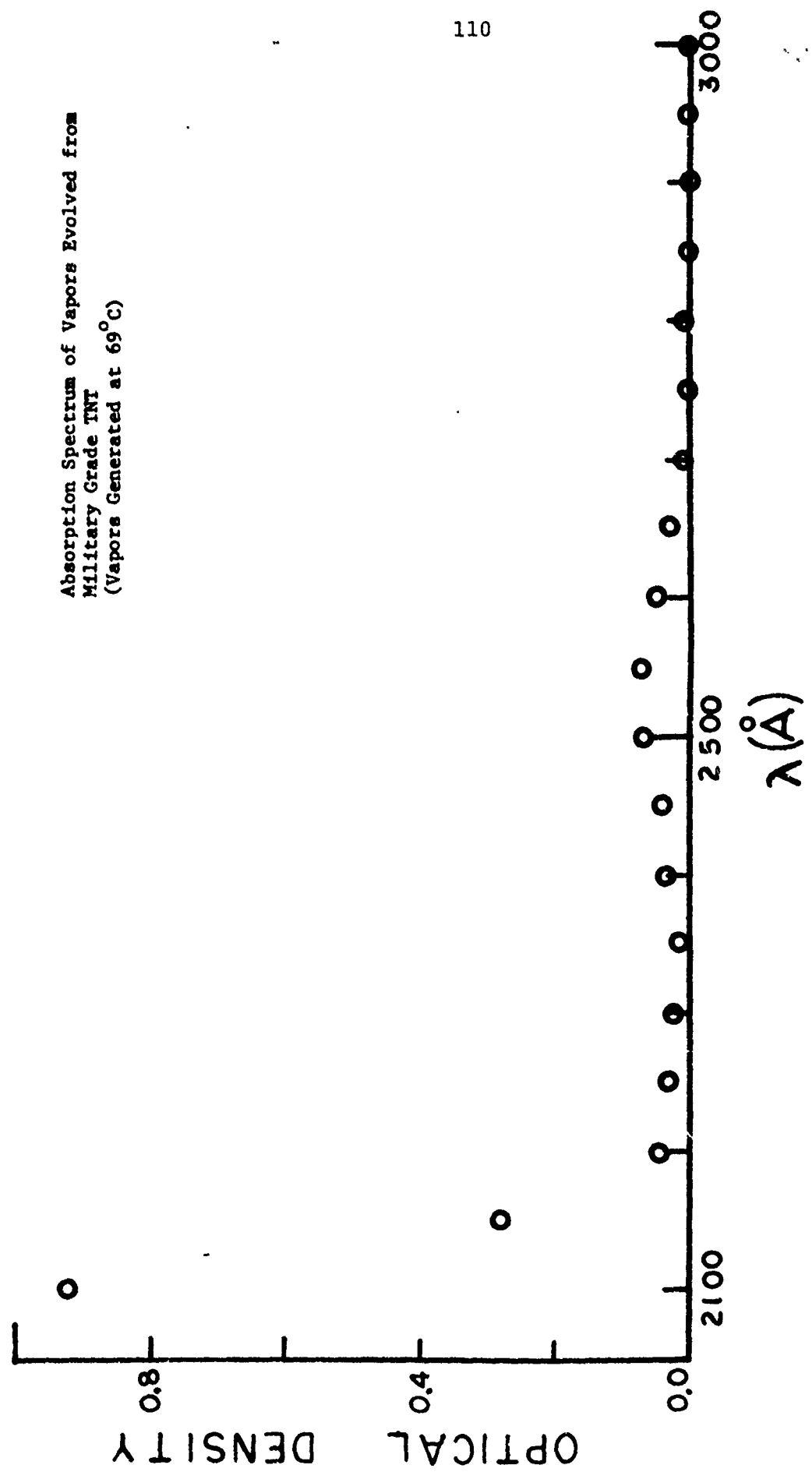


Figure 31

Absorption Spectrum of Vapors Evolved from TNT  
(Recrystallized from Military Grade and  
Pumped on for 32 Hours. Vapors Generated at  
60°C)

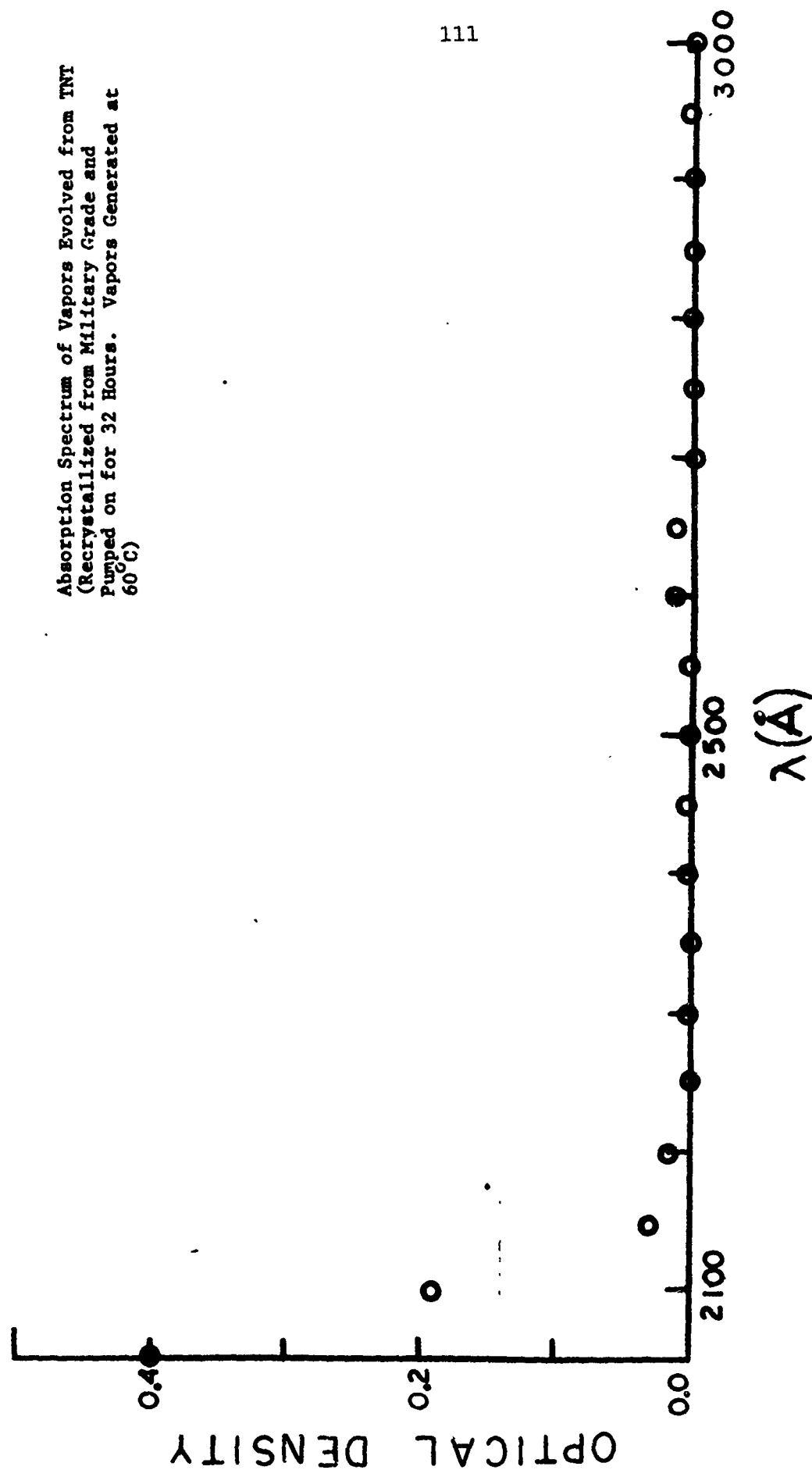


Figure 32

Absorption Spectrum of Vapors Evolved from  
Eastman 2,4,6 TNT  
(Vapors Generated at 42°C)

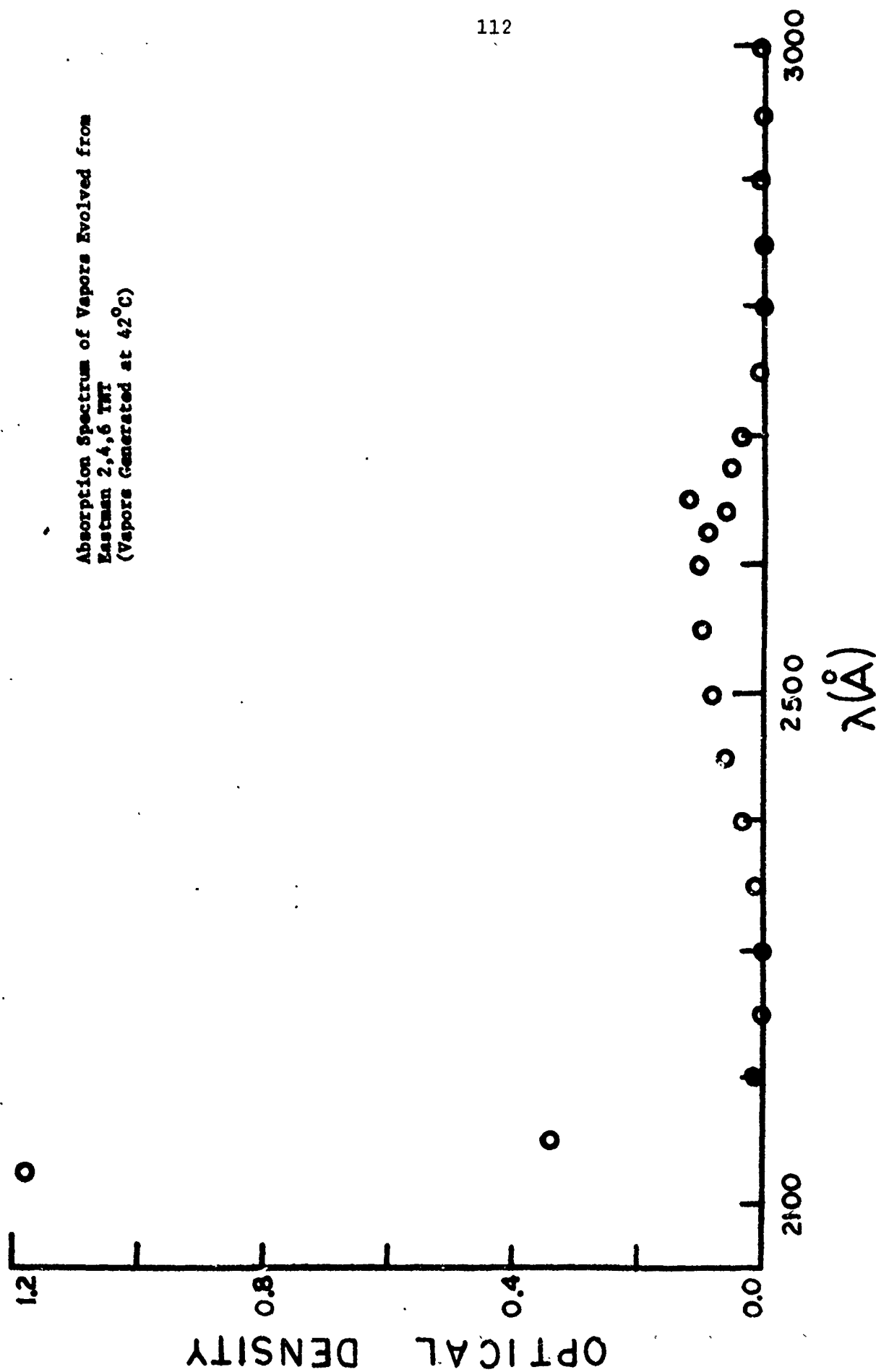


Figure 33



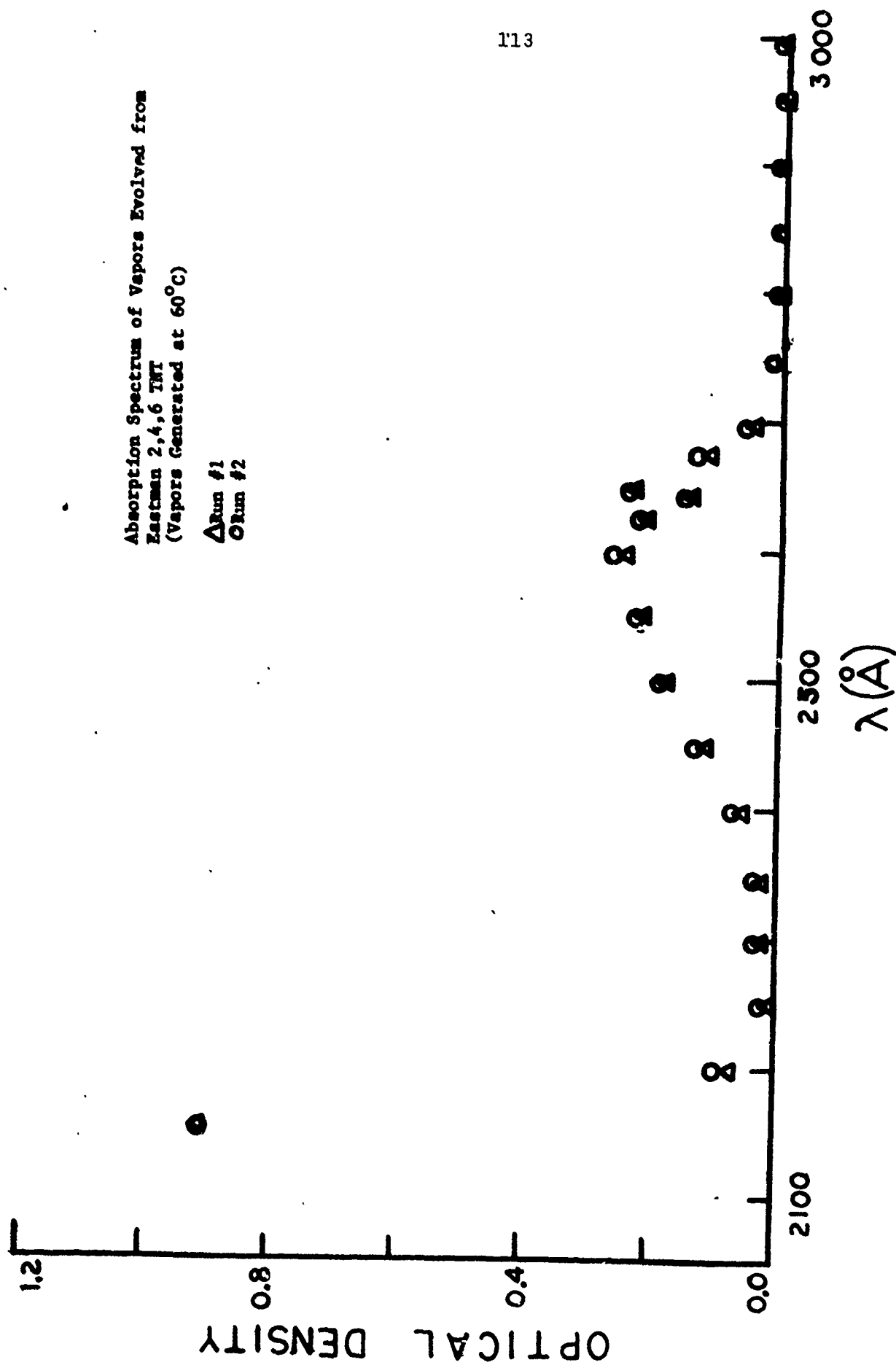


Figure 34

Absorption Spectrum of Vapors Evolved from  
Eastman 2,4,6 TNT  
(Pumped on Overnight. Vapors Generated at  
60°C)

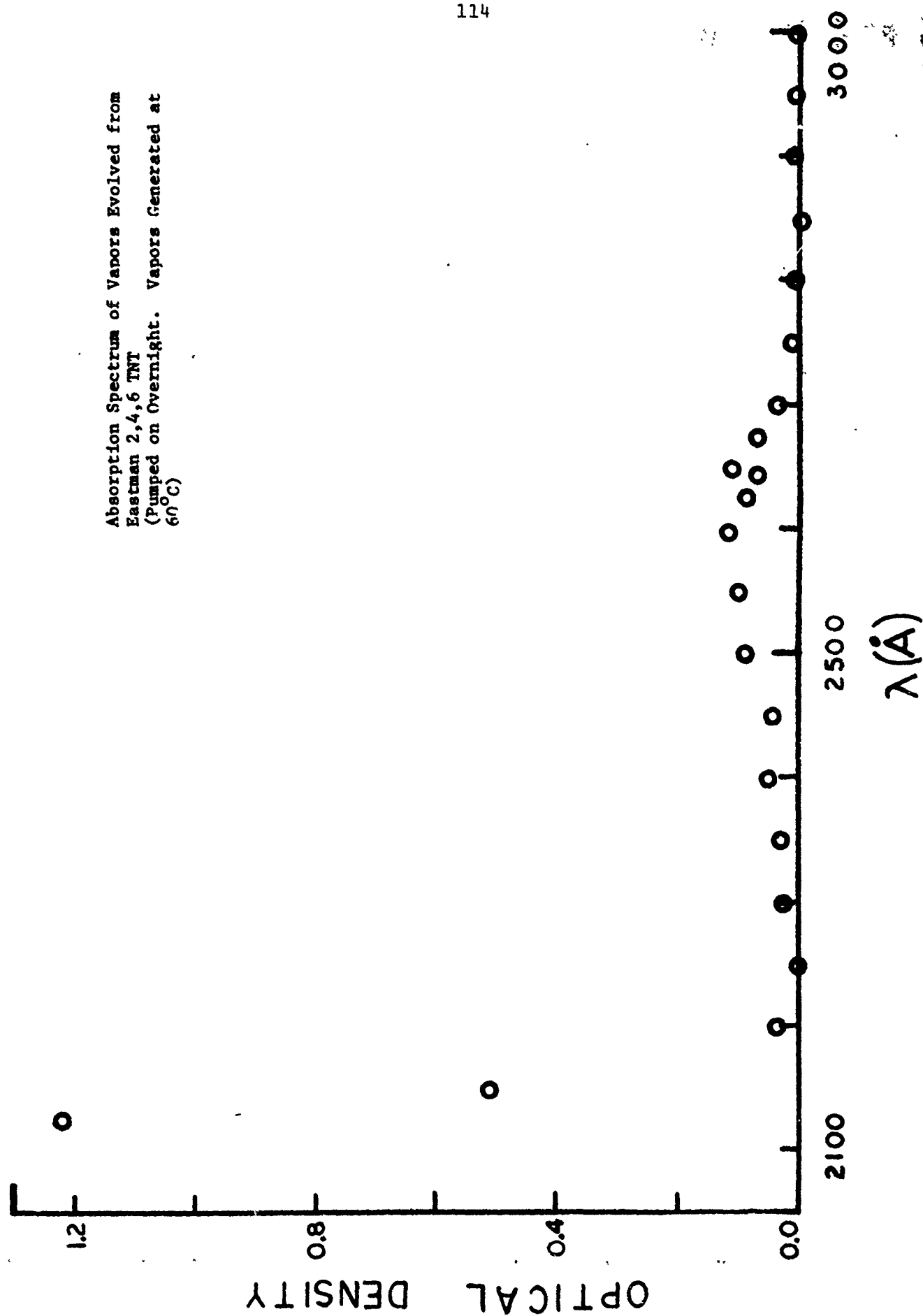


Figure 35

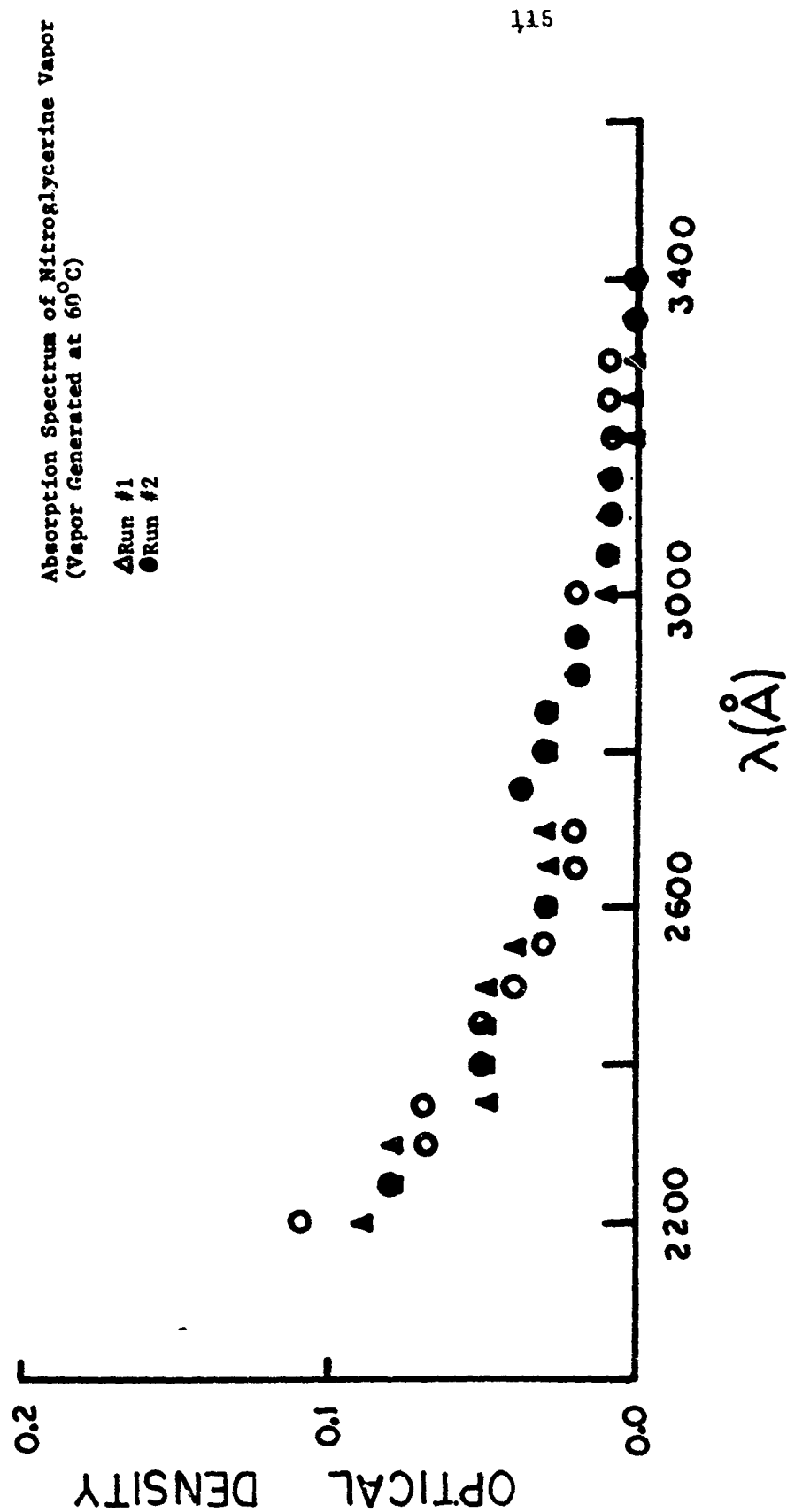
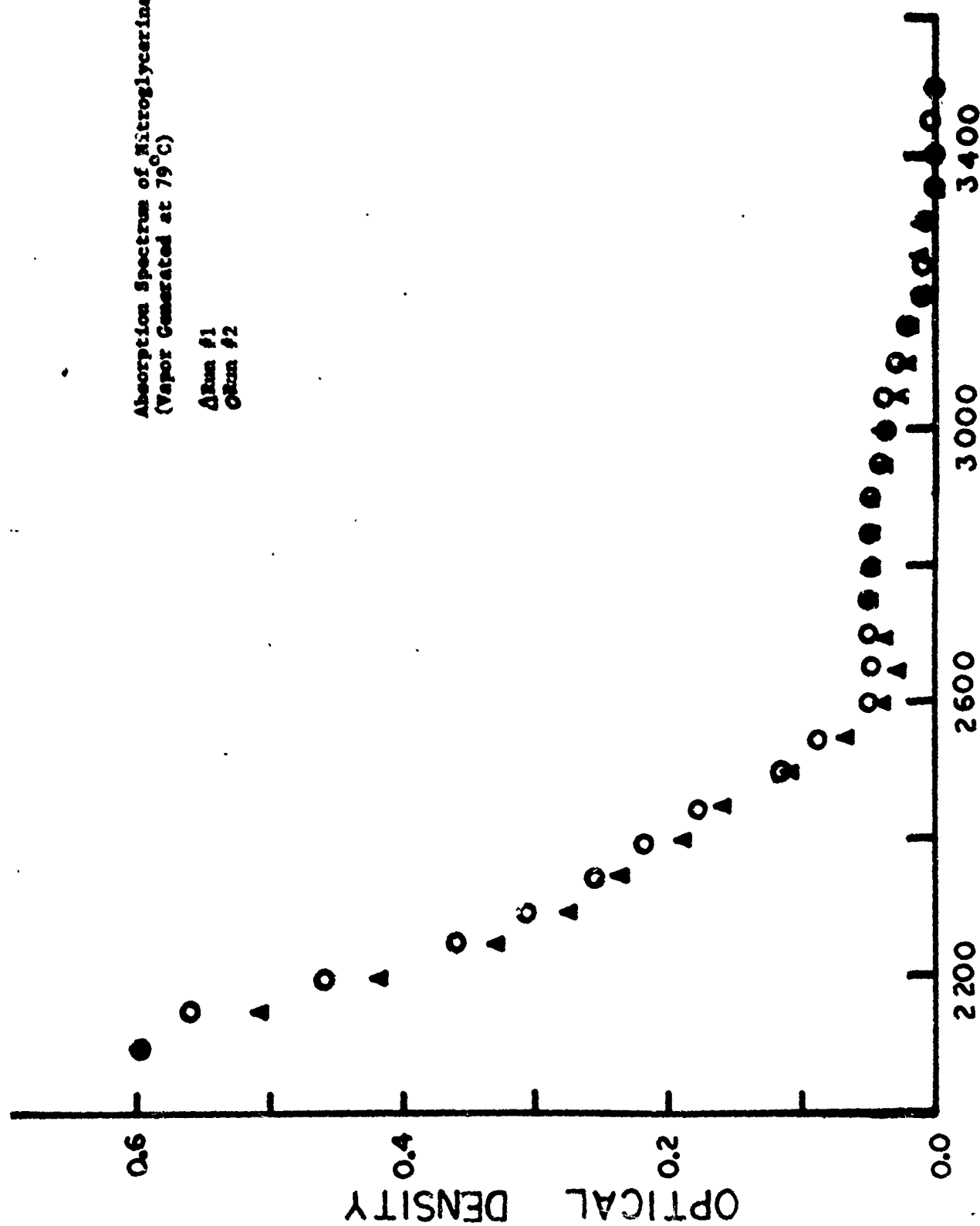


Figure 36

Absorption Spectrum of Nitroglycerine Vapor  
(Vapor Generated at 79°C)

Δ Run #1  
○ Run #2



λ(Å)

Figure 37

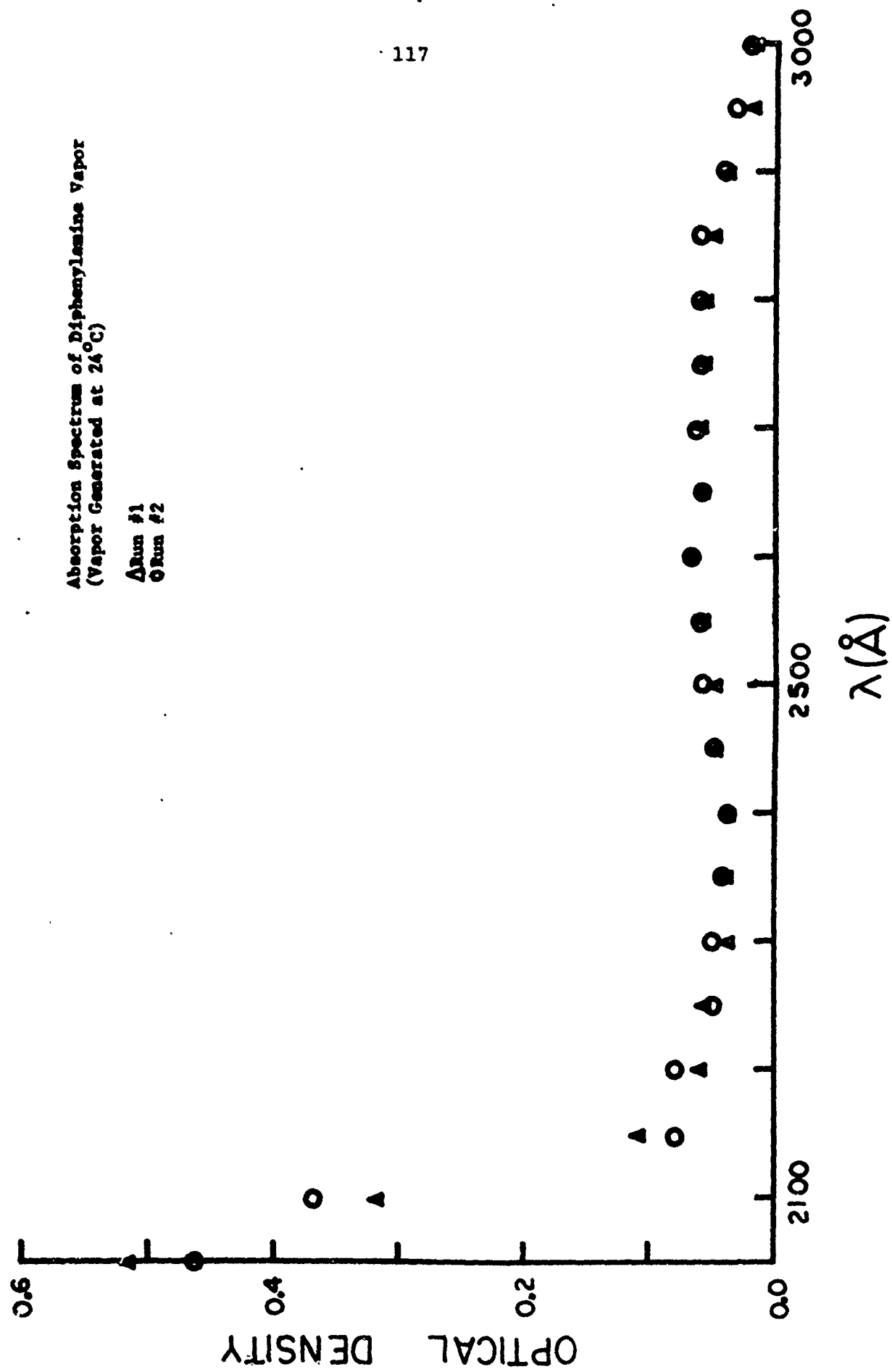
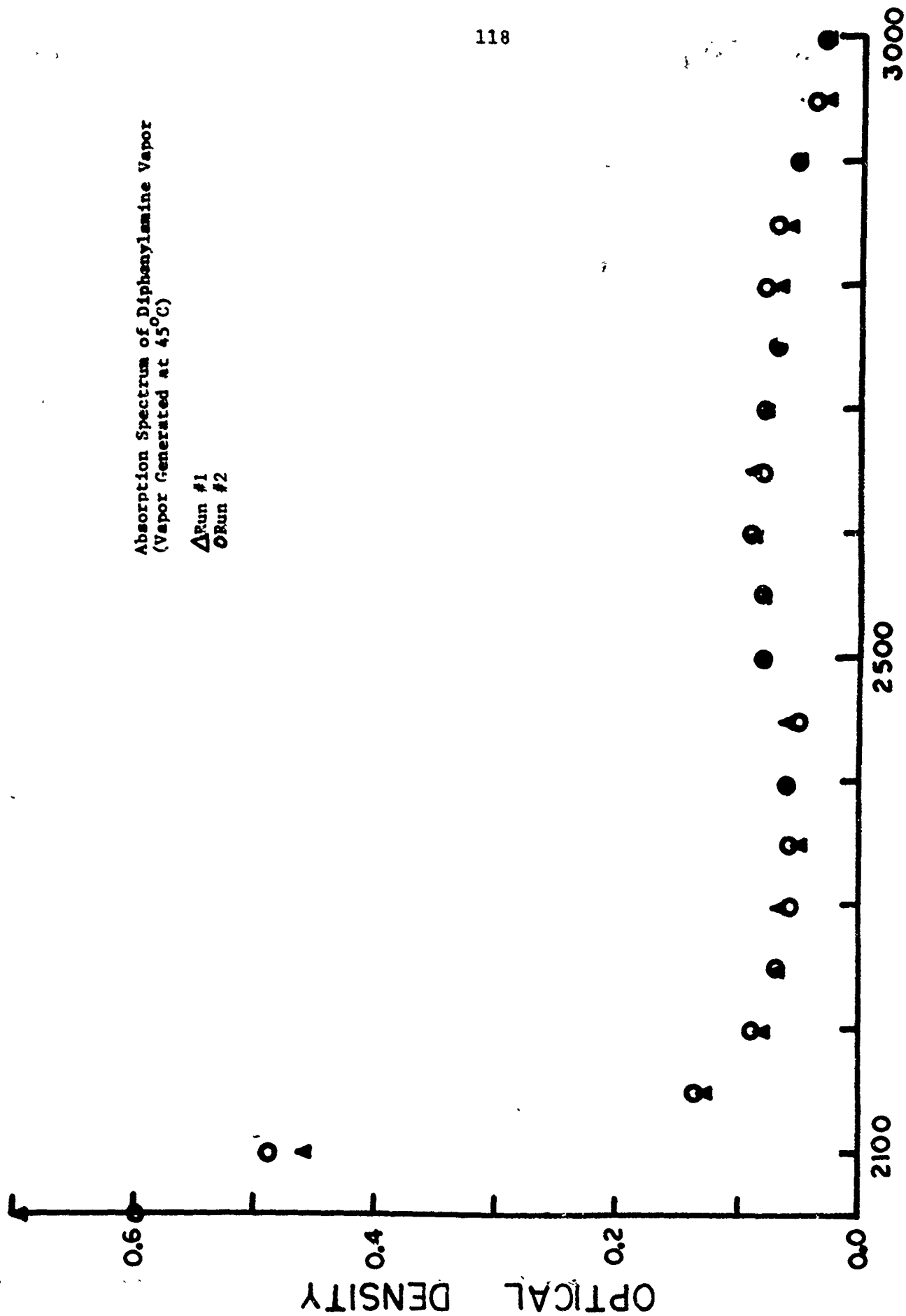


Figure 38

Absorption Spectrum of Diphenylamine Vapor  
(Vapor Generated at 45°C)

$\Delta$  Run #1  
O Run #2



$\lambda(\text{\AA})$   
Figure 39

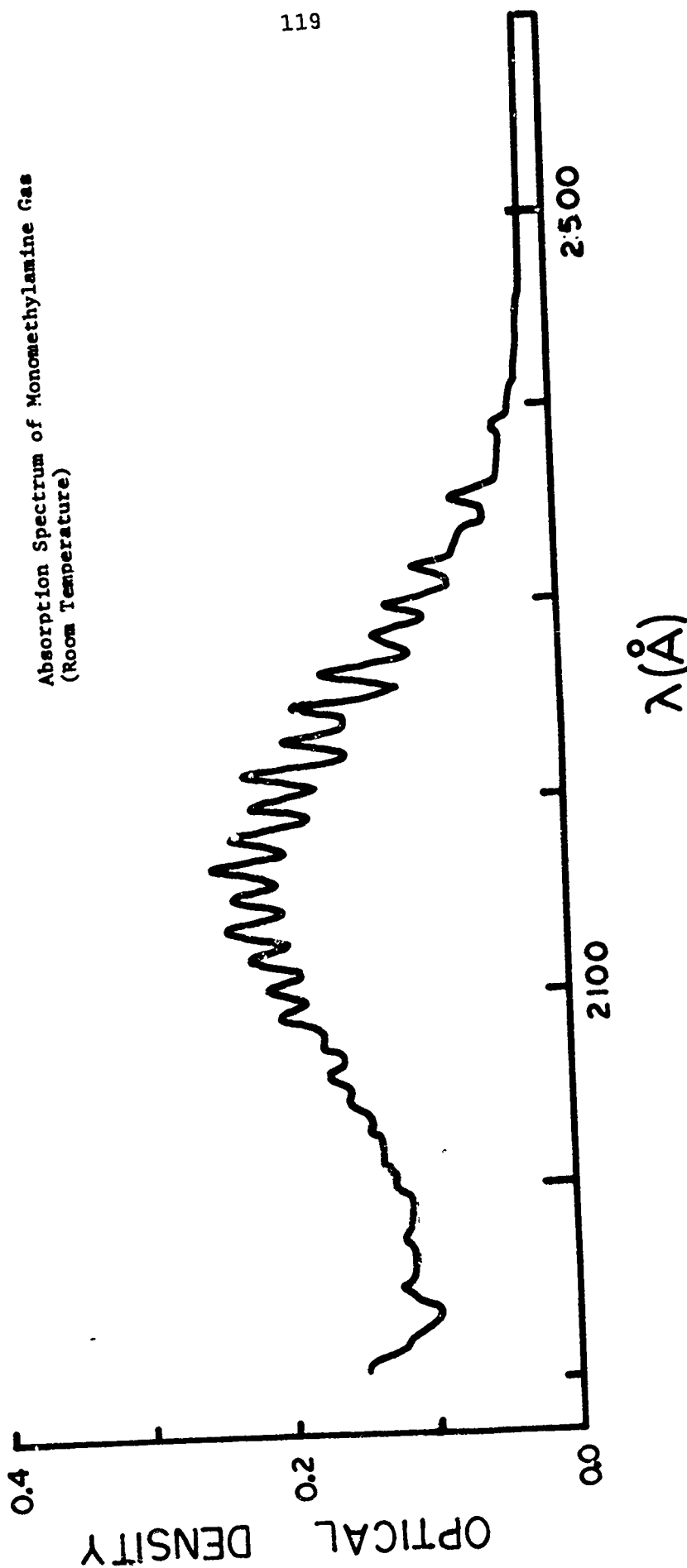


Figure 40

Absorption Spectrum of Ethyl Centralite Vapor  
(Vapor Generated at 76°C)

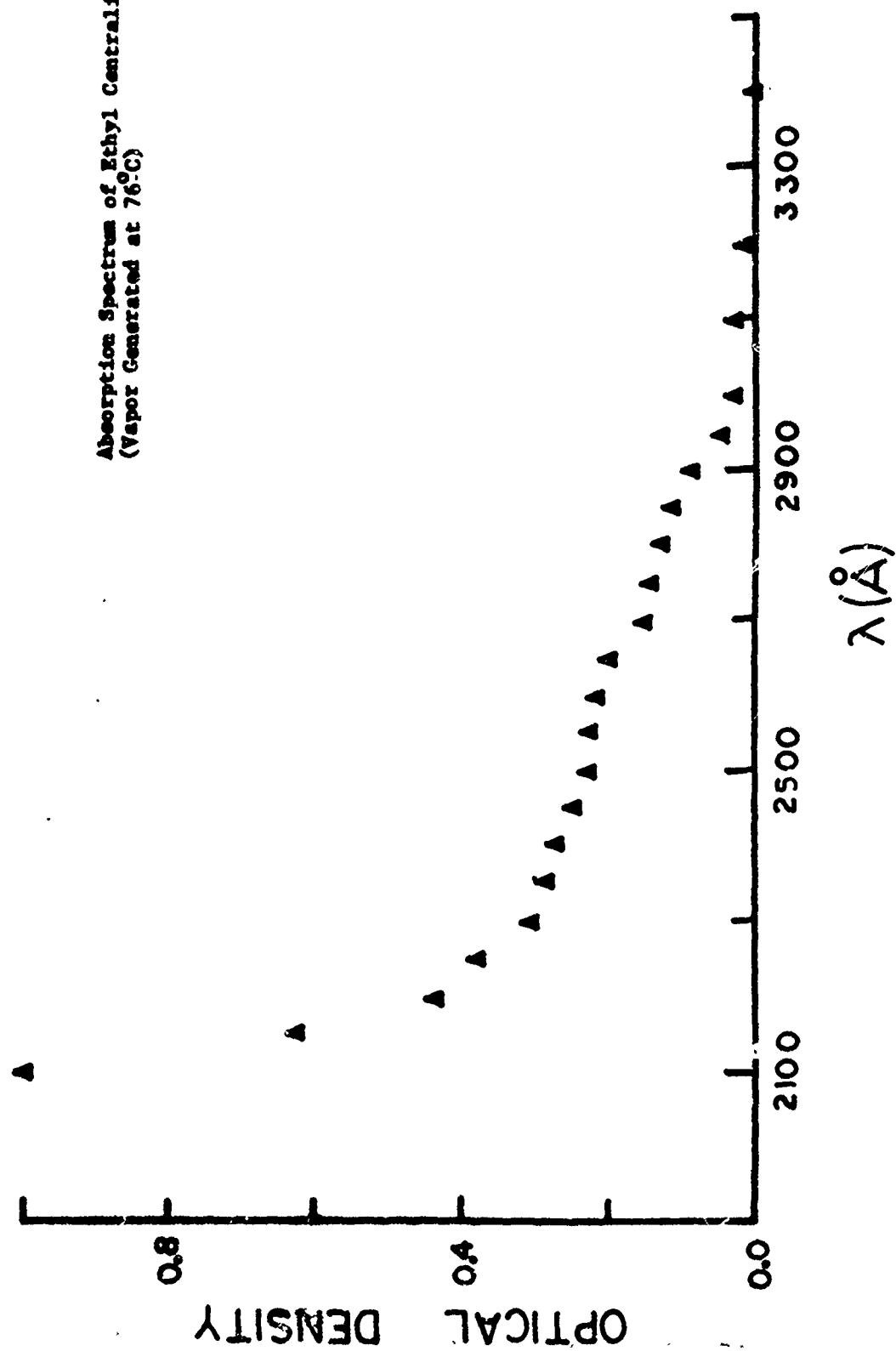


Figure 41



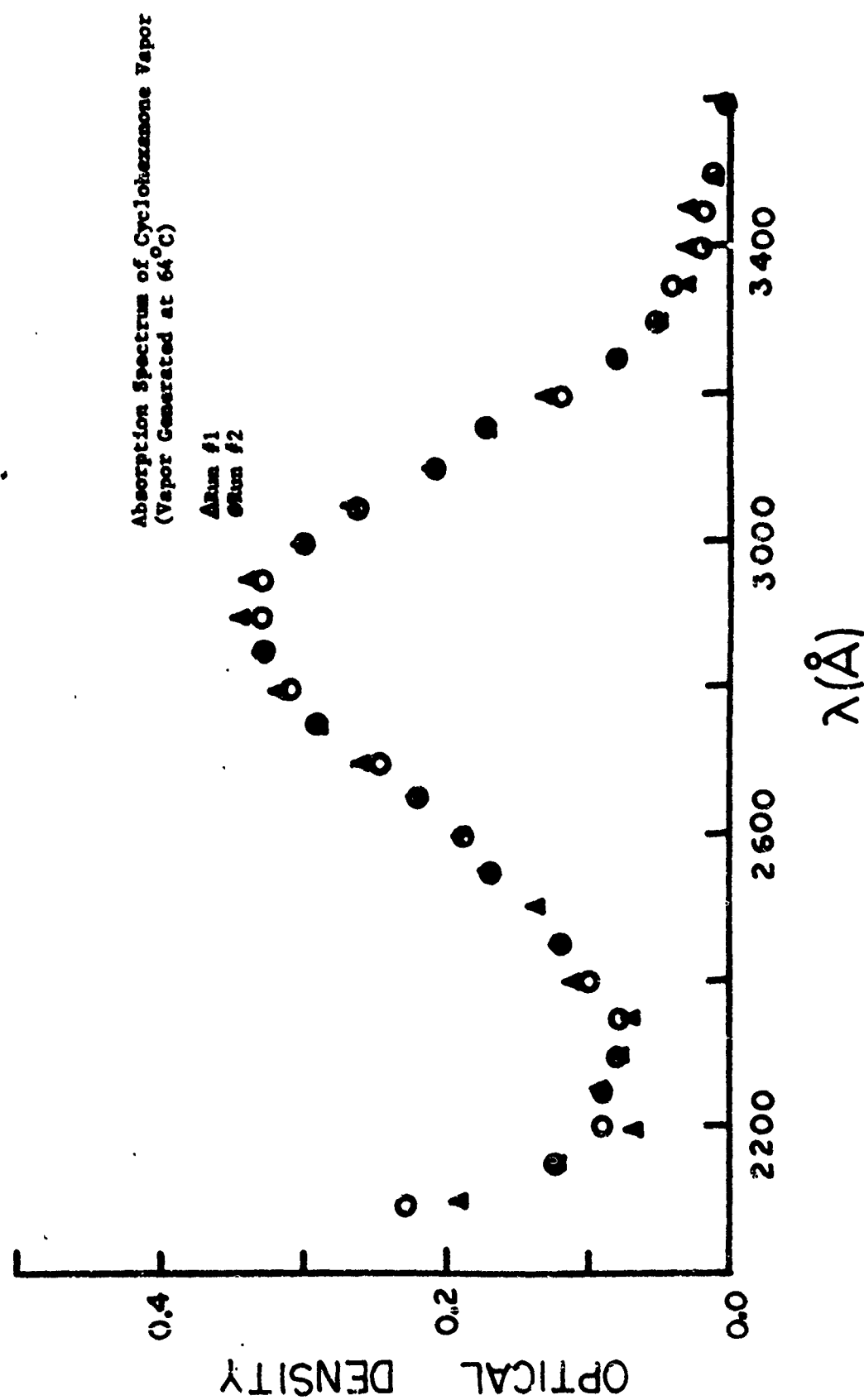


Figure 42

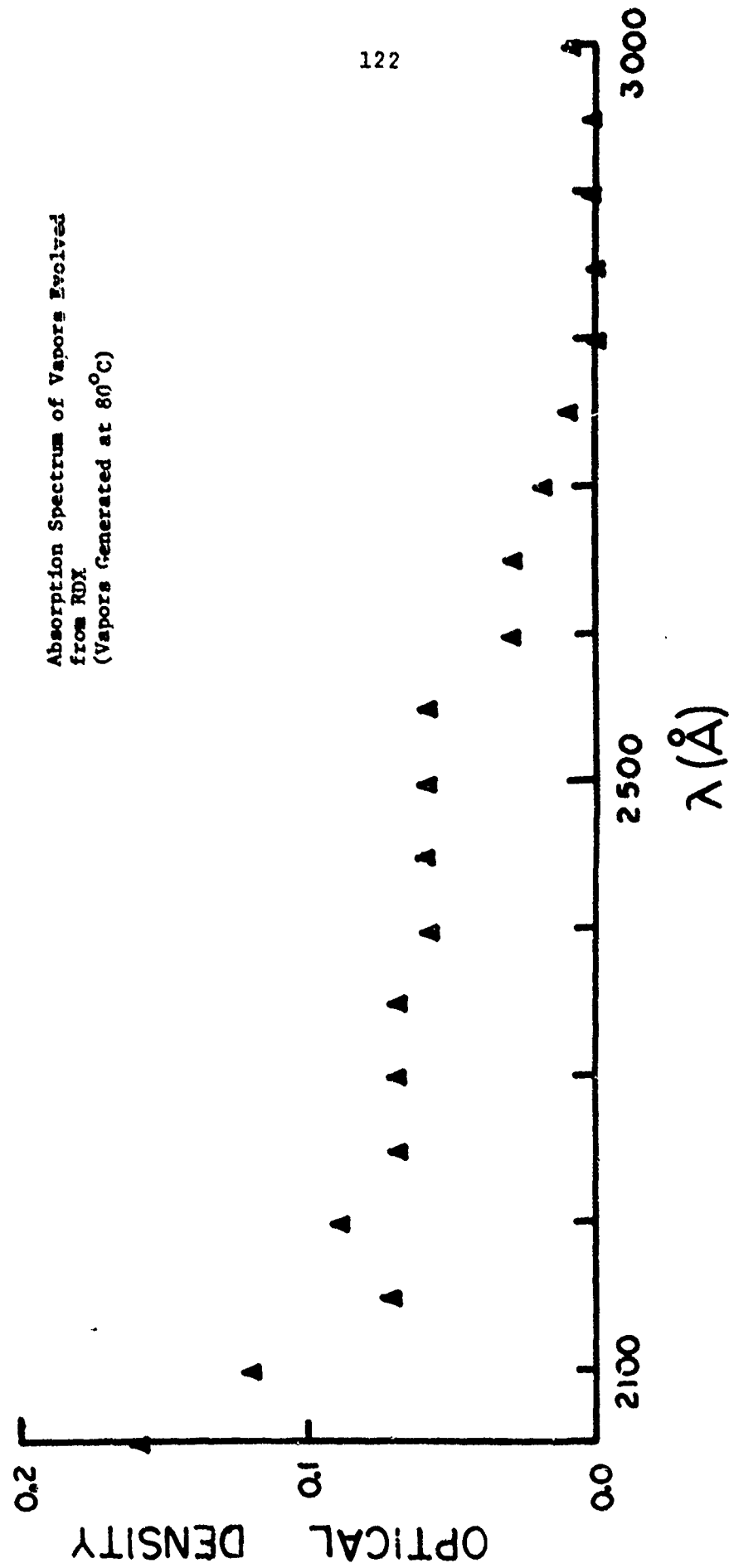


Figure 43

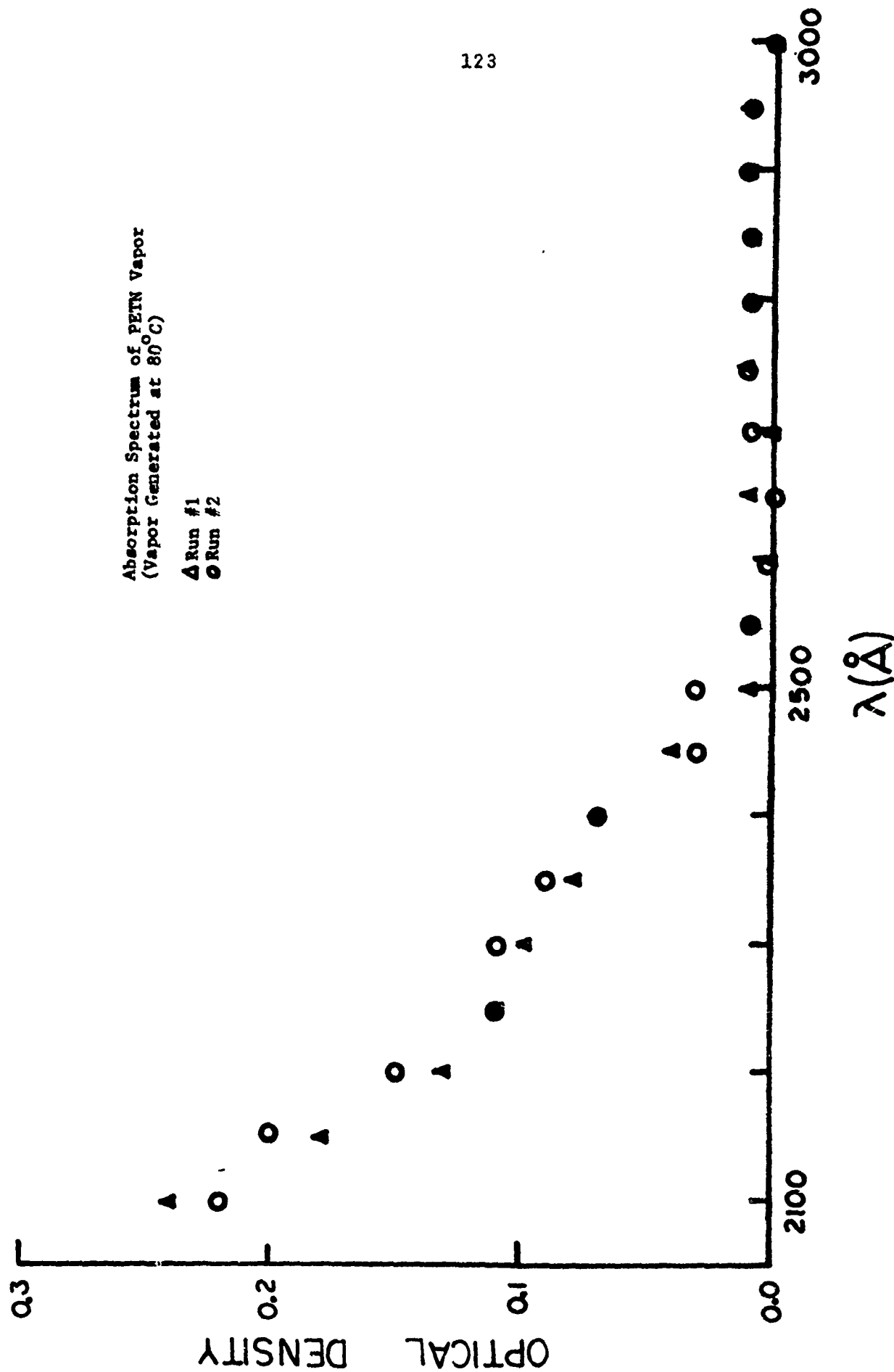


Figure 44

## FLASH PHOTOLYSIS DATA

### Introduction

The technique of flash photolysis allows the measurement of excited-state absorption of molecular species, i.e., the measurement of absorption transitions that originate from excited (metastable) levels. The photolysing flash has the purpose of populating such levels and, therefore, makes it possible to observe additional spectral features related to the absorption that proceeds from these levels. These spectral features may be observed at different times after the photolysing flash by using as a probing source either an additional smaller flash tube (spectroscopic mode) or a continuous source (kinetic mode); this allows a study of the evolution of the excited molecular species and its eventual relaxation to its fundamental state.

If the system under investigation consists of more than one chemical species, the photolysing flash may provide enough energy to start a chemical reaction; in this case the flash photolysis technique provides a means by which the kinetics of the reaction can be studied.

If the system consists of only one molecular species, the photolysing flash may bring this species to a repulsive electronic excited state and produce a photodecomposition; in some cases the fragments of the photolysed molecules may be stable species.

The behavior of complex molecules, such as those of energetic materials, following a photolysing action, may be very useful

for identification purposes. The most obvious application of this flash photolysis technique is the production of irreversible decomposition, where stable new species are formed. In such cases, the spectral data related to these stable species may be used to further characterize the original system. For this reason our first efforts have been in this direction. We have been able to observe a drastic and permanent change of the spectral features of a solution of TNT in ethanol following the irradiation of this solution with several light flashes.

It goes without saying that there is a tremendous amount of valuable information in the "kinetic" evolution of a molecular species; this information could also be used in principle for identification purposes. Our investigations will continue in this direction also.

#### Flash Photolysis of Ethanol

In flash photolysis experiments involving solutions, it is a good practice to look for possible effects that light may have on the pure solvent, in order to take these effects into account when examining the solution. For this reason we flashed pure ethanol 50 times with flashes obtained by dumping 560 joules of electrical energy into the photolysing flash tubes.

The spectrum of the irradiated ethanol was then run on the Cary 14 spectrophotometer versus non-irradiated ethanol. The result of this measurement is reported in figure 45, which presents evidence for structureless absorption starting at  $\sim 3300 \text{ \AA}$  and going up in intensity at lower wavelengths.

These findings are in accord with similar results obtained in this laboratory by D. Wu<sup>(29)</sup> on the flash photolysis of methanol, isopropanol and isobutanol. Wu observed no increased absorption at 3500 Å for these materials following the photolysing flash, and an increased absorption at 2700 Å. It must be mentioned that this absorption was reduced when the starting materials had been deaerated. Wu's studies were done in the kinetic mode at two different wavelengths (2700 and 3500 Å); no comparison is possible between the spectral features of ethanol and those of his samples on the basis of his data.

#### Spectral Characteristics of TNT

TNT is an extremely interesting explosive because, although it has a lot of shattering power when detonated, it is normally very stable. In fact, TNT can be stored at 150°C for 40 hours with no sign of decomposition; molten TNT can be stored at 85°C for two years without decomposition, and moisture does not affect the stability of solid TNT.<sup>(30)</sup> This extreme stability is the reason for the popularity of TNT as an explosive.

Little is known, however, about the stability of TNT in the presence of ultraviolet (UV) radiation. It does absorb strongly at ~2250 Å (see figure 30) due to a  $\pi \rightarrow \pi^*$  transition.<sup>(31)</sup>

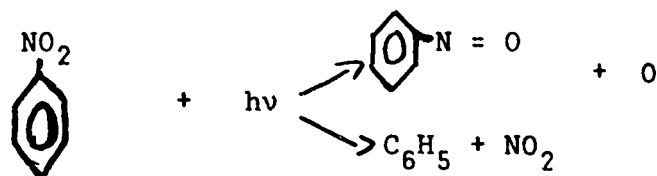
(29) D. Wu, Doctoral Dissertation, Boston College, 1977 (unpublished).

(30) Technical report of the Department of the Army and the Air Force, November, 1967; Department of the Army Technical Manual TM9-1300-214; Dept. of the Air Force Technical Order T011A-1-34.

(31) D.S. Downes and A.C. Forsyth, "Optical Absorption of TNT Single Crystals," Picatinny Arsenal Technical Report No. 4565, August, 1973.

Since  $\pi^*$  electrons are antibonding, the molecule will certainly be less stable in the excited state than in the ground state. Thus, it is possible that the molecule could decompose in the presence of strong UV radiation. In fact, in a dilute gas, the TNT will either decompose or luminesce to return to the ground state.

Evidence which indicates that TNT might decompose comes from the related compound, nitrobenzene. Upon irradiation with UV light:<sup>(32)</sup>



with ultimate products being nitrosobenzene and para-nitrophenol.

TNT is known to undergo a few other reactions. For example, it is known that in the presence of oxygen and UV radiation, TNT decomposes and becomes increasingly sensitive to impact.<sup>(30)</sup> Little is known, however, about either the identity of the decomposition products or the reason for the increased sensitivity. Also, when put in water and exposed to sunlight, TNT forms a red solution.<sup>(22)</sup> Again, little is known about the cause of the red color. Finally, in a mild base, TNT is known to form a red solution<sup>(33)</sup> owing to formation of the anion  $[\text{C}_6\text{H}_2(\text{NO}_2)_3\text{CH}_2]^-$ ;

(32) J.G. Calvert and J.N. Pitts, Jr., Photochemistry (John Wiley and Sons, Inc., New York, 1966), pg. 479.

(33) T. Abe, Bull. Chem. Soc. Japan 32, 339 (1959) and E.F. Calden and G. Long, Proc. Roy. Soc. (London) 238A, 263 (1955).

it is not expected, however, that this anion is also responsible for the red color of the irradiated aqueous solution, because the anion color disappears on addition of acid. It is doubtful that the same phenomenon would occur with the irradiated water solution. This conjecture, which is easy to check, will be verified.

Summarizing the facts about TNT, it is quite stable under common or even very warm or moist storage conditions. However, there is some evidence that it may decompose on exposure to strong UV radiation.

#### Flash Photolysis of TNT in Solution

The absorption spectrum of a solution of TNT in ethanol was obtained by using the Cary 14 spectrophotometer and is presented in figure 46. The TNT was recrystallized from military grade; a solution was obtained by dissolving 1 mg of recrystallized TNT in 100 ml of ethanol. 1 cm cells were used. The spectrum obtained is similar to the one reported in Figure 11 b.

A similar solution was flashed 25 times by using 560-joule flashes. The spectrum of the irradiated solution is presented in figure 47. It presents a stronger tail at wavelengths greater than 3000 Å; this increased absorption is responsible for the brownish color that the solution acquires. In addition, the absorption at ~2700 Å presents an increase.

These trends are more dramatically visible in figure 48. which reports the spectrum of a similar solution flashed 100



times by using 560-joule flashes. The tail is now more prominent and a new band has appeared at  $\sim 2700 \text{ \AA}$ . A most important observation is that the presence of these new spectral features is accompanied by a reduction in the absorbance of the normal spectral band of TNT; this is a clear indication of a permanent chemical change undergone by some of the TNT molecules in solution. A comparison of these spectra with the spectrum of irradiated ethanol (figure 45) clearly indicates that the solvent is not responsible for the observed effects.

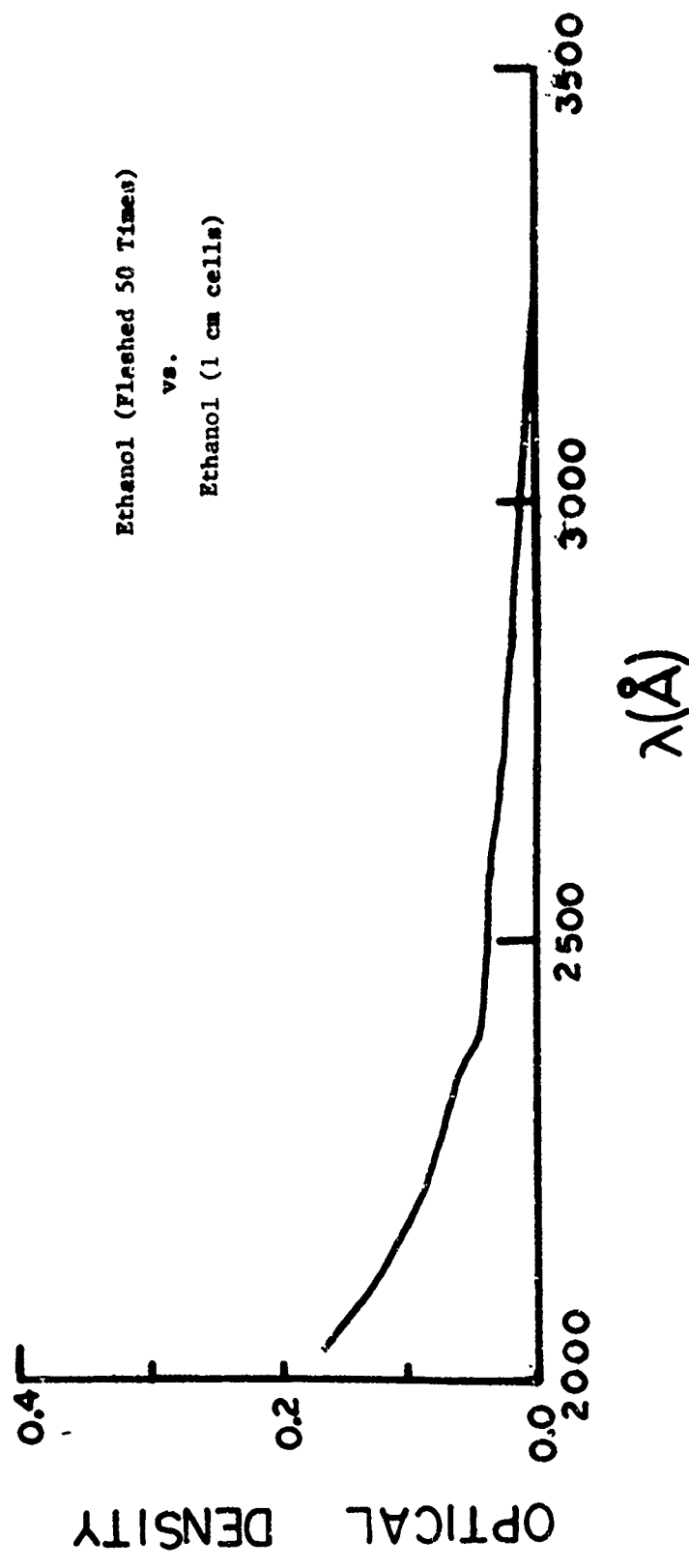


Figure 45

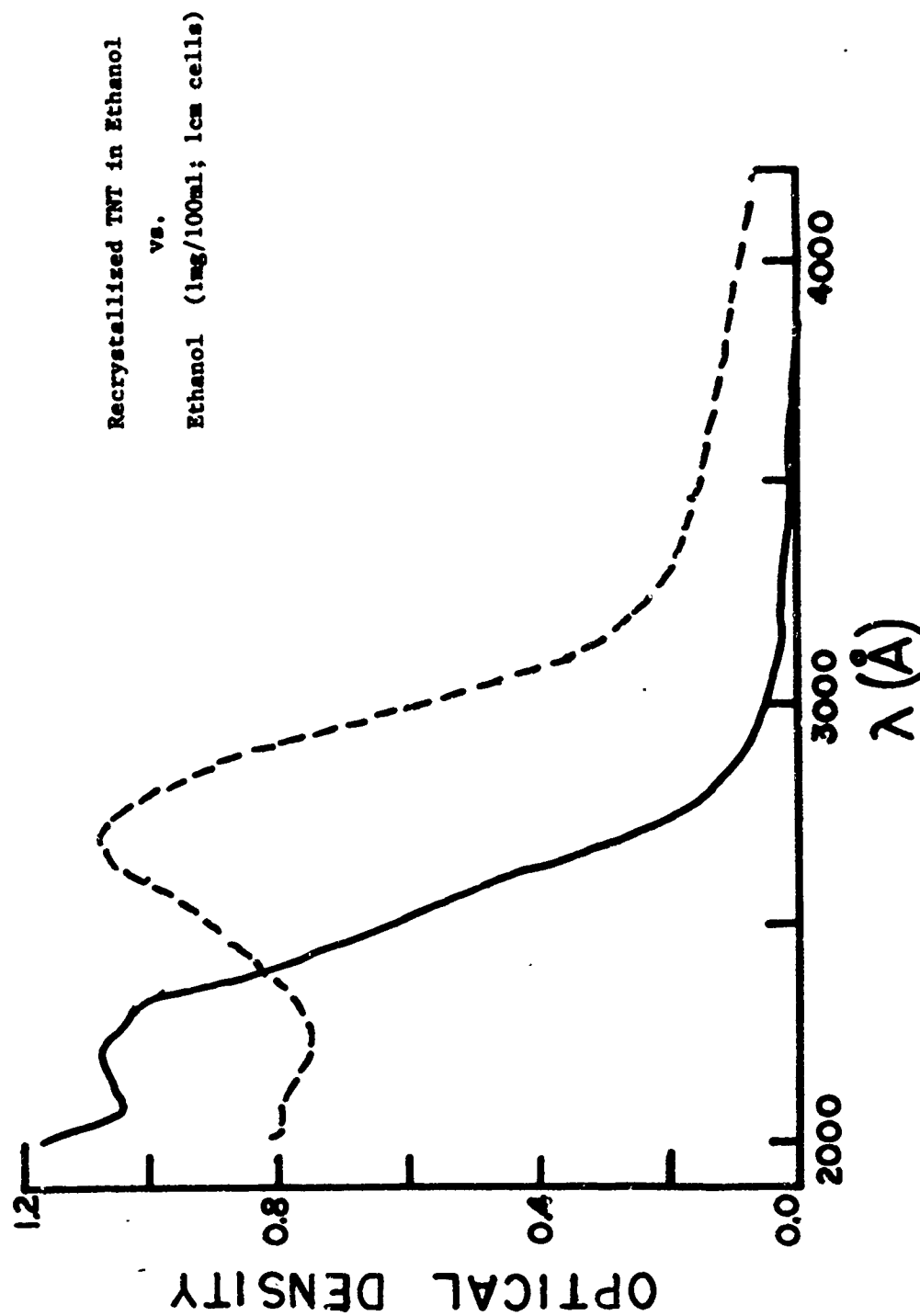


Figure 46

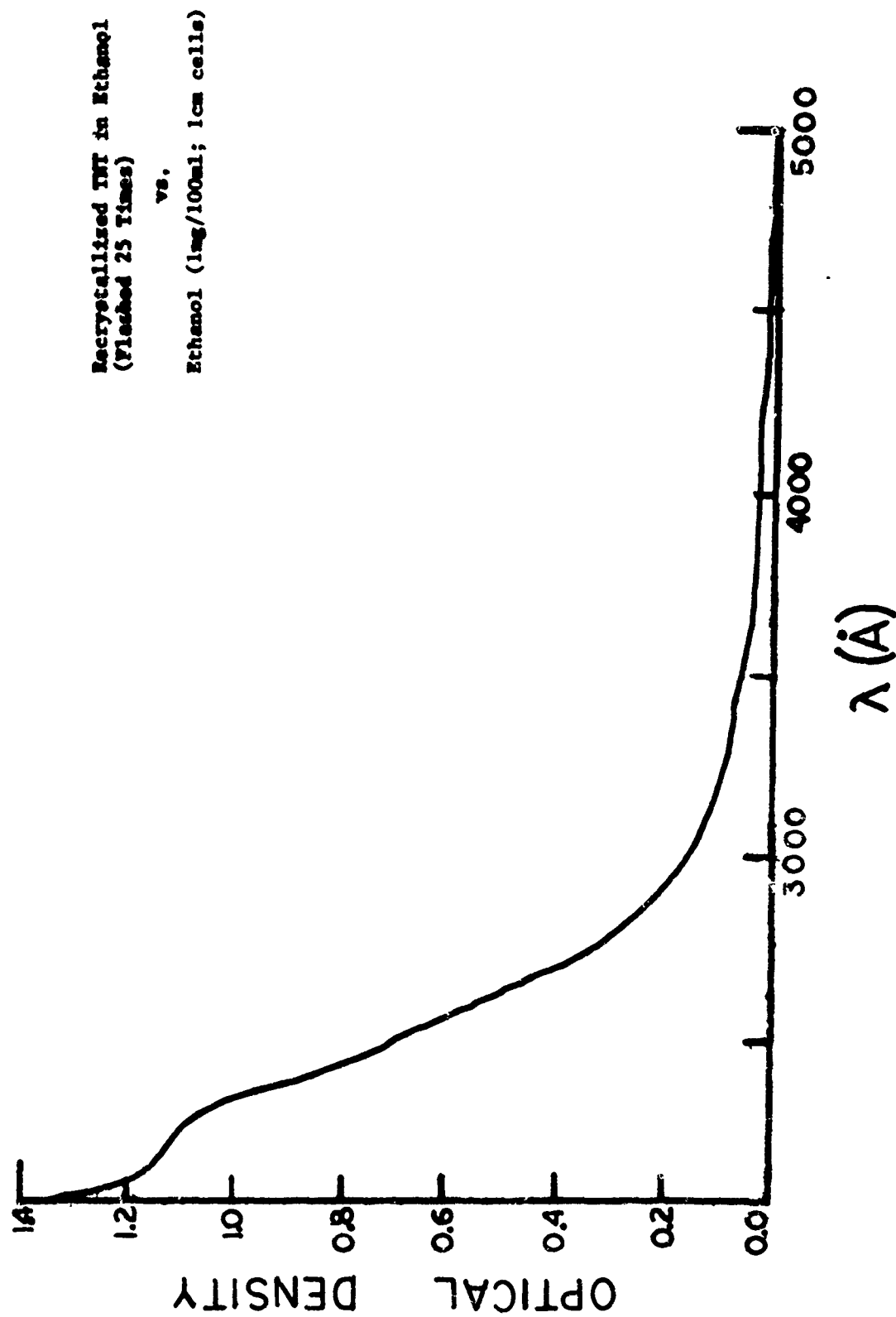


Figure 47

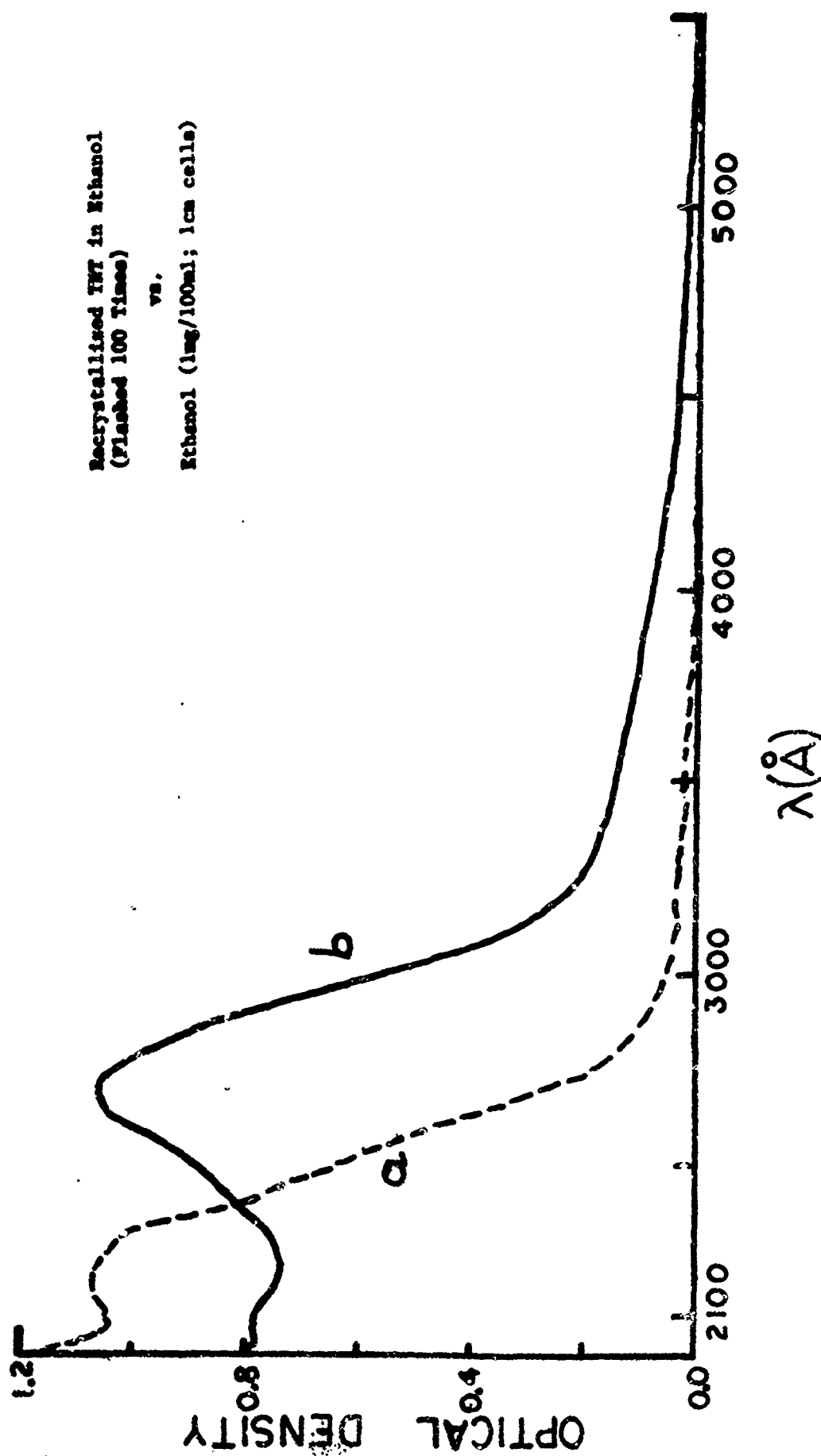


Figure 48

## CONCLUSIONS AND RECOMMENDATIONS

The absorption spectra of a number of explosive and explosive-related compounds have been obtained both in solution and in the vapor phase. The following conclusions represent the most significant findings of this investigation.

(1) Except for monomethylamine, no compound studied revealed evidence of a sharp-line absorption. For the nitrotoluene compounds, this is due to the shift of the unstructured First Primary Band into the general region of the absorption due to the Secondary Band. Because the extinction coefficient of the former is typically about an order of magnitude larger than that of the latter, all sharp-line structure is masked. For the amines ethyl centralite and diphenylamine, the reason for this lack of structure is less clear, but the amine group is known to produce a similar shift when substituted on a benzene ring.

(2) For the nitrotoluene compounds, the less polar the environment, the more the First Primary Band is shifted toward shorter wavelengths. The band at higher energy does not appear to be similarly affected. As a result, the vapor-phase absorption spectra for these materials indicate a considerable overlap between these two bands. This is especially evident for 2,6 DNT. This effect tends to wash out any distinguishing features of the spectra and hence inhibits detection by this method.

(3) For the amines, there exist two different situations. The absorption spectrum of monomethylamine shows a characteristic structure due to the presence of two predominant vibrational modes.

This property is conducive to detection by means of U.V. absorption techniques. For ethyl centralite and diphenylamine, however, the situation is more closely related to that of the nitro compounds. In going from the solution to the vapor, the main band above  $\sim 2400 \text{ \AA}$  shifts to shorter wavelengths and/or broadens. Such a behavior increases the overlap of this band with the more intense one at higher energies. The effect is to smear out the observed absorption and make detection by this method difficult.

(4) The nitroxy compounds studied (nitroglycerine and PETN) reveal no significant intrinsic absorption above  $\sim 2400\text{--}2500 \text{ \AA}$  in the vapor phase. The spectra below these wavelengths consist essentially of an absorption tail extending into the vacuum U.V. Consequently, detection of these compounds by their U.V. absorption spectra is not feasible. On the other hand, they do not interfere with the detection of other explosive-related compounds.

(5) The detection of RDX itself is intrinsically difficult because of its very low vapor pressure. Our data are inconclusive, because the observed absorption cannot at present be definitely attributed to RDX. Cyclohexanone, a common impurity in materials containing RDX, possesses a characteristic absorption band peaking at  $\sim 2900 \text{ \AA}$ . Therefore, it would appear that detection of cyclohexanone could be used to indicate the presence of RDX. As was seen in our study, however, purified RDX may contain no optical traces of cyclohexanone.

As a result of the above considerations, it would appear then that the detection of such materials by their U.V. absorption

spectra is less than promising. There are, however, two related approaches which could prove more successful in the detection of the compounds of interest. As such they warrant future study.

These approaches include:

- (1) An investigation of the optical characteristics of the species produced following photodissociation of the explosive materials and their associated impurities. When molecules are illuminated with light of the proper wavelength, they may dissociate into species which can be optically investigated. This is the basic notion behind flash photolysis spectroscopy. The complex molecule of an explosive or an associated impurity is expected to dissociate into a set of species which are optically detectable and whose summed spectra will characterize the molecule. If the molecule is dissociated and rapid recombination does not occur, then one can look at both absorption and luminescence characteristics of the dissociated species. The data generated in such a study might well point the way to a new detection technique. The existence of dye lasers make it possible to selectively dissociate the molecules of interest. (We have already undertaken some preliminary studies of the flash photolysis of TNT in solution. The details can be found earlier in this report.)
- (2) An investigation of the luminescence characteristics of the explosives and their associated impurities. While



there have been previous studies of explosives in the crystalline state, the results are not necessarily applicable to the explosives in the molecular state, since in this case non-radiative decay mechanisms could not involve energy transfer to the crystal. Data could be collected on the emission spectra and lifetimes, and estimates made of the ratio of energy absorbed to energy emitted as luminescence. The data could allow feasibility estimates on luminescence detection to be made, based on the frequency and power of the laser light source required, the emission detector sensitivity, and the likelihood of interference by atmospheric constituents.

## REFERENCES

1. CRC Handbook of Chemistry and Physics, CRC Press, 57th Ed. (1976-1977).
2. W. A. Schroeder, P. E. Wilcox, K. N. Trueblood, and A. O. Dekker, Anal. Chem. 23, 1740 (1951).
3. T. Abe, Bull. Chem. Soc. Japan 31, 904 (1958).
4. H. H. Jaffé and M. Orchin, Theory and Applications of Ultraviolet Spectroscopy (John Wiley and Sons, Inc., New York, 1962) ppg. 255-257.
5. Ibid., pg. 243.
6. C. P. Conduit, J. Chem. Soc., 3273 (1959).
7. See any introductory organic chemistry text, e.g., Morrison and Boyd, Organic Chemistry (Allyn and Bacon, 1967).
8. M. K. Orloff, P. A. Mullen, and F. C. Rauch, J. Phys. Chem. 74, 2189 (1970).
9. P. L. Marinkas, "Luminescence Properties of RDX and HMX," Picatinny Arsenal Technical Report No. 4840, August, 1975.
10. M. Ito, J. Mol. Spectroscopy 4, 106 (1960).
11. See, for example, the review by J. Yinon, CRC Critical Reviews in Analytical Chemistry, pg. 1 (December, 1977).
12. P. A. Pella, J. Chem. Thermodynamics 9, 301 (1977).
13. J. H. McReynolds, G. A. St. John, and M. Anbar, "Determination of Concentration of Explosive Vapor from Parcels and Letters," Final Report, U.S. Postal Service Contract No. 74-00810, Stanford Research Institute (January, 1975).

14. D. C. Leggett, T. F. Jenkins, and R. P. Murrmann, "Composition of Vapors Evolved from Military TNT as Influenced by Temperature, Solid Composition, Age, and Source," CRREL Special Report No. 77-16 (June, 1977).
15. T. F. Jenkins, W. F. O'Reilly, R. P. Murrmann, and C. I. Collins, "Detection of Cyclohexanone in the Atmosphere Above Emplaced Antitank Mines," CRREL Special Report No. 203 (April, 1974).
16. C. T. Pate, "Characterization of Vapors Emanating from Explosives," Final Report, LEAA Contract No. J-LEAA-025-73 (June, 1976).
17. J. A. Gelbwachs, C. F. Klein, and J. E. Wessel, "Feasibility of Doppler-Free Two-Photon Spectroscopy for Explosive Vapor Detection," Aerospace Report No. ATR-76 (7911)-3 (1976).
18. P. C. Claspy, Y.-H. Pao, S. Kwong, and E. Nodov, Appl. Optics 15, 1506 (1976).
19. J. A. Rakaczky and A. D. Coates, "The Effect of Surfaces on the Flow of Vaporized Explosives," Ballistics Research Laboratory Report No. 1597.
20. E. Tannenbaum, E. M. Coffin, and A. J. Harrison, J. Chemical Phys. 21, 311 (1953).
21. J. A. Gelbwachs, private communication.
22. T. Urbanski, Chemistry and Technology of Explosives (Pergamon Press, N.Y., 1965).
23. "Properties of Explosives of Military Interest," AMC Pamphlet 706-177, U.S. Army Materiel Command, January, 1971.

24. A. Marshall and G. Peace, J. Soc. Chem. Ind. 109, 298 (1916).
25. J. M. Rosen and C. Dickinson, "Vapor Pressures and Heats of Sublimation of Some High Melting Organic Explosives," NOL Report 69-67, 16 April 1969, AD 689112.
26. J. G. Calvert and J. N. Pitts, Jr., Photochemistry (John Wiley and Sons, Inc., N.Y., 1966) ppg. 264, 499.
27. T. Förster and J. C. Jungers, Z. physik. Chem. B36, 387 (1937).
28. J. G. Calvert and J. N. Pitts, Jr., Photochemistry (John Wiley and Sons, Inc., N.Y., 1966) pg. 409.
29. D. Wu, Doctoral Dissertation, Boston College, 1977 (unpublished).
30. Technical report of the Department of the Army and the Air Force, November, 1967; Department of the Army Technical Manual TM9-1300-214; Dept. of the Air Force Technical Order T011A-1-34.
31. D. S. Downes and A. C. Forsyth, "Optical Absorption of TNT Single Crystals," Picatinny Arsenal Technical Report No. 4565, August, 1973.
32. J. G. Calvert and J. N. Pitts, Jr., Photochemistry (John Wiley and Sons, Inc., New York, 1966), pg. 479.
- 33.. T. Abe, Bull. Chem. Soc. Japan 32, 339 (1959), and E. F. Calden and G. Long, Proc. Roy. Soc. (London) 238A, 263 (1955).

# DISTRIBUTION LIST

Defense Documentation Center (TRS) Cameron Station, Building 5 Alexandria, VA 22314	2	Commander Explosive Ordnance Disposal Group TWO Fort Story, VA 23459	2
Chief of Naval Operations (OP-9821F1) Department of the Navy Washington, DC 20350	1	Commanding Officer Naval School Explosive Ordnance Disposal (SD) Naval Ordnance Station Indian Head, MD 20640	2
Chief of Naval Operations (OP-372H) Department of the Navy Washington, DC 20350	3	Commander U.S. Army Technical Detachment Naval Explosive Ordnance Disposal Facility Indian Head, MD 20640	2
Commander Naval Sea Systems Command (SEA-033) Washington, DC 20362	2	Commander Detachment 63, HQ Ogden Air Logistics Center (AFLC) Naval Explosive Ordnance Disposal Facility Indian Head, MD 20640	2
Commander Naval Sea Systems Command (SEA-663C) Washington, DC 20362	2	Officer-In-Charge Marine Corps Detachment Naval Explosive Ordnance Disposal Facility Indian Head, MD 20640	1
Commander Explosive Ordnance Disposal Group ONE Barbers Point, HI 96862	2		

# DISTRIBUTION LIST

Defense Documentation Center (TRS) Cameron Station, Building 5 Alexandria, VA 22314	2	Commander Explosive Ordnance Disposal Group TWO Fort Story, VA 23459	2
Chief of Naval Operations (OP-9821F1) Department of the Navy Washington, DC 20350	1	Commanding Officer Naval School Explosive Ordnance Disposal (SD) Naval Ordnance Station Indian Head, MD 20640	2
Chief of Naval Operations (OP-372H) Department of the Navy Washington, DC 20350	3	Commander U.S. Army Technical Detachment Naval Explosive Ordnance Disposal Facility Indian Head, MD 20640	2
Commander Naval Sea Systems Command (SEA-033) Washington, DC 20362	2	Commander Detachment 63, HQ Ogden Air Logistics Center (AFLC) Naval Explosive Ordnance Disposal Facility Indian Head, MD 20640	2
Commander Naval Sea Systems Command (SEA-663C) Washington, DC 20362	2	Officer-In-Charge Marine Corps Detachment Naval Explosive Ordnance Disposal Facility Indian Head, MD 20640	1
Commander Explosive Ordnance Disposal Group ONE Barbers Point, HI 96862	2		